

memtrans



Project N°: 518246

**MEMTRANS**

“Membrane transporters: In vitro models for the study of their role in drug fate”

STREP

Thematic priority 1: Lifesciences-Genomics and Biotechnology for Health

**Deliverable 1 (D 1)**  
**Report with the description and number of compounds**

Due date of deliverable: 01/07/2006

Actual Submission date: 31/07/2007

Start date of project: 01/04/2006

Duration: 36 months

Organisation name for lead contractor of this deliverable: University of Valencia

Nature for the deliverable: **R** = Report

Dissemination level: **PU** = Public

## TABLE OF CONTENTS

<b>LIST OF TABLES.....</b>	<b>4</b>
<b>LIST OF FIGURES.....</b>	<b>5</b>
<b>ABBREVIATIONS .....</b>	<b>6</b>
<b>1. SELECTION OF THE TEST COMPOUNDS .....</b>	<b>8</b>
1.1. Introduction.....	8
1.2. Overview .....	8
1.3. General criteria for the selection of the compounds .....	9
1.4. Compound candidates .....	10
1.4.1. Celiprolol .....	10
1.4.2. Paclitaxel.....	11
1.4.3. Saquinavir .....	13
1.4.4. Fexofenadine.....	15
1.4.5. Digoxin .....	17
1.4.6. Talinolol.....	19
1.4.7. Loperamide .....	20
1.4.8. Quinidine .....	21
1.4.9. Ritonavir .....	22
1.4.10. Vinblastine .....	23
1.4.11. Topotecan .....	24
1.4.12. Sparfloxacin.....	26
1.4.13. Methotrexate .....	27
1.4.14. Verapamil .....	28
1.4.15. Cyclosporine A .....	29
1.4.16. Rifampin .....	30
1.4.17. Daunorubicin (daunomycin).....	30
1.4.18. Etoposide .....	31
1.4.19. Vincristine.....	32
1.4.20. Erythromycin .....	33
1.4.21. Tobramycin.....	33
1.4.22. Ivermectin .....	34
1.4.23. Doxorubicin .....	35
1.4.24. Tacrolimus .....	36
1.4.25. Nadolol .....	36
1.4.26. Labetalol .....	37
1.4.27. Docetaxel .....	38
1.4.28. Lincomycin .....	39
1.4.29. Indinavir.....	39
1.4.30. Sulpiride.....	40
1.4.31. Azithromycin .....	41
1.4.32. Salbutamol .....	41
1.4.33. Sulfasalazine .....	43

1.4.34. Rosuvastatin.....	44
1.5. Summary tables.....	46
1.6. Conclusion .....	52
<b>2. SELECTION OF THE INHIBITORS.....</b>	<b>53</b>
2.1. General criteria for selection of inhibitors .....	53
2.2. P-gp Inhibition .....	53
2.3. MRP2 Inhibition .....	54
2.4. BCRP Inhibition.....	55
2.5. Conclusion .....	56
<b>3. SELECTION OF THE SYSTEM SUITABILITY MARKERS.....</b>	<b>57</b>
3.1. Introduction.....	57
3.2. Quality control markers .....	57
3.2.1. Trans-Epithelial Electrical Resistance (TEER) measurement.....	57
3.2.2. Markers for paracellular and transcellular permeability.....	57
3.2.2.1. Mannitol.....	58
3.2.2.2. Metoprolol.....	58
3.2.2.3. Atenolol.....	59
3.3. Markers for P-gp level expression .....	60
3.3.1. Rhodamine 123.....	60
3.3.2. Calcein Assay .....	61
3.3.3. Western blot.....	61
<b>4. CELL LINE SELECTION .....</b>	<b>63</b>
4.1. Introduction.....	63
4.2. Cell lines .....	63
4.2.1. TC7 .....	63
4.2.2. LLC-PK1:MDR1 .....	64
4.2.3. LS180.....	66
4.2.4. MDCK cell lines .....	66
4.2.4.1. Wild type MDCK cell lines .....	66
4.2.4.2. Transfected MDCK cell lines.....	66
4.2.5. MDCKII cell lines .....	68
4.2.6. Caco-2 Cell Lines .....	72
4.3. Conclusion .....	73
4.3.1. Caco-2 cells .....	73
4.3.2. MDCKII cells .....	74
<b>REFERENCES .....</b>	<b>75</b>

## LIST OF TABLES

Table 1: Solubility terminology by US Pharmacopoeia NF29 .....	9
Table 2: HPLC method for Paclitaxel.....	13
Table 3: HPLC method for Saquinavir .....	15
Table 4: HPLC method for Fexofenadine.....	17
Table 5: HPLC method for Digoxin .....	19
Table 6: HPLC method for Vinblastine .....	24
Table 7: HPLC method for Topotecan.....	25
Table 8: HPLC method for Sparfloxacin .....	26
Table 9: HPLC method for Methotrexate .....	27
Table 10: Physicochemical properties of Methotrexate.....	28
Table 11: HPLC method for Sulfasalazine .....	44
Table 12: HPLC method for Rosuvastatin.....	45
Table 13: Physicochemical properties of Rosuvastatin .....	45
Table 14 : Physico-chemical properties of several candidates .....	46
Table 15: Pharmacokinetic properties of several candidates.....	47
Table 16: Permeability studies of several candidates .....	48
Table 17: Pgp effects on several candidates .....	50
Table 18: Comments on several compound candidates.....	50
Table 19 : Other suggested compounds and comments.....	51
Table 20: MEMTRANS project selected compounds .....	52
Table 21: Effect of the different inhibitor on efflux carriers .....	53
Table 22: Physicochemical properties of Zosuquidar trihydrochloride <sup>120,121,122</sup> .....	54
Table 23: Physicochemical properties of MK571 <sup>120,121,122</sup> .....	55
Table 24: Physicochemical properties of FTC <sup>120,121,122</sup> .....	55
Table 25: Proposed inhibitors for the transporter proteins P-gp, MRP2 and BCRP .....	56
Table 26: Physicochemical characteristics of Mannitol <sup>120,121,122</sup> .....	58
Table 27: Physicochemical characteristics of Metoprolol <sup>120,121,122</sup> .....	59
Table 28: Physicochemical characteristics of Atenolol <sup>120,121,122</sup> .....	59
Table 29: Physicochemical characteristics of Rhodamine 123 <sup>120,121,122</sup> .....	61
Table 30: Properties of Caco-2 cells.....	73
Table 31: Properties of MDCKII cells.....	74

## LIST OF FIGURES

Figure 1: Chemical Structure of Celiprolol .....	10
Figure 2: Chemical Structure of Paclitaxel .....	11
Figure 3: Chemical Structure of Saquinavir .....	13
Figure 4: Chemical Structure of Fexofenadine .....	15
Figure 5: Chemical Structure of Digoxin.....	17
Figure 6: Chemical Structure of Talinolol .....	19
Figure 7: Chemical Structure of Loperamide .....	20
Figure 8: Chemical Structure of Quinidine.....	21
Figure 9: Chemical Structure of Ritonavir.....	22
Figure 10: Chemical Structure of Vinblastine .....	23
Figure 11: Chemical Structure of Topotecan.....	24
Figure 12: Chemical Structure of Sparfloxacin .....	26
Figure 13: Chemical Structure of Methotrexate .....	27
Figure 14: Chemical Structure of Verapamil.....	28
Figure 15: Chemical Structure of Cyclosporine A .....	29
Figure 17: Chemical Structure of Daunorubicin.....	30
Figure 18: Chemical Structure of Etoposide.....	31
Figure 19: Chemical Structure of Vincristine .....	32
Figure 20: Chemical Structure of Erythromycin .....	33
Figure 21: Chemical Structure of Tobramycin .....	33
Figure 22: Chemical Structure of Ivermectin .....	34
Figure 23: Chemical Structure of Doxorubicin .....	35
Figure 24: Chemical Structure of Tacrolimus .....	36
Figure 25: Chemical Structure of Nadolol.....	36
Figure 26: Chemical Structure of Labetalol.....	37
Figure 27: Chemical Structure of Docetaxel .....	38
Figure 28: Chemical Structure of Lincomycin .....	39
Figure 29: Chemical Structure of Indinavir .....	39
Figure 30: Chemical Structure of Sulpiride .....	40
Figure 31: Chemical Structure of Azithromycin .....	41
Figure 32: Chemical Structure of Salbutamol .....	41
Figure 33: Chemical Structure of Sulfasalazine .....	43
Figure 34: Chemical Structure of Rosuvastatin .....	44
Figure 35: Chemical Structure of Mannitol .....	58
Figure 36 : Chemical Structure of Metoprolol.....	58
Figure 37: Chemical Structure of Atenolol.....	59
Figure 38: Chemical Structure of Rhodamine 123 .....	60
Figure 39: Sf9 membrane vesicles (10 µg/lane) containing the transporter separated by SDS page. Western blot performed using the Pgp specific C219 antibody.....	62
Figure 40: Fluorescence buildup (calcein formation) in time in the presence different concentrations of verapamil in the calcein assay using HL60-MDR1 cells.....	62
Figure 41: Expression of the P-gp in L-MDR1, LLC-PK1, Caco-2 cells <sup>58</sup> .....	65
Figure 42: Transport of HIV protease inhibitors in L-MDR1 and LLC-PK1 cells <sup>58</sup> .....	65
Figure 43: Over expression of P-gp MRP1 and MRP2 in MDCKII cells <sup>203</sup> .....	69
Figure 44: Graphics of the transport and inhibition experiments on BCRP protein <sup>205</sup> .....	70
Figure 45: Graphics of the transport experiments with all of the proteins <sup>205</sup> .....	71

## ABBREVIATIONS

<b>ABC</b>	ATP Binding Cassette
<b>AUC</b>	Area under concentration-time curve
<b>AP</b>	Apical
<b>ATCC</b>	American Type Cell culture
<b>ATP</b>	Adenosine 5'-triphosphate
<b>b</b>	Borderline class
<b>BBB</b>	Blood Brain Barrier
<b>BL</b>	Basolateral
<b>BCRP</b>	Breast cancer resistance protein
<b>Bcrp</b>	BCRP gene
<b>BCS</b>	Biopharmaceutics classification system
<b>Caco-2</b>	Human colon carcinoma cell line
<b>Cmax</b>	Maximum concentration in plasma
<b>CsA</b>	Cyclosporine A
<b>CSF</b>	Cerebro-Spinal Fluid
<b>CYP3A4</b>	cytochrome P450, family 3, subfamily A, polypeptide 4
<b>d</b>	Day
<b>DMEM</b>	Dulbecco's Modified Eagle Medium
<b>EGF</b>	Epithelial growth factor
<b>ER</b>	Ratio of basal to apical transportation to apical to basal transportation
<b>F<sub>oral</sub></b>	Oral absolute bioavailability
<b>FDA</b>	Food and Drug Administration
<b>GI</b>	Gastrointestinal
<b>HIA</b>	Human Intestinal Absorption
<b>HPLC</b>	High-performance liquid chromatography
<b>IC50</b>	Half maximal inhibitory concentration
<b>i.v.</b>	Intravenous
<b>Kd</b>	Dissociation constant
<b>Km</b>	Michaelis-Menten Constant
<b>Ki</b>	Inhibition constant
<b>KO</b>	knock out
<b>LG</b>	Chemical substance supplier
<b>LLC-PK<sub>1</sub></b>	A clone of Caco-2 cells
<b>LLC-PK<sub>1</sub>:MDR<sub>1</sub></b>	LLC-PK1 cells expressing P-gp
<b>LLC-PK<sub>1</sub>:MRP<sub>1</sub></b>	LLC-PK11 cells expressing MRP1 protein
<b>Log D</b>	Distribution coefficient
<b>Log P</b>	Octanol-Water partition coefficient
<b>MDCK or MDCK-WT</b>	Madin-Darby canine kidney (wild type)
<b>MDCK-MDR<sub>1</sub></b>	Madin-Darby canine kidney cells expressing P-gp
<b>MDCK-MRP<sub>2</sub></b>	Madin-Darby canine kidney cells expressing MRP2 protein
<b>MDCKII or MDCKII -WT</b>	A clone of MDCK cells not expressing any proteins (wild type)
<b>MDCKII-MDR<sub>1</sub></b>	MDCKII cells expressing P-gp
<b>MDCKII-MDRP<sub>2</sub></b>	MDCKII cells expressing MRP2
<b>Mdr1</b>	Gene coding for P-gp
<b>MRP1</b>	Multi drug resistance associated protein 1
<b>MRP2</b>	Multi drug resistance associated protein 2
<b>MTX</b>	Methotrexate
<b>MW</b>	Molecular Weight
<b>Na</b>	Not applicable
<b>na</b>	Not available
<b>OATP-C</b>	Organic anion-transporting polypeptide C
<b>Papp</b>	Apparent permeability
<b>Pe</b>	Efficient permeability
<b>PEG</b>	Polyethylenglycol
<b>P-gp</b>	P-glycoprotein
<b>pKa</b>	Acid dissociation constant
<b>PK</b>	Pharmacokinetic properties
<b>R<sub>BA/AB</sub></b>	Ratio Basal- Apical /Apical-Basal

<b>SA</b>	Sigma Aldrich
<b>S<sub>w</sub></b>	Water solubility
<b>t<sub>1/2</sub></b>	Time required to reach the half of C <sub>max</sub>
<b>TC7</b>	Caco-2 clone
<b>TEER</b>	Transepithelial electrical resistance
<b>t<sub>max</sub></b>	Time required to reach C <sub>max</sub>
<b>TPGS</b>	d-alpha-tocopheryl polyethylene glycol 1000 succinate
<b>USP</b>	United States Pharmacopeia
<b>UV</b>	Ultraviolet
<b>VWR</b>	Chemical substance supplier
<b>V<sub>m</sub></b>	Maximum transport rate
<b>WT</b>	Wild type

## 1. SELECTION OF THE TEST COMPOUNDS

### 1.1. INTRODUCTION

The aim of this report is to present the scientific rationale for the determination of the test compounds to be tested in the MEMTRANS project as well as the inhibitors for the transporter proteins, system suitability markers and more adequate cell lines for the project objectives.

The selection of the substances is based on the initial list of the substances present at the MEMTRANS webpage, FDA Guidelines, further literature search on the substances that are known to have efflux mechanisms mediated by ABC transporters along with the established selection criteria.

The report describes relevant physico-chemical and pharmacokinetic data for compounds that were in initial list of the substances presented at the MEMTRANS project. Some additional possible candidate compounds for MEMTRANS are proposed. The list focused on P-gp substrates, but also contained MRP2 and BCRP substrates.

Pharmacokinetic and physicochemical data for these compounds are supplied. Pharmacokinetic data in report describes absorption, bioavailability, disposition and elimination of compounds in humans and experimental animals and the effects of Pgp on pharmacokinetic of compounds.

### 1.2. OVERVIEW

Drug substances show different permeability characteristics and grouped based on their intestinal permeability. The 3 groups based on the % of the drug absorbed are as follows:

- High permeability  $\geq 85$  %
- Intermediate permeability  $40 \leq x < 85$  %
- Low permeability  $< 40$  %

In the development of an in-vitro method for screening the drug substances in terms of permeability, model drugs should represent a range of low, moderate, and high absorption for the demonstration of suitability of the method<sup>1</sup>.

There is another classification system based on both intestinal permeability and aqueous solubility of the drug substances which are the two major factors that govern the rate and extend of drug absorption. This classification system is called Biopharmaceutics Classification System (BSC) and is follows<sup>1</sup>:

- Class I: High Solubility-High permeability
- Class II: Low Solubility-High permeability
- Class III: High Solubility-Low permeability
- Class IV: Low solubility-Low permeability.

If the highest dose of the drug is soluble in 250 mL of water it is classified as “High Soluble“. And if the absolute bioavailability or intestinal absorption of the drug is more than 90 % it is classified as High Permeable according to this classification<sup>1</sup>.

Effects of the transporters and the efflux systems are different for all of the mentioned classes above. Inhibition and induction of P-gp does not show a significant affect on permeability coefficient for the drugs in Class I since they are highly permeable and soluble. Due to the low solubility observed in Class II substances the absorption site is shifted more towards to the distal intestine where P-gp effect may be pronounced. In actual in-vivo conditions since most of the dose of less permeable drugs is absorbed from the lower intestine the effect of P-gp is pronounced for the Class III substances and thus the pharmacokinetics of these drugs are highly influenced by P-gp inhibition and/or GI transit.

(Indinavir, Emetidine and Saquinavir). Class IV drugs are more likely susceptible to P-gp efflux as the concentration of the drug in the enterocytes at any time will be less to saturate the transporter (Paclitaxel, Eletriptan, Clarithromycin). Most of the P-gp substrates fall in the permeability border line limits. Thus inhibition of P-gp has a profound effect on the over all bioavailability of these drugs. Drugs with both solubility and permeability in the borderline region will be highly attenuated by P-gp and are also influenced by gastro-intestinal transit. Border line class is defined for the drugs that have apical to basal permeability coefficient of higher than 20 and lower than 100 nm.s<sup>-1</sup> determined in-vitro cell culture conditions<sup>2</sup>.

Another solubility terminology used in the extent of this report is gathered from United States Pharmacopoeia NF29 and is as follows<sup>3</sup>:

TERM	AQUEOUS SOLUBILITY (mg/ml)
Very soluble	≥ 1000
Freely soluble	100-1000
Soluble	33-100
Sparingly soluble	10-33
Slightly soluble	1-10
Very slightly soluble	0.1-1
Practically insoluble	< 0.1

Table 1: Solubility terminology by US Pharmacopoeia NF29

### 1.3. GENERAL CRITERIA FOR THE SELECTION OF THE COMPOUNDS

Selection priorities are based on the selection criteria listed in the project proposal:

- Having a reported in-vitro efflux mechanism mediated by P-gp, MRP2, BCRP
- Having available data about human bioavailability, pharmacokinetics and non-linear absorption mechanisms.
- Available and reproducible analytical methods.
- Available physicochemical data
- Being commercially available.

The first 2 statements are for sure of vital importance since the work needs to be done on the substances with efflux mechanisms based on transporters and we are not able to produce in-vivo bioavailability data for the substances in the extent of this project.

Selectivity of the substances to their transporters are also taken into consideration which will be useful for determination of the permeability when a particular transporter is inhibited with a modifier.

P-glycoprotein is the most studied transporter among others up to date. The effects of this transporter in the efflux mechanism of the substances are extensively described. The effect of the P-gp on the substances with P-gp mediated efflux mechanism can differ due to the permeability class of the substance. Since bi-directional assays may fail to identify highly permeable compounds as P-gp substrates, the failure to identify highly permeable compounds would not be a concern because in this situation P-gp is not likely to be significant barrier for these compounds to cross the membrane<sup>4</sup>. Drugs were considered as P-gp substrate when it showed ER>1.5. ER is the ratio of the permeability of the drug substance from basal to apical chamber and apical to basal chamber. High ER values indicates that the drug substance is actively secreted by P-gp to the apical chamber thus this molecule is a substrate for P-gp. 5 P-gp substrates were selected as the test compounds to be used in the project.

There are 2 other transporter proteins that are taken into consideration, MRP2 and BCRP.

MRP2 is mostly involved in resistance mechanisms of tumor cells to the chemotherapeutics. In most occasions even the molecule is a substrate for MRP2, this protein is not involved in the gastro intestinal absorption of the molecules. Secondly, most of the studied substrates for the MRP2 transporter are not only and specifically transported with MRP2. Either P-gp or BCRP are also involved in the transportation of these molecules.

BCRP is also mostly involved in the resistance mechanisms of the tumour cells and decreases the intracellular accumulation of antineoplastic agents. But role of BCRP in limiting the absorption of the drugs was also reported in previous works.

## 1.4. COMPOUND CANDIDATES

### 1.4.1. Celiprolol

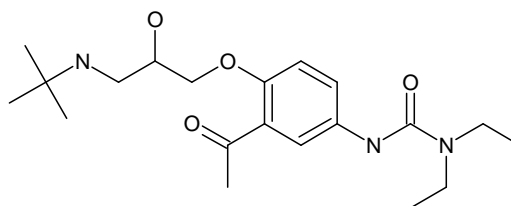


Figure 1: Chemical Structure of Celiprolol

Celiprolol is a hydrophilic  $\beta$ -adrenoreceptor blocking drug with intrinsic sympathomimetic activity and a weak vasodilating property<sup>5,6</sup>.

#### a) Reported *in vitro* efflux by P-gp, MRP2 or BCRP:

Studies performed in Caco-2 monolayers showed that Celiprolol is actively transported across the human intestinal epithelium and that the transepithelial basal-to-apical transport of celiprolol was inhibited by typical P-gp substrates (vinblastine, verapamil and nifedipine)<sup>7</sup>.

Studies in Caco-2 cells and *in situ* rat model have shown that the intestinal secretion of celiprolol is mediated by multiple transporters including P-gp<sup>8</sup>.

Studies in MDR cells that overexpress P-gp showed a reduction in drug uptake<sup>9</sup>. After *i.v.* administration of <sup>14</sup>C-celiprolol to bile duct-cannulated rats, approximately 9% of the dose was found to be associated with intestinal tissue and its contents, which is a strong evidence for carrier-mediated absorption of celiprolol<sup>8</sup>.

#### b) Effect of efflux on *in vivo* pharmacokinetic properties:

Rifampicin pre-treatment reduced plasma concentration of orally administered celiprolol ( $AUC_{0-33h}$  reduced 0.44-fold) and unaltered elimination  $t_{1/2}$ , probably by inducing P-gp expression in intestinal wall<sup>10</sup>.

P-gp inhibitor itraconazole increased the mean  $AUC_{0-33h}$  of celiprolol by 80% as a result of P-gp inhibition in the intestine<sup>11</sup>.

Orange and grapefruit juice substantially decrease the mean  $C_{max}$  and  $AUC_{0-33h}$  of concomitant administered celiprolol by about 80% and 95%, respectively probably caused by physicochemical factors<sup>11,12</sup>.

Excipients (P-gp inhibitors) changed PK profile of celiprolol in animals without effecting total  $AUC$ <sup>13</sup>.

#### c) Human bioavailability, PK and non-linear absorption mechanisms:

Human bioavailability: 30-70%<sup>14</sup>.

Celiprolol exhibits dose-dependent non-linear absorption in humans after oral dosing with bioavailabilities ranging from 30% at a 200 mg dose to 70% at a 300-400 mg dose<sup>15,16</sup>. The area under the plasma concentration-time curve (AUC) after intravenous administration is linear with dose and the terminal half-life remains unchanged with increasing dose after oral as well as after intravenous dosing<sup>5</sup>. These are not caused by altered dissolution, first pass metabolism or changes in excretion<sup>8</sup>. Thus the combined pharmacokinetic characteristics of the compound imply incomplete non-linear uptake from the gastrointestinal tract, caused by a saturable efflux mechanism in the intestinal wall<sup>16,17</sup>.

d) *Analytical methods: High Performance Liquid Chromatography Analysis:*

Matrix: blood

Sample preparation:

Dilution of stock solutions drug and internal standard (propranolol) dissolved in methanol at 1 mg/ml<sup>18,19</sup>.

Extraction using methyl-tert-butyl-ether as an organic solvent. Propranolol served as an internal standard<sup>20</sup>.

Guard column: C<sub>18</sub> column

Column: 4.6x200 mm, 5 μm

Mobile phase: 1.2% triethylamine (w/v) in acetonitrile:water (29:71, v/v), adjusted to pH 3.0 with 85% orthophosphoric acid<sup>18</sup>.

27% of acetonitrile and 73% of buffer solution (20 mM KH<sub>2</sub>PO<sub>4</sub>, pH 3.8)<sup>19</sup>.

Acetonitrile [0.1% trifluoroacetic acid (20:80, vol/vol)]<sup>20</sup>.

Detector: Spectrophotometric detection at 232-231 nm.

Limit of quantitation: 50 ng/ml<sup>18</sup> ; 2 ng/ml<sup>20</sup>.

e) *Physicochemical data:*

MW 379, logP (exp.) 1.92, logP (cal.), basic drug pKa 9.4

Soluble: Sw (exp., HCl) 138 mg/ml, Sw (cal., intrinsic) 0.13 mg/ml, Sw (cal, pH 7.4) 12.8 mg/ml (34 mM)

### 1.4.2. Paclitaxel

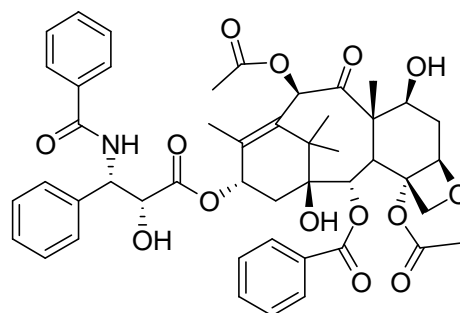


Figure 2: Chemical Structure of Paclitaxel

Paclitaxel is a taxoid antitumor agent used in treatment of breast and ovarian cancer, non-small cell lung cancer and Kaposi's sarcoma<sup>21,22,23,24</sup>.

a) *Reported in vitro efflux by P-gp, MRP2 or BCRP:*

Studies performed in Caco-2 showed highly polarized transport:

BL-to-AP flux rate of [<sup>3</sup>H]-Taxol (0.04 mM) 10–20 times faster than in the AP-to-BL direction and inhibited by 0.2 mM verapamil (P-gp inhibitor), but not by 1.0 mM probenecid (MRP inhibitor)<sup>25</sup>.

BL-to-AP flux rate of [<sup>3</sup>H]-Taxol (0.5-20 μM) 4–10 times faster than in the AP-to-BL direction and efflux inhibited by 50 μM verapamil.  $K_m$  16.5 μM,  $V_m$  1.05 nmol/h/cm<sup>2</sup>.  $P_{appAB}$  (pH 7.4, 0.5-20 μM)  $4.4 \pm 0.4 \cdot 10^{-6}$  cm/s<sup>26</sup>.

BL-to-AP flux rate of paclitaxel (5 μM) 12 fold greater than in the AP-to-BL direction. AP-to-BL flux increased twofold when 25 μM verapamil was added to the apical side. Furthermore, the addition of 25 μM verapamil analog KR-30031 to the apical side increased AP-to-BL flux twofold<sup>27</sup>.

$P_{appAB}$  (pH 7.4, 30 μM)  $2.1 \pm 0.9 \cdot 10^{-6}$  cm/s.  $K_m$  65 μM,  $V_m$  4.9 nmol/h/cm<sup>2</sup>.  $Ratio_{BA/AB}$   $4.1 \pm 0.7$ <sup>28</sup>.

Studies performed in MDCKII-MDR1 cells showed polarized transport with  $Ratio_{BA/AB} > 108$ <sup>29</sup>.

Recent studies in MDCKII cells and MDCKII-MRP2 clones showed that MRP2 transports paclitaxel and that this transport is stimulated by probenecid<sup>30</sup>.

Not substantially transported by BCRP or murine Bcrp1<sup>31</sup>.

*b) Effect of efflux on in vivo pharmacokinetic properties:*

Numerous mouse studies and clinical trials showed that coadministration of a P-gp inhibitor such as KR300031 (verapamil analog), cyclosporine A, SDZ PSC 833 (Valspodar), GF120918 (Elacridar), verapamil, and others increased oral bioavailability of paclitaxel<sup>27,32,33,34,35,36</sup>.

Using paclitaxel as model substrate, P-gp was shown to drastically limit intestinal absorption of orally administered substrates<sup>37,38</sup>.

Significant difference in plasma concentration  $C_{max}$  (2-8 fold) and  $AUC_{oral}$  (6-8 fold) in *mdr1a/b*(-/-) and wild type mice<sup>28,38</sup>.

Another group of research used *mdr1a*(-/-) mice in order to study the effect of P-gp on the pharmacokinetics of paclitaxel. The area under the plasma concentration-time curves was 2 and 6 fold higher in *mdr1a*(-/-) mice compared to wild type mice after i.v. and oral drug administration, respectively. Consequently the oral bioavailability in mice receiving 10 mg paclitaxel per kg body weight increased from 11% in control mice to 35% in *mdr1a*(-/-) mice. Thus it is concluded that P-gp limits the oral uptake of paclitaxel and mediates direct excretion of the drug from systemic circulation into intestinal lumen<sup>39</sup>.

In another study inhibition of P-gp on the oral bioavailability of paclitaxel was investigated on wild type mice. The plasma level of paclitaxel in wild type mice receiving the drug by oral route remained very low. The plasma levels hardly exceeded the 1 μM (85 ng/mL) level, which is considered of therapeutic relevance. The plasma AUC however increased significantly by 6.6 fold ( $P < 0.001$ ) when GF 120918 was given orally 10-20 minutes before the administration of paclitaxel. This result indicates that GF120918 at this dose level selectively and completely blocks P-gp in the intestines and does not notably interfere in the elimination of paclitaxel by metabolism or other transporters<sup>40</sup>.

MRP2 has a marked effect on paclitaxel plasma pharmacokinetics equal to the P-gp effect on i.v. administration but also on oral administration, especially when P-gp activity is inhibited (studies performed in *mdr1a/b*/MRP2(-/-) mice showed that the  $AUC_{oral}$  increased 2 fold compared with *mdr1a/b*(-/-) mice and 14 fold compared with WT mice<sup>38</sup>.

Effect of P-gp on the efflux of paclitaxel was studied on intestinal fragments isolated from *mdr1a*(-/-) mice. These intestinal fragments do not contain P-gp since these mice do not have the genetic information required for the expression of the P-gp. Initial studies used two compounds known to interact with P-gp, paclitaxel and digoxin, to investigate the effects of P-gp on drug permeability in different regions of the mouse intestine. An increase up to 5 fold in the absorption of paclitaxel was seen in *mdr1a*(-/-) mice compared to *mdr1a*(+/+) mice. Also the efflux activity was completely abolished in *mdr1a*(-/-) tissues in all regions<sup>41</sup>.

c) *Human bioavailability, PK and non-linear absorption mechanisms:*

Human bioavailability: Low oral bioavailability (F 4%) due to its poor solubility and its affinity for the P-gp efflux pump and presystemic extraction in the liver by cytochrome P450 in both the liver and epithelial cells of the small intestine<sup>28,42,43,44</sup>.

Non-linear pharmacokinetics explained by saturable distribution and elimination processes<sup>45,46</sup>.

Pharmacokinetics: Large volume of distribution in the body. Highly bound by the plasma proteins, primarily albumin (95–98%)<sup>47,48</sup>.

Metabolism: Liver<sup>42,43,44</sup>.

Excretion: Biliar. Less than 6–10% of the paclitaxel administered is recovered in the urine of treated patients as the unchanged drug<sup>47,49</sup>.

Total fecal excretion approximately 70% of the dose. 6-hydroxypaclitaxel is the major metabolite<sup>50</sup>.

d) *Analytical methods:*

Analytical determination of amount of paclitaxel is done with HPLC and the method is as shown below<sup>3</sup>.

Column temperature [°C]	25
Sample temperature [°C]	25
Flow [mL·min <sup>-1</sup> ]	1,5
Injection volume [µL]	10
Eluent	acetonitrile: water 9:11
Column	4,6X25 L43.
Detection	UV 227 nm

Table 2: HPLC method for Paclitaxel

e) *Physicochemical data:*

MW 854; logP (cal) 3.95, neutral drug

Poor solubility Sw (cal.) 0.012 mg/ml (14 µM).

### 1.4.3. Saquinavir

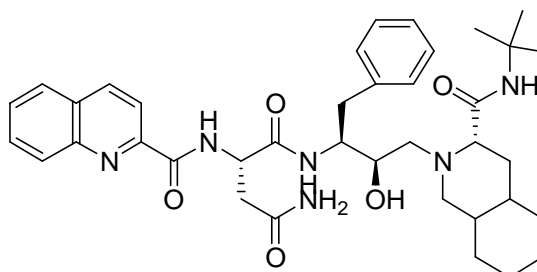


Figure 3: Chemical Structure of Saquinavir

Saquinavir is an antiviral drug. It is known that this molecule is a good substrate of P-gp<sup>51</sup>. This molecule is also used as a mesylate salt in the formulations with an induced solubility and permeability which is classified in Class I according to BCS. The molecule saquinavir that is taken into consideration for this project is classified in Class III which indicates the low permeability and high solubility of the product<sup>2,52</sup>.

a) *Reported in vitro efflux by P-gp, MRP2 or BCRP*

Studies performed in Caco-2 showed polarized apical efflux with an average 23 to 25 fold higher apparent permeability in the BL-to-AP than in the AP-to-BL direction. Secretory transport highly temperature sensitive indicating the presence of a energy dependent active transport. Cyclosporine A, verapamil and GF120918 (P-gp inhibitors) increased the net absorption by decreasing efflux and increasing influx<sup>51,53</sup>.

Although Saquinavir is mainly transported with P-gp, it is also proved that MRP2 is involved in the efflux mechanism of Saquinavir. Saquinavir efflux ratio was found to be  $6.0 \pm 0.9$  in MDCKII-MRP2 cell monolayer. The effect of concentration was also analyzed in this study. Cell lines showed decreasing basical to apical permeability and increasing apical to basical permeability with the increase in the saquinavir concentration. However the transport was not saturable in the studied concentration range up to  $47 \mu\text{M}$ . This apparent concentration dependent behaviour suggested the involvement of a carrier mediated transport process or processes. To confirm that MRP family transporters mediated the transport of saquinavir in the MDCKII-MRP2 cells inhibition studies were conducted in the presence of MK-571 a specific MRP inhibitor. The efflux ratios were found as follows. 7.2 (no MK-571), 3.9 ( $35 \mu\text{M}$  MK-571) and 1.2 ( $75 \mu\text{M}$  MK-571). Complete and concentration dependent inhibition of saquinavir transport by MK-571 indicated that an MRP family member was responsible for the saquinavir transport. Also in the same study it is showed that MRP 1 has a minor contribution to the efflux of Saquinavir<sup>54</sup>.

The specific directional efflux was measured for saquinavir using HCT-8 cell monolayers. Saquinavir and saquinavir mesylate was placed in the apical or basal side of the monolayer and drug transport was quantified over 6 hours. For saquinavir, 4.6 nmol 7% of the initial drug concentration was transported from the basolateral to the apical compartment, whereas 1.6 nmol, 3% of the initial drug, was transported in the reverse direction. The basolateral to apical  $P_e$  was  $1.83 \times 10^{-6} \text{ cm/sec}$ , whereas in the reverse direction, the  $P_e$  was  $6.24 \times 10^{-7} \text{ cm/sec}$ , with a ratio of 2.9. Addition of CsA or verapamil reduced the transepithelial flux of Saquinavir approximately 5 fold so that 1.4% of the initial drug concentration was transported into the apical compartment. These data demonstrate that saquinavir is vectorially transported across the epithelial monolayer and suggest that this flux is mediated by P-gp<sup>55</sup>.

Apical to basal and basal to apical Papp values for saquinavir were reported as 1.5 and 395 nm/s using MDRI-MDCKII monolayer bidirectional permeability assays. These results indicated the ER ratio of 261.1. In the presence of  $2 \mu\text{M}$  GF120918 this ratio is decreased to 220 which proves that saquinavir is a substrate for P-gp<sup>2</sup>. MDCKII- MDR1 cell monolayer (polarized transport, B-to-A/A-to-B ratio >100). Inhibition of efflux with GF120918<sup>56</sup>.

Permeability

Papp (caco-2, pH 7.5,  $7.5 \mu\text{M}$ ) –  $2.2 \times 10^{-6} \text{ cm/s}$ <sup>28</sup>.

b) *Effect of efflux on in vivo pharmacokinetic properties:*

Increased AUC<sub>0-24</sub> by coadministration with ritonavir<sup>57</sup>.

After oral administration of saquinavir, plasma concentrations were elevated 2-5-fold in mdr1a (-/-) mice<sup>58</sup>.

c) *Human bioavailability, PK and non-linear absorption mechanisms:*

Saquinavir's low and variable bioavailability is primarily attributed to metabolism by cytochrome P-450 3A4<sup>14,59</sup>. However, there is increasing understanding that membrane transporters contribute significantly to the biopharmaceutical characteristics of saquinavir and this entire class of drugs.

Human intestinal absorption (HIA): 30%<sup>14</sup>.

Bioavailability: Mean oral bioavailabilities ranging from 4 to 16% and highly variable, as indicated by area under the concentration time curve (AUC) coefficients of variation that are  $\geq 30\%$ <sup>14,60</sup>.

Metabolism: Very extensive metabolism and first-pass metabolism (good CYP 3A4 substrate).

Excretion: Excretion of the drug is predominantly non-renal. After i.v. administration of <sup>14</sup>C-labeled saquinavir 81% of the dose was recovered in feces<sup>14,59</sup>.

d) *Analytical methods:*

Analytical determination of amount of saquinavir is done with HPLC and the method is as shown below<sup>3</sup>.

<b>Column temperature [°C]</b>	20
<b>Sample temperature [°C]</b>	25
<b>Flow [mL·min<sup>-1</sup>]</b>	1
<b>Injection volume [μL]</b>	20
<b>Eluent</b>	Triethylamine phosphate : tetrahydrofuran: acetonitrile 14:5:1
<b>Column</b>	4.6 mm X 25 cm L1
<b>Detection</b>	UV 210 nm

Table 3: HPLC method for Saquinavir

e) *Physicochemical data:*

MW 671, logP exp. 4.7, logP cal. 3.77, weak base pKa 6.8

Sw exp. 2.2 mg/ml, Sw cal. (intrinsic) 0.17 mg/ml, Sw cal. (pH 7.4) 0.21 mg/ml (310 μM)

#### 1.4.4. Fexofenadine

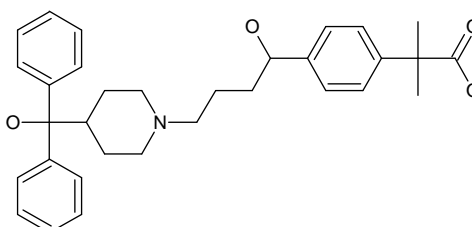


Figure 4: Chemical Structure of Fexofenadine

Fexofenadine is used as an antihistamine. It is classified in Class III according to the BCS system. In other words it has a high solubility and low permeability<sup>26</sup>. Fexofenadine hydrochloride is a racemate and exists as zwitterions in aqueous media at physiological pH. According to the common document for the Registration of Pharmaceuticals for Human Use, the recovery of total radioactivity after intravenous administration of Fexofenadine is 13 % in rats. It has been suggested that transporters play an important role in the disposition of fexofenadine. Fexofenadine has been shown to be substrate for P-gp<sup>61,62,63</sup>.

a) *Reported in vitro efflux by P-gp, MRP2 or BCRP:*

Substrate. P-gp mediated polarized transport across LLC-PK11/MDR1 cell monolayers<sup>64</sup>.

Vectorial transport of fexofenadine in the basal to apical direction was observed in Caco-2 cells and this was inhibited by inhibitors of P-gp such as verapamil and ritonavir. In a study it is demonstrated that ritonavir and verapamil reduced the p-gp mediated transport of fexofenadine by more than 80 %. Results from this in-vitro study demonstrate differential transport of fexofenadine across Caco-2 cell monolayers and inhibition of fexofenadine transport by established P-gp inhibitors<sup>62,63</sup>.

In another study it is demonstrated in humans that single dose of St John's Wort significantly ( $p < 0.05$ ) increased the maximum plasma concentration of fexofenadine by 45% and significantly ( $p < 0.05$ ) decreased the oral clearance by 20 %, with no change in half-life or renal clearance<sup>65</sup>.

Permeability

Pe cal. (pH 7.4, 500 rpm)  $> 10 \cdot 10^{-6}$  cm/s.

b) *Effect of efflux on in vivo pharmacokinetic properties:*

Effect of P-gp on PK properties of fexofenadine is unclear. In the in vivo perfusion system verapamil increased the bioavailability of fexofenadine, but intestinal permeability was unchanged. Authors suggest that the changes of bioavailability were due to decreased first-pass liver extraction. Possible mechanism – decreased sinusoidal uptake by OATP or canalicular secretion by P-gp<sup>66</sup>. Verapamil increased bioavailability in other study and inhibition of OATP have no effect<sup>67</sup>. Induction of P-gp with rifampin reduce bioavailability<sup>68</sup>

The antihistamine Fexofenadine is a sensitive probe P-gp substrate; in clinical trials, P-gp inhibitors erythromycin and ketoconazole increased fexofenadine AUC  $> 2$ -fold. Antrasentan is not a P-gp substrate, but inhibits P-gp with an  $IC_{50} \sim 12 \mu M$ <sup>69</sup>.

c) *Human bioavailability, PK and non-linear absorption mechanisms:*

Human intestinal absorption (HIA): Unknown

Predicted maximum HIA (no efflux, not solubility limited, not biased by first-pass) 100%

Bioavailability: Unknown (but probably greater than 30%)<sup>70</sup>.

Metabolism: Only about 5% of oral dose is metabolized<sup>71</sup>.

Excretion: Approximately 80% of radioactive dose is excreted in feces, however it is unclear whether it represents unabsorbed drug or it is the result of biliary secretion<sup>71</sup>.

d) *Analytical methods:*

Analytical determination of amount of fexofenadine is done with HPLC and the method is as shown below<sup>72</sup>.

<b>Column temperature [°C]</b>	35
<b>Sample temperature [°C]</b>	25
<b>Flow [mL·min<sup>-1</sup>]</b>	0,2
<b>Injection volume [µL]</b>	30
<b>Eluent</b>	10 mM ammonium acetate containing 0,1% formic acid pH 3,2
<b>Column</b>	100X2,14 µm Genesis C18
<b>Detection</b>	MS Spray interface, positive ion mode, needle voltage 5,2 kV, nebulizer gas air at 60 psi, curtain gas nitrogen at 40 psi, collision cell gas at 40 psi, turbo ionspray heater 375 C, heater gas flow 7L/ min

Table 4: HPLC method for Fexofenadine

e) *Physicochemical data:*

MW 502, logP cal. 4.35, zwitterion pKa 4.3, 8.8

Sw cal. (intrinsic) 0.012 mg/ml, Sw cal. (pH 7.5) 0.012 mg/ml (25 µM)

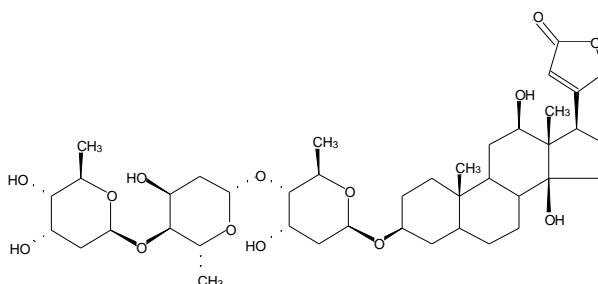
**1.4.5. Digoxin**

Figure 5: Chemical Structure of Digoxin

Digoxin, a cardiac glycoside, is the most frequently used antihypertensive agent in the treatment of congestive heart failure and atrial flutter or fibrillation<sup>73,74,75</sup>. It also had been proposed that digoxin can be used for testing a drug for the possibility that it may be an inhibitor/inducer of P-gp since it is a specific P-gp substrate<sup>4</sup>. Digoxin is classified in Class I according to the BCS classification which indicates that this molecule is highly permeable and has a high solubility.

a) *Reported in vitro efflux by P-gp, MRP2 or BCRP:*Well-known good P-gp substrates in many different in vivo and in vitro studies<sup>28, 76,77,78, 103</sup>.

The rate of bidirectional transport of digoxin in Caco-2 cells was determined for a low donor concentration of 59 nM and a high concentration of 625 nM which is the solubility limit for digoxin in the presence of 1 % DMSO. The transport rate in the absorptive direction was slower than that in the secretory direction, resulting in efflux ratios 7.7 and 1.8 for the low and high concentrations respectively<sup>79</sup>.

Polarized transport ( $R_{BA/AB} = 2.6$ , 30 µM) in Caco-2 (inhibitable with GF120918)<sup>28</sup>. $K_m$  73 µM,  $V_m = 3.4$  nmol/h/cm<sup>2(28)</sup>.

## Permeability

Papp,Caco-2 (pH 7.5, 30  $\mu$ M) –  $1.1 \cdot 10^{-6}$  cm/s,  $1.1 \cdot 10^{-6}$  cm/s (pH 7.4, 500 rpm)<sup>80</sup>.

*b) Effect of efflux on in vivo pharmacokinetic properties:*

Significant difference in plasma concentration (2 fold) and AUC (2.4) in *mdr1a/b(-/-)* and wild type mice<sup>28</sup>. P-gp efflux in the study of permeability in in situ intestinal perfusion with *mdr1a/b(-/-)* and control mice<sup>76</sup>. The effects of the inhibition of the P-gp on the Digoxin absorption were studied in rat. It was shown that inhibition of the P-gp with ketoconazole reduced the mean absorption time from the intestines from 1.1 to 0.3 h which is due to inhibition of P-gp efflux<sup>74</sup>.

Elevated digoxin plasma concentrations had been observed not only after administration of quinidine in humans but also during concomitant therapy with multiple other drugs, including clarithromycin, ritonavir, quinidine, amiodarone, itraconazole, verapamil, cyclosporine, propafenone, nifedipine, nifedipine, amiodarone and spironolactone. Many of these agents are now recognised as P-gp inhibitors<sup>81,82</sup>.

Substances as quinidine, clarithromycin and propafenone reduce the renal secretion of digoxin by blocking P-gp activity in the renal tubule. In addition, quinidine interacts with digoxin absorption in the small intestine of rats. It is also shown that inhibition of the P-gp activity by quercetin when given together with digoxin to pigs dramatically increased the plasma concentration of the pigs which resulted in the death of 2 out of the tested 3 pigs<sup>83</sup>.

Digoxin concentration and oral bioavailability increased (1.7 fold-increase of AUC<sub>0-24h</sub>) during concomitant administration of clarithromycin and this effect is dose-dependent on clarithromycin, probably due to inhibition of intestinal and renal P-glycoprotein<sup>84,85</sup>.

Multiple-dose treatment with St. John's wort extract resulted in a significant decrease of digoxin AUC (0-24) and C<sub>max</sub> values compared with placebo probably due to an activation of the efflux function in the intestinal wall<sup>86</sup>.

Mean steady-state digoxin concentrations following administration of digoxin with 80 mg atorvastatin were slightly higher compared with digoxin alone and result in an increase of C<sub>max</sub> and AUC(0-24) of 20 and 15%, respectively<sup>87</sup>. Atorvastatin (100 $\mu$ M) inhibited digoxin secretion by 58% equivalent to the extent of inhibition observed with verapamil<sup>87</sup>.

In another publication Ritonavir significantly ( $p < 0.01$ ) increased digoxin area under the plasma concentration-time curve from time 0 to infinity by 86% and its volume of distribution by 77% and decreased nonrenal and renal digoxin clearance by 48% and 35%, respectively. Digoxin terminal half-life in plasma increased by 156% ( $p < 0.01$ ) in healthy volunteers, this is also due to the inhibition of the P-gp activity by ritonavir<sup>88</sup>.

Oral coadministration of 100 mg talinolol increased the area under the concentration-time curve (AUC) from 0 to 6 hours and the AUC from 0 to 72 hours of digoxin significantly by 18% and 23%, respectively ( $5.85 \pm 1.49$  versus  $7.22 \pm 1.29$  ng . h/mL and  $23.0 \pm 3.3$  versus  $27.1 \pm 3.7$  ng. h/mL, for both  $p < 0.05$ ) and the maximum serum levels by 45% which is clearly due to the competition in binding to the P-gp between talinolol and digoxin<sup>89</sup>.

*c) Human bioavailability, PK and non-linear absorption mechanisms:*

Human intestinal absorption (HIA)

Incomplete 60-90%, formulation-dependent absorption (probably solubility limited)

Predicted maximum HIA (no efflux, not solubility limited, not biased by first-pass) 95%

Bioavailability: 75 (60-90)%<sup>90,91,92</sup>.

Metabolism: Only 16% of oral drug is metabolized. Cytochromes P450 does not involved in metabolism.

Excretion: Mainly eliminated by the kidneys.

d) *Analytical methods:*

Analytical determination of amount of digoxin is done with HPLC and the method is as follows according to USP<sup>72</sup>.

<b>Column temperature [°C]</b>	25
<b>Sample temperature [°C]</b>	25
<b>Flow [mL·min<sup>-1</sup>]</b>	1
<b>Injection volume [μL]</b>	50
<b>Eluent</b>	water: acetonitrile 55:45
<b>Column</b>	3,9 mmX30 cm that contains packing L1
<b>Detection</b>	UV 218 nm

Table 5: HPLC method for Digoxin

e) *Physicochemical data:*

MW 781, logP (exp) 1.26, (cal.) 1.38, neutral compound

Poor solubility: Sw (exp.) 0.05 mg/ml (69 μM)

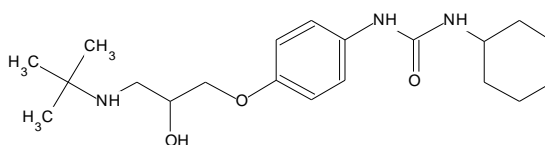
**1.4.6. Talinolol**

Figure 6: Chemical Structure of Talinolol

Talinolol is a cardiovascular agent. It is known that P-gp affects the in-vivo absorption of talinolol from the intestines.

a) *Reported in vitro efflux by P-gp, MRP2 or BCRP:*

Polarized ( $R_{BA/AB}$  7, 40 μM), saturable, verapamil-inhibited (GF120918 inh.) transport across caco-2 cell monolayers<sup>28,93</sup>.

$K_m$  100 μM,  $V_m$  5.5 nmol/h/cm<sup>2(28)</sup>.

Permeability

$P_{app,caco-2}$  (pH 7.5, 40 μM) –  $1.5 \cdot 10^{-6}$  cm/s<sup>(28)</sup>.

b) *Effect of efflux on in vivo pharmacokinetic properties:*

Intravenously administered talinolol is actively secreted into the human small intestine. This secretion is reduced by the intraluminal supply of verapamil<sup>94</sup>.

Verapamil-inhibited intestinal secretion was observed in rats (in situ intestinal perfusion)<sup>93</sup>.

Significant difference in plasma concentration (2.9 fold) in *mdr1a/b(-/-)* and wild type mice<sup>(28)</sup>.

Oral coadministration of 100 mg talinolol increased the area under the concentration-time curve (AUC) from 0 to 6 hours and the AUC from 0 to 72 hours of digoxin significantly by 18% and 23%, respectively ( $5.85 \pm 1.49$  versus  $7.22 \pm 1.29$  ng . h/mL and  $23.0 \pm 3.3$  versus  $27.1 \pm 3.7$  ng . h/mL, for both  $p < 0.05$ ) and the maximum serum levels by 45 % which is clearly due to the competition in binding to the P-gp between talinolol and digoxin<sup>89</sup>.

Rifampin is a inducer for P-gp expression. Effects of rifampin on talinolol were studied on 8 healthy volunteers. During rifampin treatment the areas under the curve of i.v. and oral talinolol were significantly lower ( 21 % and 35 %  $p < 0.05$ ). Thus it is concluded that rifampin induces P-gp mediated excretion of talinolol in the gut wall<sup>95</sup>.

TPGS is used as a surfactant in oral tablet formulations. This surfactant is known to inhibit P-gp. So the effects of TPGS were investigated on talinolol. It was found that TPGS inhibited the P-gp mediated talinolol transport in Caco-2 cells. In healthy volunteers TPGS increased the area under the plasma concentration-time curve with extrapolation to infinity of talinolol by 39% (90 % confidence interval, 1.10-1.75) and the maximum plasma concentration by 100 % (90 % confidence interval 1.39-2.88)<sup>96</sup>.

c) *Human bioavailability, PK and non-linear absorption mechanisms:*

Human intestinal absorption (HIA): Predicted maximum HIA (no efflux, not solubility limited, not biased by first-pass) 100%

Bioavailability: HIA 55% (40-60)<sup>97</sup>.

Metabolism: Not significant metabolism.

d) *Physicochemical data:*

MW 363, logP (cal.) 3.32, base pKa 9.4

Soluble: Sw (cal. intrinsic) 0.163 mg/ml, Sw (cal, pH 7.4) 17 mg/ml (45 mM)

### 1.4.7. Loperamide

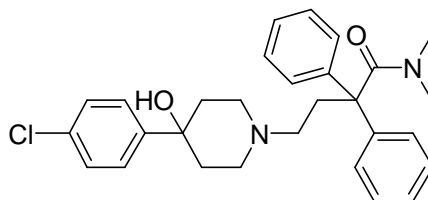


Figure 7: Chemical Structure of Loperamide

a) *Reported in vitro efflux by P-gp, MRP2 or BCRP:*

Good P-gp substrate in BBB<sup>98</sup> and transport across cell monolayers studies<sup>29</sup>. Polarized transport across MDCKII-MDR1 cell monolayers (ratio 8). Efflux is inhibited by GF120918<sup>29</sup>. Loperamide, an opioid with minimal CNS levels in genetically intact mice, becomes a psychotropic in knock-out (mdr) mice, with brain levels of drug 13.5 higher in knock-out-mice<sup>99,100</sup>.

Permeability

Pe, cal (Caco-2, 500 rpm)  $> 10 \cdot 10^{-6}$  cm/s

b) *Effect of efflux on in vivo pharmacokinetic properties:*

Significant increase (3 fold) of intestinal permeability in in situ perfusion system in mdr1a/1b(-/-) mice<sup>76</sup>.

c) *Human bioavailability, PK and non-linear absorption mechanisms:*

Human intestinal absorption (HIA): Unknown

Predicted maximum HIA (no efflux, not solubility limited, not biased by first-pass) 100%

Bioavailability: 40%<sup>14, 59</sup>.

Metabolism: Extensive<sup>59</sup>.

Excretion: Biliary/renal<sup>71</sup>.

d) *Physicochemical data:*

MW 477, logP cal. 3.86, base pKa 8.5

Sw exp. 0.02 mg/ml, Sw cal. (intrinsic) 0.07 mg/ml, Sw cal. (pH 7.5) 0.9 mg/ml (1.9 mM)

### 1.4.8. Quinidine

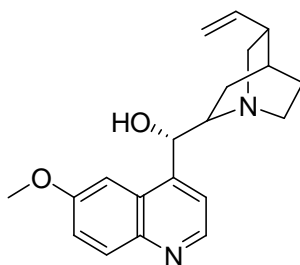


Figure 8: Chemical Structure of Quinidine

a) *Reported in vitro efflux by P-gp, MRP2 or BCRP:*

Very good P-gp substrate in many different studies. MDCKII-MDR1 (polarized transport, inhibition with GF120918)<sup>29</sup>. mdr1a(-/-) mice (increased distribution to brain)<sup>98, 101</sup> and many others. Brain/Plasma distribution ratio = 36, CSF/Plasma distribution ratio = 10 (AUC 0-5, 10 mg/kg, HPLC)<sup>98</sup>.

Permeability

Pe (pH 7.4, 1  $\mu$ M GF129018)  $>10 \times 10^{-6}$  cm/s [9], Pe app (caco-2)  $20 \times 10^{-6}$  cm/s<sup>102</sup>.

Pe cal. (pH 7.4, 500 rpm)  $>10 \times 10^{-6}$  cm/s

b) *Effect of efflux on in vivo pharmacokinetic properties:*

Probably P-gp effects permeability of quinidine across BBB, but have no or small effect on other PK properties of drug.

But: P-gp efflux was observed in the study of permeability in in situ intestinal perfusion with mdr1a/b(-/-) and control mice<sup>76</sup>.

c) *Human bioavailability, PK and non-linear absorption mechanisms:*

Human intestinal absorption (HIA): Absorption  $>80\%$ <sup>14, 90</sup>.

Predicted maximum HIA (no efflux, not solubility limited, not biased by first-pass) 100%

Bioavailability: 85 (56-95) %<sup>14, 92</sup>.

d) *Physicochemical data:*

MW 324, logP exp. 2.64, logP cal. 2.29., base pKa 8.6

Soluble: Sw exp. 0.14 mg/ml, Sw (cal. intrinsic) 0.62 mg/ml, Sw (cal. pH 7.4) 10 mg/ml (30 mM)

### 1.4.9. Ritonavir

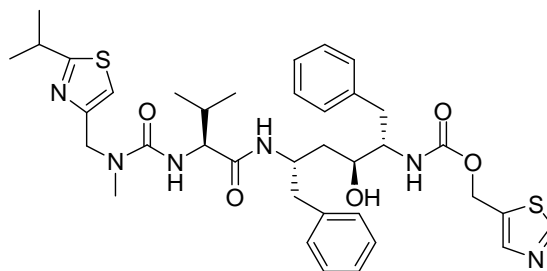


Figure 9: Chemical Structure of Ritonavir

a) *Reported in vitro* efflux by P-gp, MRP2 or BCRP:

Studies performed in MDCKII-MDR1 cells showed polarized transport with  $\text{Ratio}_{\text{BA/AB}} > 165^{29}$ .

Studies performed in LLC-PK11, parental, and transfectants L-MDR1 and L-mdr1a cells showed polarized transport inhibited by cyclosporine A<sup>103</sup>.

Studies performed in Caco-2 showed polarized apical efflux with an average 2.1 to 15 fold higher apparent permeability in the BL-to-AP than in the AP-to-BL direction. Secretory transport highly temperature dependent. Cyclosporine A, verapamil and GF120918 (P-gp inhibitors) increased the net absorption by decreasing efflux and increasing influx<sup>51,53</sup>.

Permeability

Pe cal. (pH 7.4, 500 rpm)  $> 10 \cdot 10^{-6}$  cm/s

b) *Effect of efflux on in vivo* pharmacokinetic properties:

Ritonavir increased the AUC of saquinavir more than 20 fold attributed to inhibition of the metabolism and, at least partially, to competition for efflux mechanism during drug absorption and/or elimination<sup>51</sup>.

P-gp efflux was observed in the permeability study in in situ intestinal perfusion with mdr1a/b(-/-) and control mice<sup>76</sup>.

c) *Human bioavailability, PK and non-linear absorption mechanisms:*

Human bioavailability: 70 (60-80)%<sup>59</sup>.

Metabolism: Extensive (CYP 3A4, CYP 2D6)<sup>71</sup>

Excretion: Elimination: fecal 86% (34% unchanged), renal 11% (4% unchanged)<sup>71</sup>.

d) *Analytical methods:*

High Performance Liquid Chromatography Analysis:<sup>3,72</sup>

Matrix: blood

Sample preparation: Evaporation-reconstitution

Guard column: C<sub>18</sub>

Column: 4.6x250 mm, 5 μm

Mobile phase: MeCN:40 mM disodium hydrogen phosphate containing 4% octanesulfonic acid 50:50<sup>72</sup>.

75:25 acetonitrile and H<sub>2</sub>O mixture containing 0.01% trifluoroacetic acid

Detector: UV 220

Limit of quantitation: 50 ng/mL

e) *Physicochemical data*

MW 720, logP cal. 5.64, neutral (very weak base pKa 4.1)

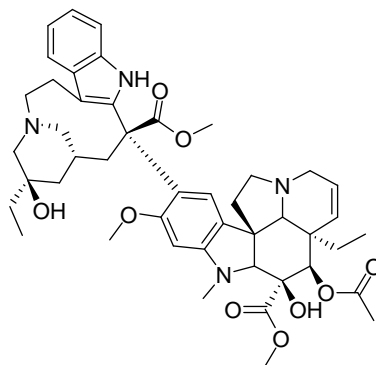
Sw cal. (intrinsic) 0.017 mg/ml, Sw (pH 7.4) 0.017 mg/ml (230  $\mu$ M)**1.4.10. Vinblastine**

Figure 10: Chemical Structure of Vinblastine

Vinblastine is a vinca alkaloid antineoplastic agent. The vinca alkaloids are structurally similar compounds comprised of 2 multiringed units, vindoline and catharanthine. Vinblastine is known as a substrate for P-gp, MRP1 and MRP2 and frequently used in the studies related to MRP2 activity.

a) *Reported in vitro efflux by P-gp, MRP2 or BCRP:*

Cytotoxicity and accumulation of drug is significantly lower in P-gp overexpressing cells<sup>103,104</sup>. Polarized transport across P-gp-overexpressing cell monolayers (ratio >10)<sup>29,103</sup>. P-gp-effect = 2.7 (in situ brain perfusion model, mdr1a(-/-) and wild-type mice)<sup>105</sup>. MRP substrate<sup>106</sup>.

Permeability

Pe cal. (pH 7.4, 500 rpm) >10\*10<sup>-6</sup> cm/sb) *Effect of efflux on in vivo pharmacokinetic properties:*

Only borderline effect of P-gp - in situ intestinal perfusion experiments with mdr1a/b(-/-) mice<sup>76</sup>. Cyclosporine increase intestinal absorption in rats<sup>107</sup>.

Vinblastine was found to be secreted by both MDCKII wild type and MDCKII-cMOAT cells. Permeability of MRP2 transfected cells (MDCKII-cMOAT) to vinblastine was greater than in the wild type cells. The magnitude of this increase varied slightly between the A to B (5 fold increase) and B to A (3 fold increase) directions. This secretion was greatly inhibited by cyclosporine A in the MDCKII cells. In contrast sulfinpyrazone treatment decreased secretion (shown only by an increase in A to B permeation) in this cell line as well as in the wild type<sup>108</sup>.

The broadly similar efflux kinetics was observed in means of P-gp mediated transport both for vinblastine and digoxin in Caco-2 cells and rat ileum. Efflux values at 100  $\mu$ M vinblastine in colon (0.9 $\pm$ 0.2 nmol.h<sup>-1</sup>.cm<sup>-2</sup>) were approximately 3 fold lower than those observed in ileum, suggesting that the difference is due to the unequal P-gp content in the different parts of the intestine. 25 % efflux of vinblastine was inhibited using MRP specific inhibitors probenecid and MK571 in Caco-2 cells<sup>109</sup>.

c) *Human bioavailability, PK and non-linear absorption mechanisms:*

Human intestinal absorption (HIA): Unknown

Predicted maximum HIA (no efflux, not solubility limited, not biased by first-pass) 100%

Bioavailability: Bioavailability unknown but suspected to be very low. Dug used only intravenously<sup>71</sup>.

Metabolism: Extensive (CYP 3A4)

d) *Analytical methods:*

Analytical determination of amount of digoxin is done with HPLC and the method is as follows according to USP<sup>72</sup>.

<b>Column temperature [°C]</b>	25
<b>Sample temperature [°C]</b>	25
<b>Flow [mL·min<sup>-1</sup>]</b>	1
<b>Injection volume [μL]</b>	10
<b>Eluent</b>	Buffer: Acetonitrile:2-aminoheptan (70:30:0,5) Buffer: 8,82 g Sodium acetate+ 33 mL glacial acetic acid /1 L
<b>Column</b>	4.6 mm X 15 cm column L1
<b>Detection</b>	UV 278 nm

Table 6: HPLC method for Vinblastine

e) *Physicochemical data:*

MW 811, logP exp. 3.83, logP cal. 5.42, base pKa 7.4.

Solubility: Sw exp. (H<sub>2</sub>SO<sub>4</sub>) 89 mg/ml, Sw cal. (intrinsic) 0.19 mg/ml, Sw cal. (pH 7.4) 0.39 mg/ml (470 μM)

### 1.4.11. Topotecan

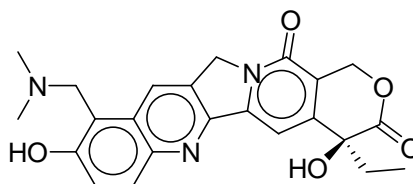


Figure 11: Chemical Structure of Topotecan

Topotecan is an anti-neoplastic drug. It is normally administrated by intravenous route since oral administration of topotecan is accompanied by a substantially increased interpatient variability in systemic exposure. Topotecan is a BCRP substrate with a very low affinity to P-gp. BCRP is the most plausible explanation for the limited absorption of orally administered topotecan<sup>110,111</sup>.

a) *Reported in vitro efflux by P-gp, MRP2 or BCRP:*

Polarized transport across caco-2 ( $R_{BA/AB}$  = 3.5, 40 uM). Km 170 μM, Vm – 7.2 nmol/h/cm<sup>2(28)</sup>.

**Permeability**

Papp,caco-2 (7.5, 40 μM) -  $1 \cdot 10^{-6}$  cm/s<sup>(28)</sup>.

Pe cal. (pH 7.4, 500 rpm)  $2.5 \cdot 10^{-6}$  cm/s (lactone)

b) *Effect of efflux on in vivo pharmacokinetic properties:*

Difference in plasma concentration (2.3 fold) and AUC (2 fold) in *mdr1a/b(-/-)* and wild type mice<sup>(28)</sup>.

Preclinical studies on knock out mice not expressing the P-gp and wild type mice which were treated with oral topotecan in combination with a single dose of GF120918, have shown that the systemic exposure of oral topotecan increased almost 10 fold due to the BCRP inhibition in the intestines and does not have an effect on the renal clearance<sup>112</sup>.

In a study on 16 patients oral GF120918 is given together with topotecan. As a result of BCRP inhibition in the intestines oral bioavailability of the molecule was increased from 40 % to 97.1%. Also the results of the patients treated with intravenous topotecan with or without GF120918 show that GF120918 had a small but significant effect of approximately 10% on AUC and systemic clearance of total topotecan, but no effect on  $t_{1/2}$  and  $C_{max}$  of oral topotecan<sup>110</sup>.

To confirm that the bioavailability of topotecan in rats is also limited by the expression of BCRP, a study was conducted to evaluate the effects of GF120918 on topotecan pharmacokinetics in SD rats. Coadministration of 50 mg/kg GF120918 significantly increased the  $AUC_{0-720}$  (the AUC from time 0 to 720 min, which is the last time point for blood sampling) [from  $1.74 \pm 0.86$  ( $\times 10^4$ ) to  $7.65 \pm 3.78$  ( $\times 10^4$ ) ng/mL.min,  $p < 0.01$ ], the  $AUC_{0-\infty}$  [from  $1.80 \pm 0.89$  ( $\times 10^4$ ) to  $7.91 \pm 3.56$  ( $\times 10^4$ ) ng/mL.min,  $p < 0.01$ ], and the bioavailability (from  $29.7 \pm 14.8\%$  to  $130 \pm 58.8\%$ ,  $p < 0.01$ ) by more than 4-fold. The mean  $C_{max}$  was also increased 3-fold (from  $86.4 \pm 42.9$  to  $257 \pm 154$  ng/ml,  $p < 0.05$ ) The  $t_{max}$  and terminal  $t_{1/2}$  were not significantly changed by GF120918. These results indicate that the bioavailability of topotecan in rats is indeed limited by the expression of BCRP and, therefore, inhibition of BCRP should increase the bioavailability of topotecan in these animals<sup>113</sup>.

c) *Human bioavailability, PK and non-linear absorption mechanisms:*

Human intestinal absorption (HIA): Predicted maximum HIA (no efflux, not solubility limited, not biased by first-pass) 78%.

Bioavailability: 30 (21-45)%<sup>34,114</sup>.

d) *Analytical methods:*

Analytical determination of amount of topotecan is done with HPLC and the method is as shown below<sup>113</sup>.

<b>Column temperature [°C]</b>	25
<b>Sample temperature [°C]</b>	25
<b>Flow [mL·min<sup>-1</sup>]</b>	1
<b>Injection volume [µL]</b>	50
<b>Eluent</b>	10 mM phosphate buffer pH 3.74, 25 % methanol, 2 % trimethylamine
<b>Column</b>	Partisphere C18 125X4.6 mm
<b>Detection</b>	Fluorimetrically excitation wavelength 361 nm emission wavelength 527 nm

Table 7: HPLC method for Topotecan

e) *Physicochemical data:*

MW 421, logP 0.29, amphiprotic (base pKa 8.6)

Sw cal. (intrinsic) 0.25 mg/ml, Sw cal. (pH 7.4) 0.9 mg/ml (2mM).

### 1.4.12. Sparfloxacin

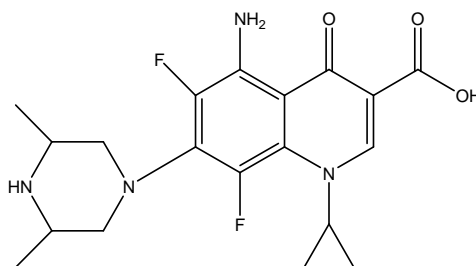


Figure 12: Chemical Structure of Sparfloxacin

Sparfloxacin is an anti-infective agent. Fluoroquinolones are only slightly metabolized in the organism, and external routes have been considered important for their elimination. In this regard the fraction of fluoroquinolones eliminated in the intestine following oral administration was estimated between 10 and 25% of the dose ingested in humans, rats and rabbits and this elimination is due to the affinity of this molecule to P-gp.

*a) Effect of efflux on in vivo pharmacokinetic properties:*

Sparfloxacin accumulation in the cells was studied in the presence of P-gp inhibitors verapamil and progesterone. Addition of 100 $\mu$ L verapamil or progesterone during 1 hour incubation significantly increased the level of accumulation of sparfloxacin in differentiated Caco-2 cells by 30 and 60 % respectively. These two inhibitors also induced four and 6 fold increases in the level of accumulation of vinblastine respectively suggesting that similar mechanisms are involved in the efflux of these drugs. In order to determine the involvement of P-gp the effect of P-gp inhibitors was also tested with undifferentiated Caco-2 cells. Neither 100  $\mu$ L progesterone nor verapamil effected the accumulation of sparfloxacin in the cells. Taken together these results support the existence of common pathways of sparfloxacin and vinblastine secretion and that these pathways involve P-gp<sup>115</sup>.

*b) Analytical methods:*

Analytical determination of amount of sparfloxacin is done with HPLC and the method is as shown below<sup>116</sup>.

<b>Column temperature [°C]</b>	25
<b>Sample temperature [°C]</b>	25
<b>Flow [mL·min<sup>-1</sup>]</b>	1
<b>Injection volume [<math>\mu</math>L]</b>	20
<b>Eluent</b>	acetonitrile–0.035 M perchloric acid 28:72, v/v, adjusted to pH 2.0 with 0.015 M triethylamine
<b>Column</b>	Luna C18 5- $\mu$ m.
<b>Detection</b>	UV 300 nm

Table 8: HPLC method for Sparfloxacin

### 1.4.13. Methotrexate

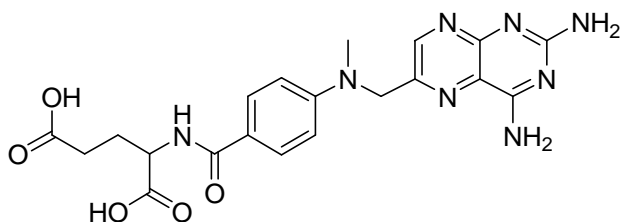


Figure 13: Chemical Structure of Methotrexate

Methotrexate is an antineoplastic anti-metabolite. Anti-metabolites masquerade as purine or pyrimidine - which become the building blocks of DNA. They prevent these substances becoming incorporated into DNA during the "S" phase (of the cell cycle), stopping normal development and division. MRP2 plays an important role in the resistance mechanism, clearance and absorption of methotrexate.

*a) Reported in vitro efflux by P-gp, MRP2 or BCRP:*

Functional characterization of various MRP homologues revealed some common features with those of methotrexate (MTX) efflux systems. The intracellular accumulation of MTX was measured in the presence and absence of 0.5 mM probenecid which is a known MRP inhibitor. Co-incubations with probenecid increased the intracellular concentration of MTX 2 fold in MRP1, MRP2, MRP3, MRP4, MRP5, MRP6, MRP7, MRP8, MRP9, MRP10, MRP11, MRP12, MRP13, MRP14, MRP15, MRP16, MRP17, MRP18, MRP19, MRP20, MRP21, MRP22, MRP23, MRP24, MRP25, MRP26, MRP27, MRP28, MRP29, MRP30, MRP31, MRP32, MRP33, MRP34, MRP35, MRP36, MRP37, MRP38, MRP39, MRP40, MRP41, MRP42, MRP43, MRP44, MRP45, MRP46, MRP47, MRP48, MRP49, MRP50, MRP51, MRP52, MRP53, MRP54, MRP55, MRP56, MRP57, MRP58, MRP59, MRP60, MRP61, MRP62, MRP63, MRP64, MRP65, MRP66, MRP67, MRP68, MRP69, MRP70, MRP71, MRP72, MRP73, MRP74, MRP75, MRP76, MRP77, MRP78, MRP79, MRP80, MRP81, MRP82, MRP83, MRP84, MRP85, MRP86, MRP87, MRP88, MRP89, MRP90, MRP91, MRP92, MRP93, MRP94, MRP95, MRP96, MRP97, MRP98, MRP99, MRP100 which are human ovarian carcinoma cell lines<sup>117</sup>.

MTX has been shown to be a substrate of MRP2 using EHBR rats that does not encode MRP2 protein. C<sub>max</sub> values both systemic and portal were 2 fold higher than (p>0,05) in EHBR than control rats<sup>118</sup>.

It is clearly shown in another publication that MTX is a substrate for MRP2. In this study membranes isolated from sf9 cells either encoding MRP1 or MRP2 were used<sup>119</sup>.

*b) Analytical methods:*

Analytical determination of amount of vinblastine is done with HPLC and the method is as shown below<sup>3</sup>.

Column temperature [°C]	25
Sample temperature [°C]	25
Flow [mL·min <sup>-1</sup> ]	1
Injection volume [µL]	10
Eluent	Phosphate buffer:acetonitrile 50:50
Column	4.6 mm X 15 cm column L1
Detection	UV 305 nm

Table 9: HPLC method for Methotrexate

*c) Physicochemical data:*

The following table shows the physicochemical properties of Methotrexate<sup>120,121,122</sup>.

<b>Category</b>	Antineoplastic agent
<b>Formula</b>	$C_{20}H_{22}N_8O_5$
<b>Molecular weight</b>	454.44
<b>Solubility</b>	Practically insoluble
<b>Availability</b>	SA
<b>Log P</b>	0.94
<b>Log D</b>	na
<b>pKa</b>	4.7
<b>In-vivo absorption (permeability %)</b>	60 %
<b>Protein binding</b>	50%
<b>Minimum dose /maximum dose (mg)</b>	2.5/2.5
<b>BCS Classification</b>	Class III

Table 10: Physicochemical properties of Methotrexate

#### 1.4.14. Verapamil

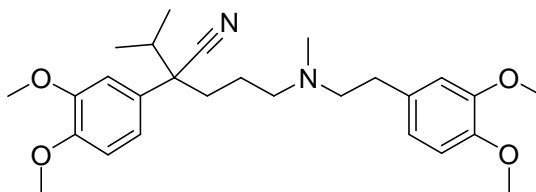


Figure 14: Chemical Structure of Verapamil

a) *Reported in vitro* efflux by P-gp, MRP2 or BCRP:

Highly permeable P-gp substrate. Verapamil is effluxed by P-gp at BBB<sup>98,123</sup> but usually there is no net secretion in cell monolayers, at least at high concentrations > 10  $\mu$ M (but transport across MDCKII-MDR1 cells is polarized at low concentrations < 2  $\mu$ M)<sup>29,56</sup>.

Caco-2 cells – no net secretion at 20  $\mu$ M<sup>28</sup>.

Permeability

$P_{app}$  (caco-2, pH 7.5, 30  $\mu$ M) –  $14.7 \cdot 10^{-6}$  cm/s<sup>28</sup>.

b) *Effect of efflux on in vivo pharmacokinetic properties:*

P-gp has no effect on PK properties of verapamil.

Plasma concentration is the same in mdr1a(-/-) mice and wild type mice<sup>28</sup>.

But, significant increase (3 fold) of intestinal permeability in in situ perfusion system in mdr1a/1b(-/-) mice<sup>76</sup>. But, P-gp effect = 6.6 (in situ brain perfusion model, mdr1a(-/-) and P-gp competent mice<sup>101</sup>).

c) *Human bioavailability, PK and non-linear absorption mechanisms:*

Human intestinal absorption (HIA): Complete absorption<sup>90,92</sup>.

Bioavailability: 22 (14-30) %, low bioavailability due to extensive first-pass metabolism<sup>14, 92</sup>.

Metabolism: Extensive (CYP 3A4, 2C8).

d) *Physicochemical data:*

MW 454, logP exp. 3.83, cal. 4.86, base pKa 9.1

Moderately soluble – Sw (exp.) 77 mg/ml (\*HCl), Sw (cal. intrinsic) 0.009 mg/ml, Sw (pH 7.4) 0.4 mg/ml (900  $\mu$ M).

### 1.4.15. Cyclosporine A

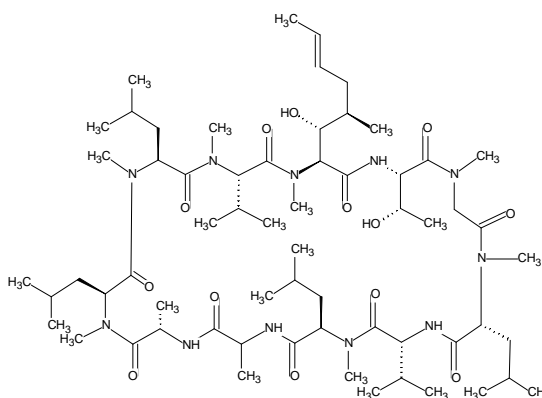


Figure 15: Chemical Structure of Cyclosporine A

a) *Reported in vitro efflux by P-gp, MRP2 or BCRP:*

Good P-gp substrate in many different studies (polarized transport across MDR1 transfected cell monolayers, increased brain distribution in P-gp deficient mice and others)<sup>29,77,78, 76,124</sup>.

Generally used as a multiple inhibitor for the P-gp, MRP1, MRP2, OATP-C (recently published FDA draft Guideline on Drug interaction studies)<sup>4</sup>.

K<sub>m</sub> 8 μM, V<sub>m</sub> 2.4 nmol/mg protein/h (LLC-GA5-COL300)<sup>102</sup>.

Permeability

Pe app (Caco-2) 1.05

Pe cal. (Caco-2, 7.4, 500 rpm) 4,6\*10<sup>-6</sup> cm/s

b) *Effect of efflux on in vivo pharmacokinetic properties:*

Effect of P-gp on PK properties of CsA is unclear.

Amlodipine (CYP3A4 and P-gp inhibitor) increased CsA (oral) AUC<sup>125</sup>.

P-gp efflux in the study of permeability in in situ intestinal perfusion with *mdr1a/b(-/-)* and control mice<sup>76</sup>.

c) *Human bioavailability, PK and non-linear absorption mechanisms:*

Human intestinal absorption (HIA): Complete absorption 100%<sup>126</sup>.

Bioavailability: Variable bioavailability 30 (10-60)% probably due to concentration of CYP 3A4 and P-gp<sup>90,92,127</sup>.

Metabolism: Extensive (CYP 3A4)

d) *Physicochemical data:*

MW 1202, logP cal. 1.02, neutral drug

Solubility: 0.591 mg/ml (490 μM)

### 1.4.16. Rifampin

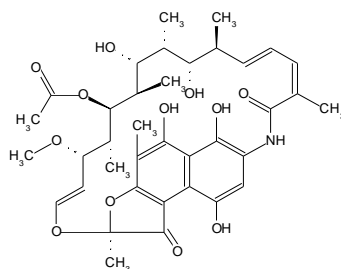


Figure 16: Chemical Structure of Rifampin

a) *Reported in vitro efflux by P-gp, MRP2 or BCRP:*

Polarized transport across Caco-2 cell monolayers ( $R_{BA/AB} = 4.2$ ,  $20 \mu\text{M}$ ). GF120918 inhibited efflux.  $K_m$   $55 \mu\text{M}$ ,  $V_m$   $4.3 \text{ nmol/h/cm}^2$ <sup>(28)</sup>.

P-gp inducer (Rifampin treatment increased intestinal P-gp content)<sup>128</sup>.

Permeability

$P_{app}$  (caco-2, pH 7.5,  $20 \mu\text{M}$ ) –  $2 \times 10^{-6} \text{ cm/s}$ <sup>28</sup>.

b) *Effect of efflux on in vivo pharmacokinetic properties:*

Difference in plasma concentration (3.5 fold) and AUC (6.4 fold) in *mdr1a/b*(-/-) and wild type mice<sup>28</sup>. Oral treatment with increasing doses of rifampicin resulted in elevated drug levels in the livers of *mdr1a* (-/-) mice compared with *mdr1a* (+/+) mice at all doses<sup>129</sup>.

c) *Human bioavailability, PK and non-linear absorption mechanisms:*

Human intestinal absorption (HIA): Well absorbed  $>80\%$ <sup>14</sup>.

Predicted maximum HIA (no efflux, not solubility limited, not biased by first-pass) 100%

Bioavailability: 70 (68-93)%<sup>14, 92, 130</sup>.

Metabolism: Biotransformation - hepatic; rapidly deacetylated by microsomal oxidative enzymes<sup>14, 71</sup>.

Excretion: Elimination - biliary/fecal (enterohepatic circulation)<sup>14, 71</sup>.

d) *Physicochemical data:*

MW 823, logP cal. 2.39, amphiprotic (base pKa 8, weak acid pKa 7.9)

Sw exp. 3.3 mg/ml, Sw cal. (intrinsic) 0.55 mg/ml, Sw cal. (7.4) 0.11 mg/ml ( $140 \mu\text{M}$ ).

### 1.4.17. Daunorubicin (daunomycin)

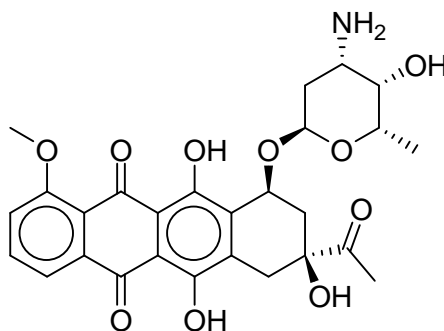


Figure 17: Chemical Structure of Daunorubicin

- a) *Reported in vitro efflux by P-gp, MRP2 or BCRP:*  
 Good substrate. MDR type anti-cancer drug<sup>104,131</sup>. Polarized transport across MDCKII-MDR1 cell monolayers (ratio 14).  
 Permeability  
 Pe, cal (Caco-2, 500 rpm)  $1.2 \cdot 10^{-6}$  cm/s.
- b) *Effect of efflux on in vivo pharmacokinetic properties:*  
 P-gp efflux was observed in the permeability study in in situ intestinal perfusion with mdr1a/b(-/-) and control mice<sup>76</sup>.
- c) *Human bioavailability, PK and non-linear absorption mechanisms:*  
 Human intestinal absorption (HIA): Unknown  
 Predicted maximum HIA (no efflux, not solubility limited, not biased by first-pass) 45%  
 Bioavailability: Not reported, but probably is very low. Used only intravenous.  
 Metabolism: Rapid to active metabolite doxorubino<sup>71</sup>.  
 Excretion: Elimination - in the urine, 25% in an active form; an estimated 40% is eliminated by biliary excretion<sup>71</sup>.
- d) *Physicochemical data:*  
 MW 528, logP exp. 1.83, logP cal. 1.01, base pKa 10  
 Sw cal. (intrinsic) 0.16 mg/ml, Sw cal. (pH 7.4) 0.98 mg/ml (1.8 mM)

#### 1.4.18. Etoposide

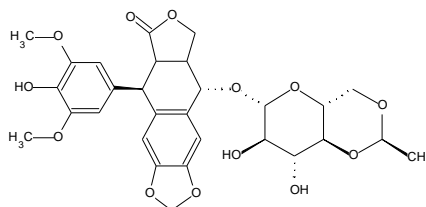


Figure 18: Chemical Structure of Etoposide

- a) *Reported in vitro efflux by P-gp, MRP2 or BCRP:*  
 Moderate substrate. MDR type anticancer drug<sup>132,133</sup>. Only slightly polarized transport across MDCKII-MDR1 cell monolayers (ratio 2.8)<sup>29</sup>. Estimated efflux Km MDCKII-MDR1 cells  $2.55 \cdot 10^{-6}$ .  
 Permeability  
 Pe, cal (Caco-2, 500 rpm)  $5 \cdot 10^{-6}$  cm/s  
 Pe (pH 7.4, 1  $\mu$ M GF129018)  $>10 \cdot 10^{-6}$  cm/s<sup>134</sup>.
- b) *Effect of efflux on in vivo pharmacokinetic properties:*  
 Polarized transport of etoposide was reduced but not abolished in mdr1a (-/-) tissues. Residual ETOP efflux in mdr1a (-/-) tissues was abolished by the MRP inhibitor MK571, indicating involvement of both P-GP and MRP<sup>135</sup>.
- c) *Human bioavailability, PK and non-linear absorption mechanisms:*  
 Human intestinal absorption (HIA): HIA-50% variable and dose-dependent absorption, probably due limited solubility<sup>90</sup>.  
 Predicted maximum HIA (no efflux, not solubility limited, not biased by first-pass) 97%

Bioavailability: 52 (17-70)%. Decreases at oral doses greater than 200 mg<sup>14,92,136</sup>.

Metabolism: No evidence of first-pass metabolism.

Excretion: Urinary recovery of etoposide after i.v. dosing is about 35-50% of the dose. The glucuronide conjugate accounts for up to 20% of the urinary recovery dose<sup>14</sup>.

d) *Physicochemical data:*

MW 588, logP exp 0.6, logP cal. 0.44, neutral

Sw exp. 0.1 mg/ml (170  $\mu$ M)

### 1.4.19. Vincristine

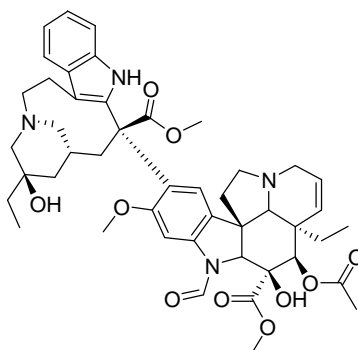


Figure 19: Chemical Structure of Vincristine

a) *Reported in vitro efflux by P-gp, MRP2 or BCRP:*

MDR-type anticancer drug<sup>132,133</sup> Polarized transport across MDCKII-MDR1 cell monolayers (ratio 6.3)<sup>29</sup>. No P-gp effect (in situ mice brain perfusion model, mdr1a(-/-) and wild-type mice<sup>105</sup>.

Permeability

Pe, cal (Caco-2, 500 rpm)  $>10 \cdot 10^{-6}$  cm/s

b) *Effect of efflux on in vivo pharmacokinetic properties:*

-

c) *Human bioavailability, PK and non-linear absorption mechanisms:*

Human intestinal absorption (HIA): Unknown

Predicted maximum HIA (no efflux, not solubility limited, not biased by first-pass) 100%

Bioavailability: Not reported. Probably very low. Drug used intravenously.

Metabolism: Rapid and extensive (CYP3A4)<sup>71</sup>.

Excretion: Primary route of elimination – biliary (80%)<sup>71</sup>.

d) *Physicochemical data:*

MW 825, logP exp. 2.82, logP cal. 3.71, base pKa 7.4

Sw exp. (\*H<sub>2</sub>SO<sub>4</sub>) 440 mg/ml, Sw cal. (intrinsic) 0.19 mg/ml. Sw cal. (pH 7.4) 0.5 mg/ml (570  $\mu$ M)

### 1.4.20. Erythromycin

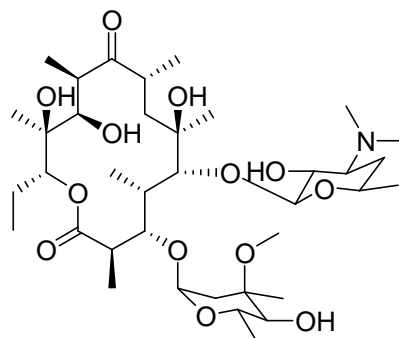


Figure 20: Chemical Structure of Erythromycin

a) *Reported in vitro* efflux by P-gp, MRP2 or BCRP:

Polarized transport across MDR1 transfected and caco-2 cell monolayers<sup>29,78,137</sup>. BA/AB ration 14 in MDCKII-MDR1 cells<sup>29</sup>. Studies in *mdr1a* disrupted mice confirmed that erythromycin was a P-gp substrate<sup>137</sup>.

Permeability

Pe  $1.13 \cdot 10^{-6}$  cm/s (pH 7.4, 500 rpm)<sup>138</sup>.

Pe cal. (pH 7.4, 500 rpm)  $5.6 \cdot 10^{-6}$  cm/s

b) *Effect of efflux on in vivo* pharmacokinetic properties:

c) *Human bioavailability, PK and non-linear absorption mechanisms:*

Human intestinal absorption (HIA): Unknown

Predicted maximum HIA (no efflux, not solubility limited, not biased by first-pass) 97%.

Bioavailability: 30 (10-60) %<sup>59,92,136</sup>.

Metabolism: CYP3A4

Excretion: Primarily elimination – biliary (more than 60% of i.v. dose)<sup>71</sup>.

d) *Physicochemical data:*

MW 734, logP exp. 2.54, logP cal. 1.87, base pKa 8.6

Sw exp. 2 mg/ml, Sw cal. (intrinsic) 12.8 mg/ml, Sw cal. (pH 7.4) 180 mg/ml (>100 mM)

### 1.4.21. Tobramycin

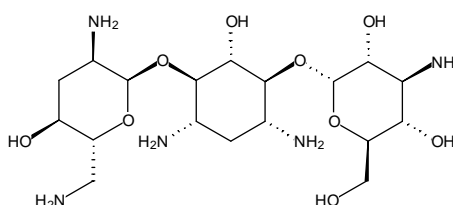


Figure 21: Chemical Structure of Tobramycin

- a) *Reported in vitro efflux by P-gp, MRP2 or BCRP:*  
 Can be P-gp substrate (?)<sup>139</sup>.  
 Permeability  
 Pe cal. (pH 7.4, 500 rpm)  $0.08 \cdot 10^{-6}$  cm/s.
- b) *Effect of efflux on in vivo pharmacokinetic properties:*  
 Inhibition of P-gp with copolymer CRL-1605 increased bioavailability of drug in mice<sup>139</sup>.
- c) *Human bioavailability, PK and non-linear absorption mechanisms:*  
 Human intestinal absorption (HIA): 1%  
 Predicted maximum HIA (no efflux, not solubility limited, not biased by first-pass) 3%.  
 Bioavailability: 1 %<sup>14,136</sup>.  
 Metabolism: Not metabolized or non-significant metabolism<sup>14</sup>.  
 Excretion: Renal<sup>14</sup>.
- d) *Physicochemical data:*  
 MW 467, logP<2, base pKa 9.9  
 Highly soluble Sw exp. 650 mg/ml

#### 1.4.22. Ivermectin

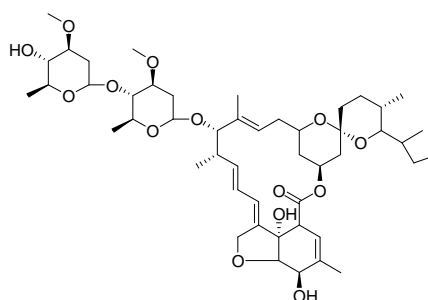


Figure 22: Chemical Structure of Ivermectin

- a) *Reported in vitro efflux by P-gp, MRP2 or BCRP:*  
 P-gp substrate in BBB permeability studies in vivo. P-gp deficient mice displayed increased sensitivity to the centrally neurotoxic pesticide ivermectin (100-fold)<sup>140</sup>.  
 Permeability  
 Pe cal. (pH 7.4, 500 rpm)  $>10 \cdot 10^{-6}$  cm/s
- b) *Effect of efflux on in vivo pharmacokinetic properties:*  
 -
- c) *Human bioavailability, PK and non-linear absorption mechanisms:*  
 Human intestinal absorption (HIA): Rapidly absorbed 60% (incomplete absorption probably due to poor solubility or reported HIA value biased by first-pass metabolism)<sup>14</sup>.  
 Predicted max. HIA (no efflux, not solubility limited, not biased by first-pass) 100%.  
 Bioavailability: -  
 Metabolism: Metabolized (demethylation)  
 Excretion: The major route of excretion is in the feces.

d) *Physicochemical data:*

MW 875, logP 3.25, neutral,

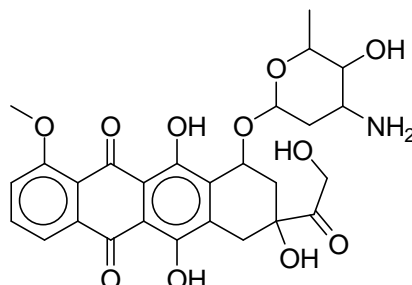
Poor solubility Sw 0.0038 mg/ml (4.6  $\mu$ M)**1.4.23. Doxorubicin**

Figure 23: Chemical Structure of Doxorubicin

a) *Reported in vitro efflux by P-gp, MRP2 or BCRP:*

Pharmacokinetic analyses indicated that, compared to *mdr1a*(+/+) mice, *mdr1a*(-/-) mice showed a significantly higher accumulation of doxorubicin<sup>141</sup>.

Permeability

Pe app Caco-2  $0.16 \times 10^{-6}$  cm/s<sup>102</sup>.Pe cal. Caco-2 (pH 7.4, 500 rpm)  $0.3 \times 10^{-6}$  cm/s.b) *Effect of efflux on in vivo pharmacokinetic properties:*

P-gp substrate. MDR type anticancer<sup>104,133</sup>. Studies in *mdr1a* disrupted mice confirmed that doxorubicin was a P-gp substrate<sup>137</sup>.

Not polarized transport across MDCKII-MDR1 cell monolayers<sup>29</sup>. Probably transport across P-gp expressing cells is not polarized (slightly polarized) at high concentrations (10  $\mu$ M and >) and can be polarized at lower concentrations.

c) *Human bioavailability, PK and non-linear absorption mechanisms:*Human intestinal absorption (HIA): Dose-limited absorption (about 10%)<sup>90</sup>.

Predicted maximum HIA (no efflux, not solubility limited, not biased by first-pass) 12%.

Bioavailability: 5%<sup>14,136</sup>.Metabolism: Rapid biotransformation to active metabolite doxorubicinol<sup>71</sup>.

Excretion: Biliary/renal

d) *Physicochemical data:*

MW 543, logP cal. 0.32, base pKa 8.1

Sw cal. (intrinsic) 0.26 mg/ml, Sw cal. (pH 7.4) 1.6 mg/ml (3 mM)

### 1.4.24. Tacrolimus

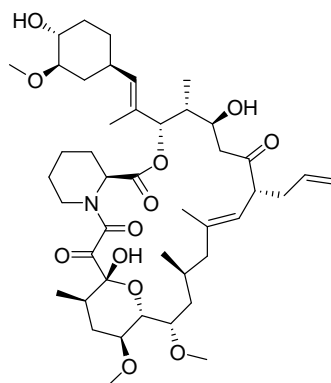


Figure 24: Chemical Structure of Tacrolimus

a) *Reported in vitro efflux by P-gp, MRP2 or BCRP:*

Polarized transport across caco-2 ( $R_{BA/AB} = 7.5$ , 40  $\mu\text{M}$ ). Efflux not saturable in 0-40  $\mu\text{M}$  [4].  
Permeability

Papp,caco-2 (7.5, 40  $\mu\text{M}$ ) -  $2.1 \cdot 10^{-6} \text{ cm/s}^{28}$ .

Pe cal. (pH 7.4, 500 rpm)  $> 10 \cdot 10^{-6} \text{ cm/s}$

b) *Effect of efflux on in vivo pharmacokinetic properties:*

Difference in plasma concentration (8.3 fold) and AUC (8.2 fold) in *mdr1a/b(-/-)* and wild type mice<sup>28</sup>.

c) *Human bioavailability, PK and non-linear absorption mechanisms:*

Human intestinal absorption (HIA): Predicted maximum HIA (no efflux, not solubility limited, not biased by first-pass) 97%.

Bioavailability: 16% (9-23)%<sup>14,59,136</sup>.

Metabolism: Extensive (CYP 3A4)

Excretion: The majority of the dose ( $>90\%$ ) is excreted as metabolites in urine and feces<sup>14</sup>.

d) *Physicochemical data:*

MW 804, logP 4.45, neutral

Sw 0.059 mg/ml (70  $\mu\text{M}$ )

### 1.4.25. Nadolol

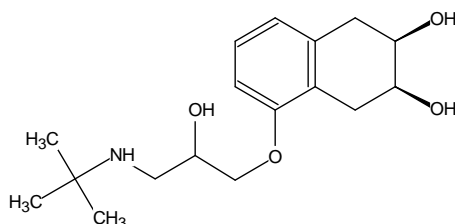


Figure 25: Chemical Structure of Nadolol

a) *Reported in vitro efflux by P-gp, MRP2 or BCRP:*

Decreased accumulation in P-gp-overexpressing K562/ADM cells<sup>9</sup>.

Permeability

Pe  $1.13 \cdot 10^{-6}$  cm/s (pH 7.4, 500 rpm)<sup>80</sup>.

Pe cal. (pH 7.4, 500 rpm)  $1.3 \cdot 10^{-6}$  cm/s.

b) *Effect of efflux on in vivo pharmacokinetic properties:*c) *Human bioavailability, PK and non-linear absorption mechanisms:*

Human intestinal absorption (HIA): Variable, Dose-dependent absorption 57% 30-70% (absorption from the ratio of urinary excretion of drug related material following oral and i.v.administration)<sup>90</sup>.

Predicted maximum HIA (no efflux, not solubility limited, not biased by first-pass) 58%.

Bioavailability: 30-40%<sup>14, 92, 136</sup>. Non-linear pharmacokinetics<sup>142</sup>.

Metabolism: Not metabolized<sup>14</sup>.

Excretion: Excreted unchanged by the kidney (73%) and bile (27%)<sup>14</sup>.

d) *Physicochemical data:*

MW 309, logP cal. 0.54, base pKa 9.4

Highly soluble: Sw (intrinsic) 4.2 mg/ml, Sw cal. (pH 7.4) 240 mg/ml (>100 mM)

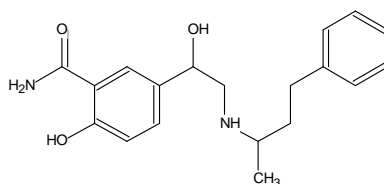
**1.4.26. Labetalol**

Figure 26: Chemical Structure of Labetalol

a) *Reported in vitro efflux by P-gp, MRP2 or BCRP:*

Polarized transport across MDRI-MDCKII cell monolayers (B-A/A-B 8.8). Inhibition of efflux with GF120918<sup>143</sup>.

Permeability

Pe app Caco-2 -  $9 \cdot 10^{-6}$  cm/s<sup>102</sup>.

Pe cal. (pH 7.4, 500 rpm)  $>10 \cdot 10^{-6}$  cm/s.

b) *Effect of efflux on in vivo pharmacokinetic properties:*c) *Human bioavailability, PK and non-linear absorption mechanisms:*

Human intestinal absorption (HIA): Absorption 95% (urinary excretion data)<sup>90</sup>.

Predicted maximum HIA (no efflux, not solubility limited, not biased by first-pass) 100%

Bioavailability: 18 (13-50)%<sup>14, 92, 136</sup>.

Metabolism: Elimination of labetalol is mainly by hepatic biotransformation to glucuronides<sup>136</sup>.

Excretion: Less than 5% of labetalol is excreted unchanged in urine. Its metabolites are mainly excreted in urine (55-60%) but 12-27% are excreted in feces<sup>136</sup>.

d) *Physicochemical data:*

MW 328, logP 2.24, amphiprotic: base pKa 8.6, weak acid pKa 7.5

Soluble: Sw cal. (intrinsic) 0.7 mg/ml, Sw cal (pH 7.4) 0.2 mg/ml (500 µM)

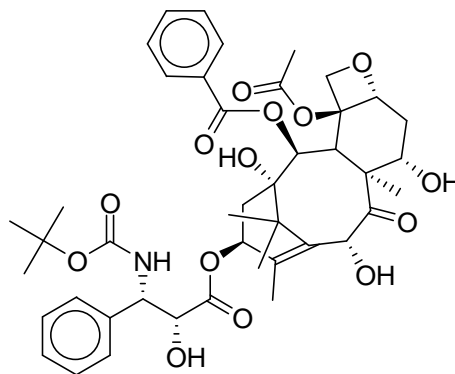
**1.4.27. Docetaxel**

Figure 27: Chemical Structure of Docetaxel

a) *Reported in vitro efflux by P-gp, MRP2 or BCRP:*Good P-gp substrate, MDR-type anticancer drug<sup>144</sup>.Polarized transport across caco-2 cell monolayers ( $R_{BA/AB}$  20). This polarized transport was inhibited by verapamil, chlorpromazine and reserpine<sup>145</sup>.

Permeability

Pe cal. (pH 7.4, 500 rpm)  $>10 \cdot 10^{-6}$  cm/sb) *Effect of efflux on in vivo pharmacokinetic properties:*Coadministration of cyclosporine A (P-gp and CYP 3A4 inhibitor) strongly enhances the oral bioavailability of docetaxel<sup>146</sup>.c) *Human bioavailability, PK and non-linear absorption mechanisms:*

Human intestinal absorption (HIA): Predicted maximum HIA (no efflux, not solubility limited, not biased by first-pass) 100%

Bioavailability: 8 (2-14) %<sup>147</sup>.Metabolism: Extensive metabolism (CYP3A4)<sup>71</sup>.Excretion: Primarily biliary/fecal<sup>71</sup>.d) *Physicochemical data:*

MW 808, logP cal 3.60, neutral

Poor solubility Sw cal. 0.0065 mg/ml (8 µM)

### 1.4.28. Lincomycin

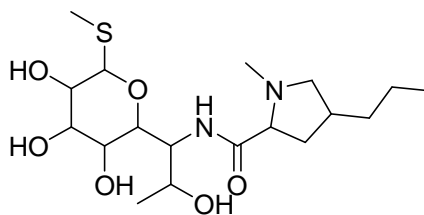


Figure 28: Chemical Structure of Lincomycin

a) *Reported in vitro* efflux by *P-gp*, *MRP2* or *BCRP*:

Moderate or weak substrate. Polarized transport across MDCKII-MDR1 cell monolayers (50  $\mu$ M, efflux ratio 3.2)<sup>143</sup>.

Permeability

Pe cal. (pH 7.4, 500 rpm)  $1.6 \cdot 10^{-6}$  cm/s.

b) *Effect of efflux on in vivo* pharmacokinetic properties:

-

c) *Human bioavailability, PK and non-linear absorption mechanisms:*

Human intestinal absorption (HIA): Absorption 20-35%<sup>90</sup>.

Predicted maximum HIA (no efflux, not solubility limited, not biased by first-pass) 51%

Bioavailability: 20-30%<sup>136</sup>.

Metabolism: -

Excretion: -

d) *Physicochemical data:*

MW 406, logP cal 0.72, base pKa 7.7

Highly soluble, Sw cal (intrinsic) 9.5 mg/ml, Sw cal (pH 7.4) 30 mg/ml (70 mM)

### 1.4.29. Indinavir

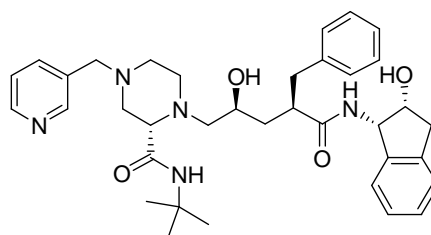


Figure 29: Chemical Structure of Indinavir

a) *Reported in vitro* efflux by *P-gp*, *MRP2* or *BCRP*:

Good substrate in many different studies

Indinavir showed polarized transport in the BBB model, LLC-PK11:MDR1 and Caco-2 cell line. PSC 833, verapamil and LY335979 inhibited polarized transport<sup>148</sup>.

Permeability

Pe cal. (pH 7.4, 500 rpm)  $>10 \cdot 10^{-6}$  cm/s

b) *Effect of efflux on in vivo pharmacokinetic properties:*

c) *Human bioavailability, PK and non-linear absorption mechanisms:*

Human intestinal absorption (HIA): Predicted maximum HIA (no efflux, not solubility limited, not biased by first-pass) 100%

Bioavailability: 18-30%<sup>14</sup>.

Metabolism: Metabolized by CYP3A4<sup>14</sup>.

Excretion: -

d) *Physicochemical data:*

MW 614, logP cal 2.69, weak base pKa 6.8

Sw cal (intrinsic) 0.06 mg/ml, Sw cal. (pH 7.4) 0.07 mg/ml (120 µM)

### 1.4.30. Sulpiride

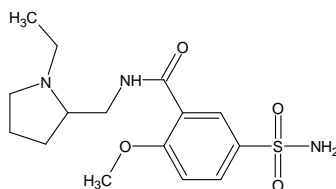


Figure 30: Chemical Structure of Sulpiride

a) *Reported in vitro efflux by P-gp, MRP2 or BCRP:*

Moderate substrate.

Polarized transport across Caco-2 cell monolayers. Inhibition of efflux with verapamil<sup>149</sup>. The B-to-A transport is mediated by the basolateral peptide transporter and organic cation transporter OCT1 on the basolateral membrane and by P-glycoprotein on the apical membrane (Caco-2)<sup>150</sup>. Increased distribution (2 fold) to the brain in P-gp deficient mice<sup>98</sup>.

Permeability

Pe caco-2  $0.39 \times 10^{-6}$  cm/s (pH 7.4, 500 rpm)<sup>149</sup>.

Pe app caco-2  $0.39 \times 10^{-6}$  cm/s<sup>102</sup>.

b) *Effect of efflux on in vivo pharmacokinetic properties:*

Quinidine and verapamil increased bioavailability of sulpiride after intestinal administration in rats<sup>151</sup>.

c) *Human bioavailability, PK and non-linear absorption mechanisms:*

Human intestinal absorption (HIA): Moderate absorption 30-70%<sup>90,152</sup>.

Predicted maximum HIA (no efflux, not solubility limited, not biased by first-pass) 78%

Bioavailability: 18-36%<sup>14,153</sup>.

Metabolism: Not extensive metabolism (5-oxypiperidyl sulpiride)<sup>14</sup>.

Excretion: Up to 50% of sulpiride is excreted unchanged in urine. 50-70% of dose was eliminated in feces<sup>14</sup>.

d) *Physicochemical data:*

MW 341, logP cal 0.6, base pKa 9.3

Sw exp 0.54 mg/ml, Sw cal (intrinsic) 0.56 mg/ml, Sw cal (pH 7.4) 10 mg/ml (30 mM)

### 1.4.31. Azithromycin

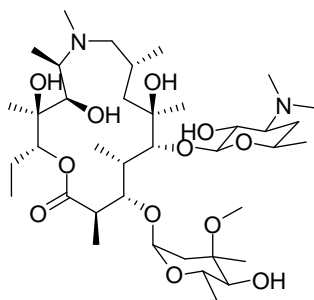


Figure 31: Chemical Structure of Azithromycin

a) *Reported in vitro efflux by P-gp, MRP2 or BCRP:*

Polarized transport across Caco-2 cell monolayers (BA/AB ratio 67 at 50  $\mu$ M. Significant inhibition of efflux with verapamil<sup>154</sup>.

Permeability

Pe cal. (pH 7.4, 500 rpm)  $0.3 \cdot 10^{-6}$  cm/s

b) *Effect of efflux on in vivo pharmacokinetic properties:*

Drug-drug interactions with nelfinavir and CsA<sup>155,156</sup>.

c) *Human bioavailability, PK and non-linear absorption mechanisms:*

Human intestinal absorption (HIA): 37% dose limited absorption<sup>90</sup>.

Predicted maximum HIA (no efflux, not solubility limited, not biased by first-pass) 9%

Bioavailability: 37%<sup>14,157</sup>.

Metabolism: Moderately metabolized (demethylation)<sup>14,71</sup>.

Excretion: A large fraction of the absorbed dose of azithromycin remains unmetabolized. The major route of elimination is biliary excretion of the unchanged compound<sup>14</sup>.

d) *Physicochemical data:*

MW 749, logP 1.98, base pKa 9.7

Highly soluble Sw cal. (intrinsic) 25 mg/ml, Sw cal (pH 7.4) >1 g/m (>100 mM)

### 1.4.32. Salbutamol

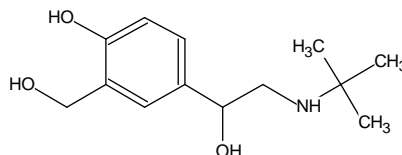


Figure 32: Chemical Structure of Salbutamol

Salbutamol is a respiratory agent normally used by inhalation. Oral tablet formulations are also present for salbutamol. It has been previously found that salbutamol absorption from the intestines is limited by P-gp.

a) *Reported in vitro efflux by P-gp, MRP2 or BCRP:*

Possible substrate (based on only one study)<sup>158</sup>.

Permeability

Pe cal. (pH 7.4, 500 rpm)  $1.1 \times 10^{-6}$  cm/s

b) *Effect of efflux on in vivo pharmacokinetic properties:*

Possible P-gp substrate - in vivo absorption study (effect of verapamil and absorption correlation with P-gp expression). The intrinsic absorption of salbutamol in different intestinal segments of the rat was measured and related with the corresponding intestinal P-glycoprotein (P-gp) expression levels. The apparent absorption rate constants ( $k_a$ ,  $h^{-1}$ ) observed in each fraction by means of the *in situ* rat gut absorption method after perfusion of a 0.29-mM isotonic solution of salbutamol were used as absorption indexes. In a separate series of studies, a semiquantitative analysis of the mRNA expression of P-gp by means of polymerase chain reaction and Western blot with an antibody raised against the P-gp were also performed. The *in situ*  $k_a$  values determined in the different segments ( $h^{-1}$ ) showed that the absorption is not homogeneous along the intestinal tract, that is,  $0.499 \pm 0.054$  for colon,  $0.474 \pm 0.052$  for the proximal segment,  $0.345 \pm 0.014$  for the mean, and  $0.330 \pm 0.023$  for the distal fraction. Addition of verapamil to the perfusion fluid did provide a better absorption of salbutamol in the distal segment. The analysis of the mRNA expression and levels of P-gp showed that the enzyme content in each section of the intestine was inversely related to salbutamol absorption<sup>158</sup>.

In another study, the objective was to develop a semiphysiological population pharmacokinetic model that describes the complex salbutamol sulphate absorption in rat small intestine. *In situ* techniques were used to characterize the salbutamol sulphate absorption at different concentrations (range: 0.15-18 mM). Salbutamol sulphate at concentration of 0.29 mM was administered in presence of verapamil (10 and 20 mM), grapefruit juice and sodium azide ( $NaN_3$ ) (0.3, 3 and 6 mM). Different pharmacokinetic models were fitted to the dataset using NONMEM. Parametric and non-parametric bootstrap analyses were employed as internal model evaluation techniques. The validated model suggested instantaneous equilibrium between salbutamol sulphate concentrations in lumen and enterocyte, and the salbutamol sulphate absorption was best described by a simultaneous passive diffusion ( $k_a = 0.636 h^{-1}$ ) and active absorption ( $V_{Max} = 0.726$  mM/h,  $K_m = 0.540$  mM) processes from intestinal lumen to enterocyte, together with an active capacity-limited P-gp efflux ( $V_{max} = 0.678$  mM/h,  $K_m = 0.357$  mM) from enterocyte to intestinal lumen. The extent of salbutamol sulphate absorption in rat small intestine can be improved by  $NaN_3$ , grapefruit juice and verapamil<sup>159</sup>.

c) *Human bioavailability, PK and non-linear absorption mechanisms:*

Human intestinal absorption (HIA): Predicted maximum HIA (no efflux, not solubility limited, not biased by first-pass) 49%.

Bioavailability: 50% (45-55)%<sup>14,160,161</sup>.

Metabolism: Considerable (sulphate conjugation)<sup>14,71</sup>.

Excretion: Elimination renal 69 to 90% (60% as metabolite), fecal 4%<sup>71</sup>.

d) *Physicochemical data:*

MW 239, logP 0.23, base pKa 8.6

Highly soluble: Sw cal. (intrinsic) 10 mg/ml, Sw cal. (pH 7.4) 110 mg/ml (>100 mM)

### 1.4.33. Sulfasalazine

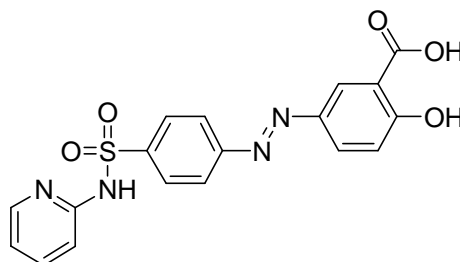


Figure 33: Chemical Structure of Sulfasalazine

Sulfasalazine is an anti-inflammatory agent indicated for the treatment of ulcerative colitis and rheumatoid arthritis. BCRP protein is an important determinant for the absorption of the sulfasalazine. And it is stated that sulfasalazine has the potential to be utilized as a specific in-vivo probe of BCRP.

*a) Reported in vitro efflux by P-gp, MRP2 or BCRP:*

Permeability coefficients of sulfasalazine across Caco-2 monolayers were approximately 342, 261 and 176 fold higher from basolateral to apical direction than from apical to basolateral direction for 100, 200 and 500  $\mu$ M sulfasalazine respectively. In this study also effect of the transporters on efflux of sulfasalazine was investigated by using selective inhibitors. Inhibition of P-gp with verapamil and Rhodamine 123 did not affect the transport of sulfasalazine in both directions. On the other hand 3-4 fold decrease was observed in the permeability ratios when MRP protein is inhibited with indomethacin and calcein. Hence it is decided that the efflux of sulfasalazine in Caco-2 cells was dependent on MRP but not on P-gp transporters<sup>162</sup>.

Recent studies using the T-cell line (CEM) have shown that sulfasalazine is a substrate for BCRP. After oral administration of 20 mg/kg sulfasalazine, the area under the plasma concentration profile in Bcrp2(abcg2)(-/-) KO mice which can not express BCRP protein was 13 fold higher than in control mice expressing BCRP protein. Moreover treatment of control mice with single dose of gefitinib (50 mg/kg), a known inhibitor of BCRP, given 2 h prior to administering a single oral dose of sulfasalazine(20 mg/kg), resulted in a 13 fold increase in the AUC of sulfasalazine compared to the AUC in vehicle treated mice. Since gefitinib is also an inhibitor of P-gp the impact of P-gp on sulfasalazine absorption was also investigated in-vivo. The sulfasalazine AUC in mdr1a(-/-) KO versus control mice did not differ significantly after either oral or intravenous dose<sup>163</sup>.

*b) Human bioavailability, PK and non-linear absorption mechanisms:*

Bioavailability: Sulfasalazine is absorbed poorly with an estimated bioavailability of 3-12 %<sup>162</sup>.

*c) Analytical methods:*

Analytical determination of amount of sulfasalazine is done with HPLC and the method is as shown below<sup>3</sup>.

<b>Column temperature [°C]</b>	25
<b>Sample temperature [°C]</b>	25
<b>Flow [mL·min<sup>-1</sup>]</b>	1
<b>Injection volume [μL]</b>	10
<b>Eluent</b>	acetonitrile: water:isopropanol:glacial acetic acid 7:22:11:0.4:
<b>Column</b>	4.6 mm X 25 cm column L1
<b>Detection</b>	UV 254 nm

Table 11: HPLC method for Sulfasalazine

#### 1.4.34. Rosuvastatin

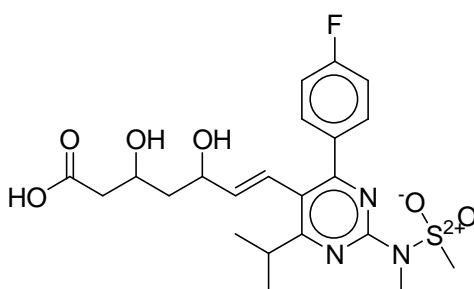


Figure 34: Chemical Structure of Rosuvastatin

Rosuvastatin is a statin used as an antilipemic agent and a competitive HMG-CoA reductase inhibitor effective in lowering LDL cholesterol and triglycerides.

##### a) Reported *in vitro* efflux by P-gp, MRP2 or BCRP:

Rosuvastatin is known to be a BCRP substrate. It is also proved that P-gp does not appear to play a role in rosuvastatin disposition<sup>164</sup>.

A study was designed to determine whether rosuvastatin is a substrate for MDR1, MRP2, or BCRP. Rosuvastatin transport was measured at concentrations of 10 and 50 μM in the absence or presence of 2 μM GF120918 using MDCK-MDR1 cells. Rosuvastatin transport in both B to A and A to B directions was similar, with Papp value of 8 nm/s and was not affected by the inhibitor. This proves that rosuvastatin is not a substrate for P-gp. Membranes isolated from Sf9 cells either containing MRP2 or not were used for the investigation of rosuvastatin transport. It was shown that ATP dependent transport of rosuvastatin between control and MRP2-Sf9 membranes was not significantly different (p>0.05). Thus it was concluded that rosuvastatin is not carried by MRP2. Whereas in MXR-M-VT membranes isolated from mammalian cells expressing BCRP rosuvastatin transport was inhibited by 89 % (p<0.05) when GF120918 was used<sup>165</sup>.

##### b) Effect of efflux on *in vivo* pharmacokinetic properties:

Ketoconazole is known to inhibit both CYP3A4 and P-gp. Thus ketoconazole was administrated together with rosuvastatin to healthy subjects to investigate if P-gp and CYP3A4 play a role in the absorption and disposition of rosuvastatin. Following the Coadministration of ketoconazole with rosuvastatin there was no change in the pharmacokinetics of the drug compared to the placebo. Therefore, these results suggests that rosuvastatin is not a ligand for P-gp<sup>166</sup>.

The ATP dependent activity of BCRP on rosuvastatin was also evaluated using BCRP expressing membrane vesicles. The results are as follows for the members of the group statin<sup>167</sup>.

c) *Analytical methods:*

Analytical determination of amount of rosuvastatin is done with HPLC and the method is as shown below<sup>3</sup>.

<b>Column temperature [°C]</b>	25
<b>Sample temperature [°C]</b>	25
<b>Flow [mL·min<sup>-1</sup>]</b>	1
<b>Injection volume [µL]</b>	50
<b>Eluent</b>	0.05 M formic acid:acetonitrile 55:45
<b>Column</b>	Kromasil KR 100-5C18 4.6 × 250 mm, 5 µm.
<b>Detection</b>	UV 240 nm

Table 12: HPLC method for Rosuvastatin

d) *Physicochemical data:*

The following table shows the physicochemical properties of Rosuvastatin<sup>120,121,122</sup>.

<b>Category</b>	Antilipemic agent
<b>Formula</b>	C <sub>22</sub> H <sub>28</sub> FN <sub>3</sub> O <sub>6</sub> S
<b>Molecular weight</b>	481.539
<b>Solubility</b>	Sparingly soluble in water
<b>Availability</b>	VWR
<b>Log P</b>	3.135
<b>Log D</b>	-0,88
<b>pKa</b>	na
<b>In-vivo absorption (permeability %)</b>	20 %
<b>Protein binding</b>	88 %
<b>Minimum dose /maximum dose (mg)</b>	5/40
<b>BCS Classification</b>	Class III

Table 13: Physicochemical properties of Rosuvastatin

## 1.5. SUMMARY TABLES

The following tables show a summary of different properties and studies conducted on the compound candidates:

Drug	MW	logP	Ionization	Sw (pH 7.4) µM	Sw (intrinsic) mg/ml
Celiprolol	379	1.92	Base pKa 9.4	>1000	0.13
Paclitaxel	854	3.95	neutral	14	0.012
Talinolol	363	3.32	Base pKa 9.4	>1000	0.163
Digoxin	781	1.26	neutral	69	0.05
Verapamil	454	3.83	Base pKa 9.1	900	0.009
Cyclosporin A	1202	1.02	neutral	490	0.59
Quinidine	324	2.64	base pKa 9.6	>1000	0.14
Vinblastine	811	3.83	weak base pKa 7.4	470	0.19
Fexofenadine	502	4.35	Zwitterion pa 4.3, 8.8	25	0.012
Saquinavir	671	4.7	weak base pKa 6.8	310	0.17
Ritonavir	720	5.64	neutral	230	0.017
Rifampin	823	2.39	amphiprotic pKb 7.9, pKa 8	140	0.55
Loperamide	477	3.86	Base pKa 8.5	>1000	0.07
Daunorubicin	528	1.83	Base pKa 10	>1000	0.16
Etoposide	588	0.6	neutral	170	0.1
Vincristine	825	2.82	Base pKa 7.4	570	0.19
Erythromycin	734	2.54	Base pKa 8.6	>1000	2
Tobramycin	467	<-2	base pKa 9.9	>1000	>5
Ivermectin	875	3.25	neutral	4.6	0.04
Doxorubicin	543	0.32	Base pKa 8.1	>1000	0.26
Tacrolimus	804	4.45	neutral	70	0.06
Topotecan	421	0.29	amphiprotic bas pKa 8.6	>1000	0.25
Nadolol	309	0.54	base pKa 9.4	>1000	4.2
Labetalol	328	2.24	amphiprotic pKb 8.6, pKa 7.5	500	0.7
Docetaxel	808	3.60	neutral	8	0.067
Lincomycin	406	0.72	Base pKa 7.7	>1000	>5
Indinavir	614	2.68	weak base pKa 6.8	120	0.06
Sulpiride	341	0.6	Base pKa 9.3	>1000	0.54
Azithromycin	749	1.98	Base pKa 9.7	>1000	>5

Table 14 : Physico-chemical properties of several candidates

Drug	Dose	% F <sub>oral</sub>	Aborption (HIA)	Max HIA* (cal.)	Metabolism	Excretion
Celiprolol	100-200 mg	30-70	30-70%, dose-dependent	100	minor (no)	biliary, renal
Paclitaxel	60 mg/m <sup>2</sup>	4 (first-pass)	na	100	extensive (3A4)	biliary
Talinolol	50 mg	40-60	40-60%	100	minor (no)	-
Digoxin	0.25	60-90	60-90% formulation dependent	95	not extensive	-
Verapamil	80 mg	14-30 (first-pass)	complete	100	extensive (3A4, 2C8)	-
Cyclosporin A	700	Variable 10-60%	complete	100	extensive (3A4)	-
Quinidine	160 mg	good >80%	56-95%	100	-	-
Vinblastine	7 mg	na (iv used only)	na	100	extensive (3A4)	-
Fexofenadine	60 mg	na	na	100	minor (5%)	biliary
Saquinavir	600 mg	4% (first-pass)	30%	100	extensive	biliary
Ritonavir	600 mg	60-80%	na	100	extensive (3A4, 2D6)	biliary (renal small amount)
Rifampin	600 mg	68-93	good >80%	100	extensive (rapid)	biliary
Loperamide	2-4 mg	40%	na	100	extensive	biliary, renal
Daunorubicin	45 mg/m <sup>2</sup>	na (iv used only) Variable 17-70%,	na	45	extensive (rapid)	biliary, renal
Etoposide	100 mg	decreases with doses >100 mg	variable	97	moderate	renal
Vincristine	1.5 mg	na (used iv only)	na	100	extensive (3A4)	biliary
Erythromycin	250 mg	10-60%	na	97	metabolized (3A4)	biliary
Tobramycin	-	1%	1%	3	not metabolized	biliary
Ivermectin	-	na	60% (solubility limited?)	100	metabolized	biliary, renal
Doxorubicin	300 mg/m <sup>2</sup>	5%	10% (dose dependent)	12	extensive (rapid)	biliary, renal
Tacrolimus	0.1 mg	9-23%	na	97	extensive (3A4)	biliary, renal
Topotecan	1 mg/m <sup>2</sup>	21-45%	na	78	-	-
Nadolol	40 mg	30-40%	30-70% (dose dependent)	58	not metabolized	biliary, renal
Labetalol	100 mg	13-50%	95%	100	extensive (glucuronidation)	renal
Docetaxel	75 mg/m <sup>2</sup>	2-14% (first-pass)	na	100	Extensive (3A4)	biliary
Lincomycin	500 mg	20-35%	20-35%	51	-	-
Indinavir	800 mg	18-30%	-	100	metabolized (3A4)	-
Sulpiride	100-200 mg	18-36%	30-70%	78	not extensive	biliary, renal
Azithromycin	500 mg	37%	37%	9	not extensive	biliary

Table 15: Pharmacokinetic properties of several candidates

\*Max HIA (cal) - predicted human intestinal absorption assuming that there is no efflux, no solubility limitation and absorption is not biased by first-pass

Drug	Pe, Caco-2 *10 <sup>6</sup> cm/s	R <sub>BA/AB</sub>	V <sub>m</sub> efflux	K <sub>m</sub> efflux
Celiprolol	-	5 (50 µM, Caco-2)	113 pmol/10 <sup>6</sup> cells/min Caco-2	1000 µM (Caco-2)
Paclitaxel	4.4	4-10 (0.5-20 µM, Caco-2)	1.05 nmol/h/cm <sup>2</sup> Caco-2	16.5 µM (Caco-2)
Talinolol	1.5	7 (40 µM, caco-2)	5.5 nmol/h/cm <sup>2</sup> Caco-2	100 µM (Caco-2)
Digoxin	1.1		3.4 nmol/h/cm <sup>2</sup> Caco-2	7.3 µM (Caco-2)
Verapamil	14.7	1 (30 µM, caco-2)	no net secretion	no net secretion
Cyclosporin A	1.05	-	2.4 nmol/mg protein/h (LLC-GA5-COL300)	8 µM (LLC-GA5-COL300)
Quinidine	>5	-	-	-
Vinblastine	>5	>10 (MDR1 transfected cells)	-	-
Fexofenadine	>5	MDR1 transfected cells – polarized	-	-
Saquinavir	2.2	>10 (MDR1 transfected cells)	-	-
Ritonavir	>5	MDR1 transfected cells – polarized	-	-
Rifampin	2	4.2 (20 µM, Caco-2)	4.3 nmol/h/cm <sup>2</sup> , Caco-2	55 µM
Loperamide	>5	8 (MDR1-MDCKII)	-	-
Daunorubicin	1.2	14 (MDR1-MDCKII)	-	-
Etoposide	5	2.8 (MDR1-MDCKII)	-	255 µM (MDR1-MDCKII)
Vincristine	>5	6.3 (MDR1-MDCKII)	-	-
Erythromycin	1.13	14 (MDR1-MDCKII)	-	-
Tobramycin	0.08	-	-	-
Ivermectin	>5	-	-	-
Doxorubicin	0.16	Not polarized (?)	no net secretion (?)	no net secretion (?)
Tacrolimus	2.1	7.5 (40 µM, Caco-2)	no saturation	no saturation
Topotecan	1	3.5 (40 µM, Caco-2)	7.2 nmol/h/cm <sup>2</sup> , Caco-2	170 µM
Nadolol	0.28	-	-	-
Labetalol	9	8.8 (MDR1-MDCKII)	-	-
Docetaxel	>5	20 (Caco-2)	-	-
Lincomycin	1.6	3.2 (MDR1-MDCKII)	-	-
Indinavir	>5	Polarized (Caco-2)	-	-
Sulpiride	0.39	Polarized (Caco-2)	-	-
Azithromycin	0.3	67 (Caco-2)	-	-

Table 16: Permeability studies of several candidates

Drug	Transport	Pgp effect in vivo	In vivo Pgp effect on PK properties
Celiprolol	Possible Pg substrate	?	Pgp effect on PK is not clear (not significant data)
Paclitaxel	Pgp substrate (very good)	Yes	Proved Pgp effect in vivo (difference in PK properties in mdr1a(-/-) and wild type mice). Probably Inhibition of Pgp caused increase in % Foral in humans.
Talinolol	Pgp substrate	Yes	Proved Pgp effect in vivo (difference in PK properties in mdr1a(-/-) and wild type mice). Possible intestinal secretion in humans.
Digoxin	Pgp substrate (good)	Yes	Proved Pgp effect in vivo (difference in PK properties and in situ intestinal permeability in mdr1a/1b(-/-) and wild type mice).
Verapamil	Highly permeable Pgp substrate	No (?)	Pgp probably does not effect PK properties in vivo. Plasma concentration is the same in mdr1a(-/-) mice and wild type mice
Cyclosporin A	Pgp substrate (moderate or good)	Yes (?)	Increased permeability in in situ intestinal perfusion system in mdr1a/1b(-/-) mice.
Quinidine	Pgp substrate (very good)	?	Pgp efflux was observed in the study of permeability in in situ intestinal perfusion with mdr1a/b(-/-) and control mice. But effect of Pgp on quinidine PK is not clear (good bioavailability)
Vinblastine	Substrate (Pgp & MRP)	?	Only small increase in intestinal permeability in in situ perfusion system in mdr1a/1b(-/-) mice. CsA increased absorption in rats.
Fexofenadine	Substrate (Pgp & others?)	Yes (?)	Contradictive. Verapamil increases %Foral, but have no effect on intestinal permeability in human perfused system.
Saquinavir	Pgp substrate (very good)	Yes	Proved Pgp effect in vivo (difference in PK properties in mdr1a(-/-) and wild type mice). Bioavailability increases with coadministration with ritonavir (Pgp inhibitor).
Ritonavir	Pgp substrate (moderate or good)	Yes (?)	Pgp efflux was observed in the permeability study in in situ intestinal perfusion with mdr1a/b(-/-) and control mice
Rifampin	Pgp substrate (probably moderate) & inducer	Yes	Proved Pgp effect in vivo (difference in PK properties in mdr1a(-/-) and wild type mice).
Loperamide	Pgp substrate (moderate or good)	Yes (?)	Significant increase (3 fold) of intestinal permeability in in situ perfusion system in mdr1a/1b(-/-) mice.
Daunorubicin	Pgp substrate (good)	Yes	Pgp efflux was observed in the permeability study in in situ intestinal perfusion with mdr1a/b(-/-) and control mice
Etoposide	Pgp substrate (moderate or poor) & MRP substrate	Yes (?)	Polarized transport of ETOP was reduced but not abolished in mdr1a (-/-) tissues. Residual ETOP efflux in mdr1a (-/-) tissues was abolished by the MRP inhibitor MK571.
Vincristine	Probably Pgp substrate (contradictive BBB data)	?	No data
Erythromycin	Pgp substrate (moderate or good)	?	No data
Tobramycin	Can be Pgp substrate (not enough data)	?	Not clear (not significant data)
Ivermectin	Pgp substrate (probably good)	?	No data
Doxorubicin	Pgp substrate (moderate, contradictive transport data across cell monolayers)	Yes	Proved Pgp effect in vivo (difference in PK properties in mdr1a(-/-) and wild type mice).
Tacrolimus	Pgp substrate (moderate or good)	Yes	Proved Pgp effect in vivo (difference in PK properties in mdr1a(-/-) and wild type mice).
Topotecan	Pgp substrate (probably moderate)	Yes	Proved Pgp effect in vivo (difference in PK properties in mdr1a(-/-) and wild type mice).
Nadolol	Possible substrate	?	No data
Labetalol	Pgp substrate (moderate)	?	No data
Docetaxel	Pgp substrate (very good)	Yes (?)	Cyclosporine A strongly enhances the oral bioavailability.

Lincomycin	Substrate (moderate or weak)	?	No data
Indinavir	Substrate (good)	?	No data
Sulpiride	Substrate (Pgp, Pept, OCT1)	Yes (?)	Quinidine and verapamil increased bioavailability of sulpiride after intestinal administration in rats
Azithromycin	Substrate (good)	?	Not enough data. Drug-drug interaction with cyclosporine A.

Table 17: Pgp effects on several candidates

Compound	Inclusion	Notes
Paclitaxel	ok	# oral PK data in Pgp KO and WT mice* # published estimation of Vm,Km for Pgp
Digoxin	ok	# oral PK data in Pgp KO and WT mice # published estimation of Vm,Km for Pgp
Saquinavir	ok	# absorption 30%, vs 6% bioavailability # oral PK data in Pgp KO and WT mice # published estimation Vm,Km for Pgp
Celiprolol	ok	# not metabolised, dose-dependent absorption # possible Pgp substrate
Fexofenadine	ok	# not metabolised, bioavailability 2% in mice # oral PK data in Pgp KO and WT mice # good Pgp substrate
Loperamide	ok	# proved Pgp efflux in intestine (intestinal perfusion with KO and WT mice)
Talinolol	ok	# published estimation of Vm,Km for Pgp # very good Pgp substrate
Quinidine	questionable	# proved Pgp efflux in intestine (intestinal perfusion with KO and WT mice)
Vinblastine	Almost ok	# oral PK data in Pgp KO and WT mice
Topotecan	questionable	# oral PK data in Pgp KO and WT mice # published estimation of Vm,Km for Pgp
Rifampin	questionable	# oral PK data in Pgp KO and WT mice # published estimation Vm,Km for Pgp
Verapamil	questionable	# oral PK data in Pgp KO and WT mice # control: no effect of Pgp on PK # good Pgp substrate
Daunorubicin	Questionable	# proved Pgp efflux in intestine (intestinal perfusion with KO and WT mice)
Cyclosporin A	Questionable	# proved Pgp efflux in intestine (intestinal perfusion with KO and WT mice)
Tacrolimus	questionable	# oral PK data in Pgp KO and WT mice # tested Vm,Km for Pgp – no saturation

Table 18: Comments on several compound candidates

\*Pgp KO and WT mice – Pgp knock out mdr1a(-/-) and wild type mdr1a(+/+) mice

Compound	Inclusion	Notes
Doxorubicin	problematic	# no data of Pgp effect on PK in vivo
Ritonavir	questionable	# proved Pgp efflux in intestine (intestinal perfusion with KO and AT mice)
Etoposide	questionable	#reduced but not abolished polarized transport in mrd1a(-/-) tissues #MRP1 substrate
Erythromycin	problematic	# no data of Pgp effect on PK in vivo
Tobramycin	problematic	# no data of Pgp effect on PK in vivo
Ivermectin	problematic	# no data of Pgp effect on PK in vivo
Vincristine	problematic	# contradictory BBB studies on Pgp efflux # no data of Pgp effect on PK in vivo
Salbutamol (albuterol)	almost ok	#possible Pgp substrate # verapamil-inhibited intestinal secretion
Rosuvastatin	questionable	#BCRP substrate
Sparfloxacin	questionable	# possible Pgp substrate (and other transporters) # do not find data of Pgp effect on PK in vivo (?)
Sulfasalazine	questionable	# oral PK data in Pgp KO and WT mice (no Pgp effect) # BCRP substrate
Methotrexate	problematic	# MRP substrate # no intestinal absorption – bicarbonic acid # incomplete dose-dependent absorption, not metabolized
Nadolol	questionable	# possible Pgp substrate (decreased accumulation in Pgp+ cells) # no data of Pgp effect on PK in vivo
Indinavir	problematic	# relevant Pgp substrate # no data of Pgp effect on PK in vivo
Docetaxel	problematic	# oral PK data in Pgp KO and WT mice (small effect of Pgp)
Labetalol	questionable	# moderate Pgp substrate # Intestinal Pgp efflux (perfusion experiments in rats)

Table 19 : Other suggested compounds and comments

## 1.6. CONCLUSION

The following is the criteria that was taken into consideration to extract from the final list of selected compounds the studied compound candidates (note that some of the candidates are extracted from the list for more than one reason):

- Substrates of the MRP2 and BCRP transporter proteins, due to the final decision that the only focus of the project will be the MRP1 protein, thus compounds such as topotecan, rosuvastatin, sulfasalazine, methotrexate, vinblastine and vincristine were extracted from the list.
- Compounds that are known to be substrate of more than one transporter protein (non-P-gp selective substrates), thus compounds such as ritonavir, vinblastine, cyclosporine A, verapamil, etoposide, and sulpiride were extracted from the list.
- Compounds with a lack of data or no effect of P-gp on PK *in vivo*, thus compounds such as sparfloxacin, verapamil, erythromycin, tobramycin, ivermectin, doxorubicin, nadolol, indinavir and vincristine were extracted from the list.
- Moderate, weak or non-clear P-gp substrates, thus compounds such as tacrolimus, rifampin, doxorubicin, labetalol, nadolol, lincomycin, azitromycin and salbutamol were extracted from the list.

As it was decided during Mentrans 2<sup>nd</sup> meeting, the final list of selected model compounds include only specific and proved substrates for P-gp, a total number of 8 compounds are proposed, which would be enough for the establishment of in-vitro in-vivo correlations.

For all the reasons mentioned above the list of compounds that will be used in MEMTRANS project include: celiprolol, paclitaxel, saquinavir, fexofenadine, digoxin, talinolol, loperamide and quinidine. Table 20 show a summary of the selected compounds properties and their BCS classification.

Drug	%F <sub>oral</sub>	Efflux transporter	Analytical method available	BCS	Log P
Celiprolol	30-70	P-gp	yes	na	1.92
Paclitaxel	4 (first-pass)	P-gp	yes	II/IV <sup>168</sup>	5.02/3.95
Saquinavir	4% (first-pass)	P-gp/MRP2	yes	I <sup>52</sup> /II <sup>1,169</sup> /IV <sup>120,121,122</sup>	4.7
Fexofenadine	na (approx. 33%)	P-gp	yes	III <sup>120,121,122,168</sup>	4.35
Digoxin	60-90	P-gp	yes	I <sup>52,120,121,122</sup> /III <sup>52, 168</sup>	1.7/1.26
Talinolol	40-60	P-gp	yes	II <sup>1,169</sup>	3.32
Loperamide	40	P-gp	yes	I/b <sup>2</sup>	3.86
Quinidine	>80%	P-gp	yes	I <sup>1,168,169</sup> /b <sup>2</sup>	2.64

Table 20: MEMTRANS project selected compounds

## 2. SELECTION OF THE INHIBITORS

### 2.1. GENERAL CRITERIA FOR SELECTION OF INHIBITORS

The criteria for the selection of the inhibitors are listed below:

- a) Selective for the transporter.
- b) Inhibition with low  $K_i$  or  $IC_{50}$  values ( $IC_{50} < 10 \mu M$ )
- c) No significant metabolism in the cell
- d) Being commercially available

### 2.2. P-GP INHIBITION

P-gp substrates that have high affinity to the protein can be used as inhibitors of this protein as well as the modifiers that are not actually substrates of this protein but inhibits the protein. Most of the inhibitors that were used in the previous works are not highly specific to the P-gp and also inhibit the other transporters such as MRPs and BCRP. The list of some of the inhibitors and their substrates that are previously used for the P-gp are given in the table below.

Inhibitor	Substrate
Cyclosporine <sup>4,108</sup>	P-gp, MRP1, MRP2, OATP-C
Verapamil <sup>4</sup>	P-gp, various organic cation transporters
GF 120918 <sup>54,73,170,171,172</sup>	P-gp, BCRP
LY 33579 <sup>173,174</sup>	P-gp

Table 21: Effect of the different inhibitor on efflux carriers

Because of the high selectivity to the P-gp, LY33579 (Zosuquidar trihydrochloride) is proposed for the inhibition of P-gp. A previous study examines in more detail the in-vitro properties of LY 33579. Equilibrium binding studies using radiolabeled LY 33579 indicated that P-gp has a very high affinity for this molecule, with a  $K_i$  of 59 nM and  $K_d$  of 73 nM. It was also found that  $IC_{50}$  of LY33579 is 0.024  $\mu M$  when used in Caco-2 cells<sup>4</sup>. Furthermore it is demonstrated that binding of the modulator is ATP independent. This modulator binds to an ATP-independent conformation of P-gp and does not serve as a substrate of P-gp. The lack of affinity of this molecule to MRP2 and BCRP was also shown by transport experiments using MRP transfected Hela cells and Caco-2 cells. LY33579 modulates drug resistance much longer than other P-gp modulators, Verapamil, even after being washed<sup>173,174</sup>. Also GF 120918 a relatively selective inhibitor although it also has an affinity to BCRP can be used alone or together with LY335979 to determine the effect of different inhibitors on the efflux ratios or when P-gp and BCRP inhibition is required for unselective substrates.

<b>Category</b>	Multidrug-Resistance Modulator
<b>Formula</b>	$C_{32}H_{31}F_2N_3O_2$
<b>Molecular weight</b>	527.61 g/mol
<b>Solubility</b>	na
<b>Availability</b>	Eli Lilly Company
<b>Log P</b>	na
<b>Log D</b>	na
<b>pKa</b>	na
<b>In-vivo absorption (permeability %)</b>	na
<b>Protein binding</b>	na
<b>Minimum dose /maximum dose (mg)</b>	na
<b>BCS Classification</b>	na

Table 22: Physicochemical properties of Zosuquidar trihydrochloride<sup>120,121,122</sup>.

### 2.3. MRP2 INHIBITION

MRP2 functions as an efflux pump for drugs and their glutathione conjugates. MRP2 is quite similar to P-gp, transporting many of the same substrates such as vinblastin, cyclosporine and verapamil. It is known that a highly specific inhibitor of MRP2 is clearly lacking<sup>108</sup>. Different inhibitors for the MRP2 transporter protein were previously studied. One of these inhibitors is sulfinpyrazone. Inhibition of this molecule is highly dependent on the substrate since some substrates may be sensitive to sulfinpyrazone, whereas others are not<sup>54,108</sup>. A known P-gp inhibitor GF120918 was found to be effective on the MRP1 transporter at above 10 $\mu$ M concentration<sup>149,61</sup>. MK571 (E)-3-[[[3-[2-(7-Chloro-2-quinolinyl) ethenyl] phenyl]-[3-dimethylamino)-3-oxopropyl]thio]methyl]thio]-propanoic Acid) is the most selective inhibitor to the MRP-family transporters compared to the above listed ones. It is shown that MRP-specific inhibitor MK571 caused a concentration dependent decrease of Ochratoxin A secretion while absorption increased. Effects of 4 multidrug resistance-reversing agents on transporting activity of MRP2 were also studied in another publication. It was stated that Ki values of PAK-104P, CsA, MK571 and PSC833 were 3.7, 4.7, 13.1, 28.9 respectively<sup>149,171,175</sup>. Although Ki observed with PAK-104P and CsA are lower than the Ki of MK571; MK571 is proposed for the MRP 2 inhibition due to its selectivity on MRP family.

<b>Category</b>	Multidrug-Resistance Modulator
<b>Formula</b>	$C_{26}H_{26}ClN_2O_3S_2$
<b>Molecular weight</b>	514.1 g/mol
<b>Solubility</b>	soluble
<b>Availability</b>	VWR
<b>Log P</b>	na
<b>Log D</b>	na
<b>pKa</b>	na
<b>In-vivo absorption (permeability %)</b>	na
<b>Protein binding</b>	na
<b>Minimum dose /maximum dose (mg)</b>	na
<b>BCS Classification</b>	na

Table 23: Physicochemical properties of MK571<sup>120,121,122</sup>

## 2.4. BCRP INHIBITION

Fumitremorgin C (FTC), a fungal toxin, is a potent and specific chemosensitizing agent in cell lines selected for resistance to mitoxantrone that do not over express P-gp or multidrug resistance protein. The gene encoding a novel transporter, the breast cancer resistance protein (BCRP), was recently found to be over expressed in a mitoxantrone selected human colon cell line S1-M1-3.2, which was used to identify FTC. It is reported that FTC almost completely reverses resistance mediated by BCRP in vitro and is a pharmacological probe for the expression and molecular action of this transporter. It is also shown that FTC treatment increased the amount of daunorubicin (1.8-2.3 fold) and doxorubicin (1.8 fold), retained by the cells and it increased the toxicity of mitoxantrone (29.4 fold), doxorubicin (6.6 fold), topotecan (6.5 fold)<sup>173,174,175,176,177,178</sup>. Thus FTC is proposed as a selective inhibitor for the BCRP transporter. FTC was selected instead of Kol143 for the project for the availability reasons since FTC is readily available.

<b>Category</b>	Multidrug-Resistance Modulator
<b>Formula</b>	$C_{22}H_{25}N_3O_3$
<b>Molecular weight</b>	379.5 g/mol
<b>Solubility</b>	Practically insoluble
<b>Availability</b>	SA/Axxora
<b>Log P</b>	na
<b>Log D</b>	na
<b>pKa</b>	na
<b>In-vivo absorption (permeability %)</b>	na
<b>Protein binding</b>	na
<b>Minimum dose /maximum dose (mg)</b>	na
<b>BCS Classification</b>	na

Table 24: Physicochemical properties of FTC<sup>120,121,122</sup>.

## 2.5. CONCLUSION

Specific inhibition of the transporters is the first point of evaluation of the inhibitors in case the cell lines such as Caco-2 that are able to produce more than one protein, are used for the project. Thus, the following selective inhibitors are proposed for the transporter proteins P-gp, MRP2 and BCRP:

<b>LY33579</b>	Highly specific P-gp inhibitor.
<b>MK571</b>	Highly specific MRP2 inhibitor
<b>Fumitremorgin</b>	Highly specific BCRP inhibitor

Table 25: Proposed inhibitors for the transporter proteins P-gp, MRP2 and BCRP.

Since it was decided that the main focus of the MEMTRANS project will be the P-gp, the only inhibitor that will be used in the content of the project was decided to be LY33579. The inhibitor will be present at the same concentration in both the Apical and Basolateral compartments throughout the time course of the permeability experiments. GF120918 could be used as a second option.

### 3. SELECTION OF THE SYSTEM SUITABILITY MARKERS

#### 3.1. INTRODUCTION

A potential issue with cell based models is that the integrity of the tight junctions in the cell monolayers can be compromised. The permeability across the compromised monolayer is often much higher compared with the intact monolayers, and the permeability becomes high in both directions. In that case, the efflux ratio often becomes unity, and the test compound is classified as a non-substrate even it is a true substrate. Thus cell integrity and permeability should be checked before and after conducting the experiment since in some cases drug substances used in high concentrations may damage the integrity of the cells. For example several influx and efflux transporters are expressed in Caco-2 cells under standard cell culture conditions. However the functional expression of drug transporters in Caco-2 cells may vary significantly depending on the passage number and minor changes in culture conditions. Thus activity of the transporters should also be checked for the standardisation of the experimental conditions<sup>73</sup>.

Quality control markers will be selected in order to control the suitability of the cell lines for the different levels of transport levels, such as low and high permeability markers, along with the control for the level of P-gp expression are for sure of crucial importance for the development of the novel in-vitro system. The efficiency of the cells should be checked before every experiment to ensure the suitability of the cells for the further transport experiments.

The selection of the markers has been based on literature data and on the feasibility of implementing the measurements in the partner's laboratories.

#### 3.2. QUALITY CONTROL MARKERS

Different quality control markers can be used to check if a cell barrier is acceptable for transport studies. Markers for paracellular, transcellular, and stagnant aqueous layer resistance will be selected as these parameters are used as covariables for transport modelling in order to reduce the interlaboratory variability.

##### 3.2.1. Trans-Epithelial Electrical Resistance (TEER) measurement

The ability to form tight epithelial-like monolayers will be checked by means of the trans-epithelial permeability measurement (TEER) with chopstick electrodes. This method provides a quick, non-destructive and easy evaluation of monolayer tight junction integrity. The TEER value option is particularly cost-effective in its ability to identify unusable membranes, thus saving the time and media associated with performing an assay on unsuitable membranes. Higher electrical resistance across a membrane indicates well-formed junctions and a healthy membrane suitable for permeability tests. The measure will be performed before and after the permeability experiments<sup>179,180</sup>.

##### 3.2.2. Markers for paracellular and transcellular permeability

Paracellular flux (or permeability) represents a marker for the status of the intercellular junctions when polarized monolayers are formed. When correctly constitutes as a polarized and selective barrier sealed by tight junctions, they present no or minimal paracellular flux leaving the transcellular pathway as the only way to cross the monolayer. The use of molecules, such as Mannitol or Lucifer Yellow, that are unable to cross transcellularly and the study of their flux and permeability values allow to evaluate the barrier status of the polarized cell monolayers grown on top of microporous membranes.

Two permeability markers; a hydrophobic paracellular marker (lucifer yellow or mannitol) and a hydrophilic paracellular marker (metoprolol) showed to demonstrate consistent permeability values over the different passage numbers<sup>73,181,182,183,184,185</sup>. There is another hydrophilic paracellular

permeability marker (Propranolol) that has been stated in the literature but in the recent publications this marker was found to be a substrate and an inhibitor of P-gp<sup>115</sup>.

The first mentioned three compounds are widely used in the literature for controlling the cell integrity<sup>73,79,149,181,182,183,184,185,186,187,188</sup>. Thus it is proposed that reproducibility of the results for mannitol, lucifer yellow and metoprolol, can be used within this project for the confirmation that the cell monolayers are not compromised with demonstrating both non-permeability and 100% permeability through the cell junctions respectively.

Another marker is needed that will demonstrate 50% intestinal permeability through the cell junctions for the optimisation of the in-vitro system. Atenolol is previously tested in terms of permeability using Caco-2 cells.  $P_{app}$  value was found to be  $0.59 \pm 0.056 \times 10^{-6}$  cm/s. This molecule can be used as a marker for the system suitability tests corresponding to the 50% in-vivo permeability<sup>149</sup>.

Chemical structure and physicochemical properties of the substances are as follows:

### 3.2.2.1. Mannitol

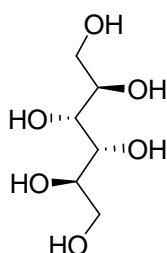
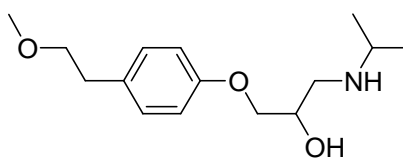


Figure 35: Chemical Structure of Mannitol

<b>Category</b>	Diuretic
<b>Formula</b>	$C_6H_{14}O_6$
<b>Molecular weight</b>	182.17 g/mol
<b>Solubility</b>	Freely soluble
<b>Availability</b>	SA/LGC/VWR
<b>Log P</b>	-3.506
<b>Log D</b>	- 3,10
<b>pKa</b>	na
<b>In-vivo absorption (permeability %)</b>	7 %
<b>Protein binding</b>	0 %
<b>Minimum dose /maximum dose (mg)</b>	na
<b>BCS Classification</b>	na

Table 26: Physicochemical characteristics of Mannitol<sup>120,121,122</sup>.

### 3.2.2.2. Metoprolol



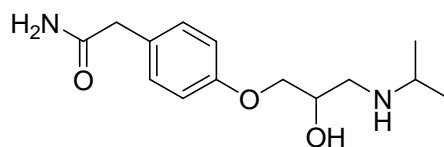
metoprolol

Figure 36 : Chemical Structure of Metoprolol

<b>Category</b>	Cardiovascular agent
<b>Formula</b>	C <sub>15</sub> H <sub>25</sub> NO <sub>3</sub>
<b>Molecular weight</b>	267.364 g/mol
<b>Solubility</b>	Sparingly soluble
<b>Availability</b>	SA/LGC/VWR
<b>Log P</b>	2.477
<b>Log D</b>	0,07
<b>pKa</b>	na
<b>In-vivo absorption (permeability %)</b>	100 %
<b>Protein binding</b>	12 %
<b>Minimum dose /maximum dose (mg)</b>	25/100
<b>BCS Classification</b>	Class I

Table 27: Physicochemical characteristics of Metoprolol<sup>120,121,122</sup>.

## 3.2.2.3. Atenolol



atenolol

Figure 37: Chemical Structure of Atenolol

<b>Category</b>	Cardiovascular agent
<b>Formula</b>	C <sub>14</sub> H <sub>22</sub> N <sub>2</sub> O <sub>3</sub>
<b>Molecular weight</b>	266.336 g/mol
<b>Solubility</b>	Sparingly soluble
<b>Availability</b>	SA/LGC/VWR
<b>Log P</b>	0.5
<b>Log D</b>	-0,54
<b>pKa</b>	na
<b>In-vivo absorption (permeability %)</b>	50 %
<b>Protein binding</b>	6-16 %
<b>Minimum dose /maximum dose (mg)</b>	25/100
<b>BCS Classification</b>	Class III

Table 28: Physicochemical characteristics of Atenolol<sup>120,121,122</sup>.

### 3.3. MARKERS FOR P-GP LEVEL EXPRESSION

Decision on methods to determine the level of P-gp expression along with the activity of this protein was showed during MEMTRANS 2<sup>nd</sup> meeting. It was proposed that P-gp expression can be checked with Rhodamine 123 as well as with Calcein using this fluorescence probes as P-gp substrates.

Functional expressions of efflux systems can be demonstrated with techniques such as bi directional transport studies demonstrating a higher rate of transport in the basolateral to apical direction as compared to apical to basolateral direction using selected model drugs and chemicals at concentrations that do not saturate the efflux system. (e.g. Cyclosporine A, Vinblastin, Rhodamine 123)<sup>1</sup>.

Other method to determine the level of P-gp expression along with the activity of this protein is the use of fluorescence probes as P-gp substrates such as Calcein Assay.

#### 3.3.1. Rhodamine 123

Rhodamine 123 is a lipophilic cationic fluorescent dye that has often been used for studying the functional activity of P-gp. When used as a probe for study of the P-gp activity either release or accumulation of the substance in the presence or absence of P-gp modulators can be used<sup>189</sup>. A general efflux modifier Cyclosporine A (CsA) can be used for the inhibition of transporters. The fluorescence intensity after efflux in the absence of CsA is subtracted that of in the presence of CsA to minimize the effects of the transport not mediated by P-gp and non specific changes in the fluorescent activity. It was shown that there is a good over all concordance between measurement of Rhodamine efflux and mdr1 expression which is responsible for the P-gp secretion. The Pearson correlation coefficient for the tested 58 cell lines were reported as 0,788 with a p value of <0,0001<sup>104,190,191</sup>. Thus Rhodamine 123 is proposed as the control agent of P-gp expression in the cells. The chemical structure and physicochemical properties of Rhodamine 123 are as follows:

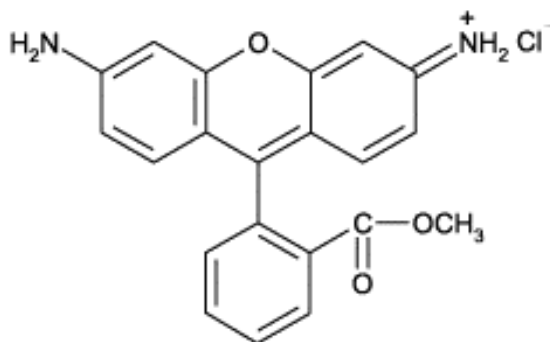


Figure 38: Chemical Structure of Rhodamine 123

<b>Category</b>	na
<b>Formula</b>	C <sub>21</sub> H <sub>17</sub> N <sub>2</sub> O <sub>3</sub>
<b>Molecular weight</b>	345.3 g/mol
<b>Solubility</b>	Practically insoluble
<b>Availability</b>	SA/VWR
<b>Log P</b>	na
<b>Log D</b>	na
<b>pKa</b>	na
<b>In-vivo absorption (permeability %)</b>	na
<b>Protein binding</b>	na
<b>Minimum dose /maximum dose (mg)</b>	na
<b>BCS Classification</b>	na

Table 29: Physicochemical characteristics of Rhodamine 123<sup>120,121,122</sup>

### 3.3.2. Calcein Assay

The Calcein Assay is an in vitro assay to assess the expression and the activity of MDR1/Pgp (ABCB1) as well as other non-Pgp efflux systems relevant to drug transport. This method allows each laboratory to characterize their cell lines for MDR activity.

The functions of the multidrug resistance protein ABCB1/MDR1/Pgp is assessed by measuring the accumulation of a fluorescent dye, calcein, in cells e.g. by flow cytometry. In the in vitro assay calcein AM is added to the cells, and this compound is converted into free calcein by intracellular esterases. Since calcein AM is extruded from multidrug-resistant cells, the reduced intracellular fluorescence reflects MDR1 activity. The quantitative MDR1 activity factors (MAFMDR) are calculated from the calcein AM extrusion assay by using efficient inhibitors of the multidrug resistance protein. This relatively simple and rapid in vitro functional assay provides a reliable quantitative measure for cellular multidrug resistance and the activity of the MDR1 protein. For flow cytometry measurements of calcein uptake, cells are pre-incubated with verapamil or with solvent (HBSS) for 5 minutes at RT. Thereafter 0.25 µM calcein AM is added and the cells are incubated for 10 min at 37 °C. Reaction is stopped by rapid centrifugation. Non-living cells are detected and gated out by propidium iodide staining.

### 3.3.3. Western blot

Western blot is a technique to measure the amount of transporter proteins in the assay system. The method is set up and validated using recombinant rat Mdr1b and human MDR1 (Pgp) expressed in Sf9 cells using baculoviral transfection. Both proteins could be successfully detected using the antibody C219 (figure 39). Then, the calcein assay is used to monitor the activity of the transporter. HL-60-MDR cells expressing human MDR1 (Pgp) were incubated with 250 nM calcein AM and different concentrations of verapamil (Pgp inhibitor). Increasing concentrations of verapamil increased the rate of calcein AM permeability across the cell membrane yielding higher rate of calcein formation and fluorescence buildup (figure 40).

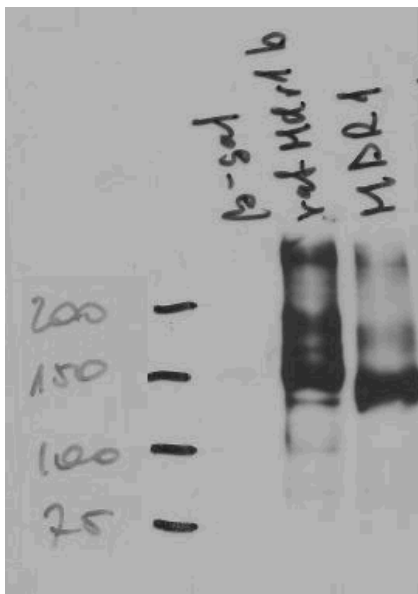


Figure 39: Sf9 membrane vesicles (10 µg/lane) containing the transporter separated by SDS page. Western blot performed using the Pgp specific C219 antibody.  
 Lane 1. control, lane 2: rat Mdr1b, lane 3: human MDR1.

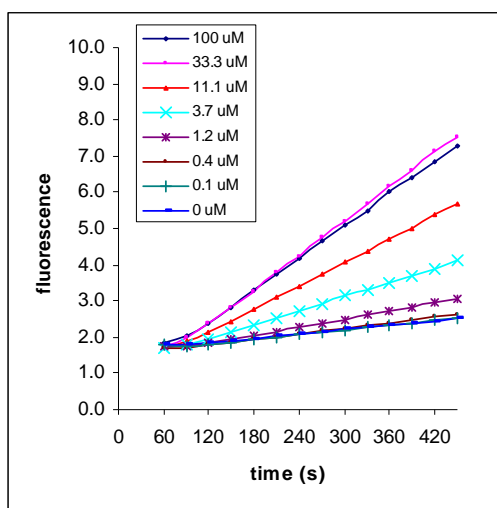


Figure 40: Fluorescence buildup (calcein formation) in time in the presence different concentrations of verapamil in the calcein assay using HL60-MDR1 cells.

## 4. CELL LINE SELECTION

### 4.1. INTRODUCTION

Cells that are evaluated in the extend of this report are selected from previous studies based on in-vitro prediction of drug absorption, initial list of the cells that are listed at the Memtrans web page, further literature search, recently released FDA guideline<sup>192</sup> and Memtrans project proposal.

The main criteria for the selection of the cell line is based on transporter expression profiles of the cells, morphological and biological similarities to the intestinal mucosa, previous correlations with the intestinal absorption that are gathered from the publications, availability of the cells during and after the project.

### 4.2. CELL LINES

#### 4.2.1. TC7

These cells are cloned from Caco-2 cells and can be provided by ATCC. They generally share the same characteristics with the Caco-2 cells other than 2-fold lower expression of the P-gp and 26 hours of doubling time which is 30 for Caco-2 cells. There is also a TC7 3-day model which completes its maturation in 3 days. Previous works on these cell lines are given below

TC7 cells cultured for 21 days differentiated in a single monolayer of polarized enterocyte-like cells with apical brush border, cell-to-cell tight junctions and basolateral membrane adherent to the support. Furthermore, the presence of a homogeneous cell population in its morphological aspect was shown by ultra structure analysis suggesting that most TC7 cells were at the same degree of differentiation. These characteristics highlighted the TC7 clone as a suitable model for permeation assays but required a time-consuming and costly culture period. High levels of growth factors added in the culture media (*e.g.*, EGF, insulin, progesterone, butyric acid) reduce maturation from 21 to 3 d. Observations showed that incomplete cell differentiation occurred with heterogeneous cell aspect and dimension, poor apical microvilli and important intercellular spaces by culturing TC7 cells with the standard Biocoat® serum-free culture media. These results indicated that the 3-d model is undifferentiated compared with the 21-d model and even these images did not allow to conclude whether cells are at different maturation levels or whether they expressed various phenotypes as described for other cell. TC7 cells cultured in conventional and accelerated culture media, it is found that the level of maturation of the 3-d model was lower in both morphologic and biochemical aspects. This indicated the limited application of TC7/3-d cultures for study of the impact of metabolism in drug absorption. The expression of carrier-mediated transport also appeared too low to evaluate the potential of absorption of compounds actively absorbed. However, using the TC7 cell line without fetal calf serum, comparable results were found between the 3-d and the 21-d culture systems for passively absorbed compounds with high potential of rank ordering of compounds. The in vitro/in vivo correlations obtained with both systems suggested that they are valuable tools to determine the absorption of passively permeable compounds. They are less time consuming and have increased efficiency when the 3-d model is used<sup>193</sup>.

The TC-7 clone exhibits morphological characteristics similar to those of the parental Caco-2 cell line, concerning apical brush border, microvilli, tight junctions and polarization of the cell line. The TC-7 clone however appeared more homogenous in terms of cell size. Both cell lines achieved similar monolayer integrity towards mannitol and PEG-4000. Monolayer integrity was achieved earlier for the TC-7 clone, mainly due to its shorter doubling time, *i.e.* 26 versus 30 hours for parental Caco-2 cells. When using cyclosporine A as a P-glycoprotein substrate, active efflux was lower in the TC-7 clone than in the parental Caco-2 cells. The Papp and mechanisms of transport (paracellular or transcellular routes, passive diffusion and active transport) were determined for 20 drugs. A relationship was

established between the *in vivo* oral absorption in humans and Papp values, allowing to determine a threshold value for Papp of 2 10<sup>-6</sup> cm/sec, above for which a 100% oral absorption could be expected in humans. Both correlation curves obtained with the two cell types were almost completely super imposable. These studies also confirmed that the dipeptide transporter is under expressed in both cell lines<sup>194</sup>.

Although the fast maturation TC7 model is time efficient, its morphological characteristics such as leaky tight junctions and undifferentiated structure along with the inability to express P-gp shows the inappropriateness of this cell line for Memtrans. 21 day cultured TC7 cells are similar in different aspects to the parental Caco-2 cell line as mentioned above. But this cell line express the P-gp 2-fold less than the parental Caco-2 cell line which also contradicts with the aim of the Memtrans project. So it is proposed that no further evaluation of these two cell lines is necessary in the extent of the project.

#### 4.2.2. LLC-PK1:MDR1

LLC-PK<sub>1</sub> are pig kidney epithelial cells. They are transformed with human MDR1 gene for the construction of the LLC-PK1:MDR1 clone. These cell lines stably express the p-gp. It is possible to determine if a substance is a substrate and actively transporter with P-gp by the comparison of apparent permeability values between transfected and not transfected cell lines. LLC-PK1 cells are available in ATCC but the MDR1 transfected cell line is not commercially available. Previous works carried out with this cell line is given below.

The LLC-PK1:MDR1, LLC-PK1 and Caco-2 cell lines were used to investigate whether Rhodamine-123 or doxorubicin would be the preferred substrate to study P-glycoprotein (P-gp) functionality *in vitro*. Both Rhodamine-123 and doxorubicin showed highly polarized transport in the Caco-2 cell line and the LLC-PK1:MDR1 cell line, indicating that P-gp is actively transporting these drugs. However, for Rhodamine-123 polarized transport was also seen in the monolayers of the wild-type LLC-PK1 cell line, indicating the presence of another active transporter for this compound. Polarized transport of doxorubicin in the Caco-2 and the LLC-PK1:MDR1 cell lines could be inhibited by the P-gp inhibitors SDZ-PSC 833 (PSC 833), Cyclosporin A (CsA), verapamil and quinine, but not by the inhibitors for the organic cation carrier systems cimetidine and tetraethylammonium (TEA). Polarized transport of Rhodamine-123 in the Caco-2 cell line could only be inhibited by P-gp inhibitors. In the LLC-PK1:MDR1 and LLC-PK1 cell lines transport was also inhibited by inhibitors for the organic cation transport systems<sup>195</sup>.

The transport behaviour of ritonavir, indinavir and amprenavir in the presence and absence of P-gp modulators and probenecid was investigated in an *in vitro* blood-brain barrier (BBB) co-culture model and in monolayers of LLC-PK1, LLC-PK1:MDR1, LLC-PK1:MRP1 and Caco-2 cells. All three HIV protease inhibitors showed polarized transport in the BBB model, LLC-PK1:MDR1 and Caco-2 cell line. The P-gp modulators SDZ-PSC 833, verapamil and LY 335979 inhibited polarized transport, although their potency was dependent on both the cell model and the HIV protease inhibitor used. Ritonavir and indinavir also showed polarized transport in the LLC-PK1 and LLC-PK1:MRP1 cell line, which could be inhibited by probenecid. HIV protease inhibitors were not able to inhibit competitively polarized transport of other HIV protease inhibitors in the LLC-PK1:MDR1 cell line. It has been found that P-gp inhibitors were not able to completely inhibit the polarized fashion thus it is suggested that other transporters also plays a role in the active transport of these drugs. And ritonavir as well as indinavir showed polarized transport due to the effect of a transporter other than P-gp<sup>148</sup>.

Immunoblot analysis of P-glycoprotein expression using the mAb anti-P-glycoprotein C219 revealed that L-MDR1 cell expressed high levels of P-glycoprotein, while the parental cell line, LLC-PK1, showed little if any detectable P-glycoprotein (Fig. 1). Caco-2 cells, however, had a readily detectable, but significantly lower amount of expressed P-glycoprotein than L-MDR1 cells (Fig. 1). Indinavir, nelfinavir, and saquinavir cellular translocation was markedly greater when [14C]-labelled drug was administered to the basal side of cultured, L-MDR1, and Caco-2 cells and its appearance measured on the apical side (basal-apical) compared to addition of drug to the opposite compartment

(apical-basal). In LLC-PK1 cells, such apical basal and basal-apical transport differences were absent for nelfinavir and saquinavir; however with indinavir, a significantly greater basal-apical versus apical-basal transport was observed in LLC-PK1 cells, although the net basal-apical transport was greater in the L-MDR1 cells. Furthermore, the addition of quinidine or PSC-833 to Caco-2 cells markedly reduced the directional transport difference<sup>58</sup>.

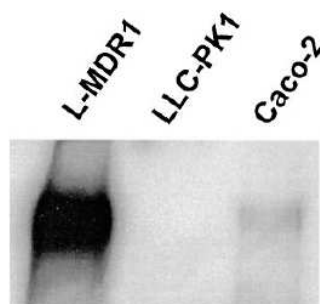


Figure 41: Expression of the P-gp in L-MDR1, LLC-PK1, Caco-2 cells<sup>58</sup>

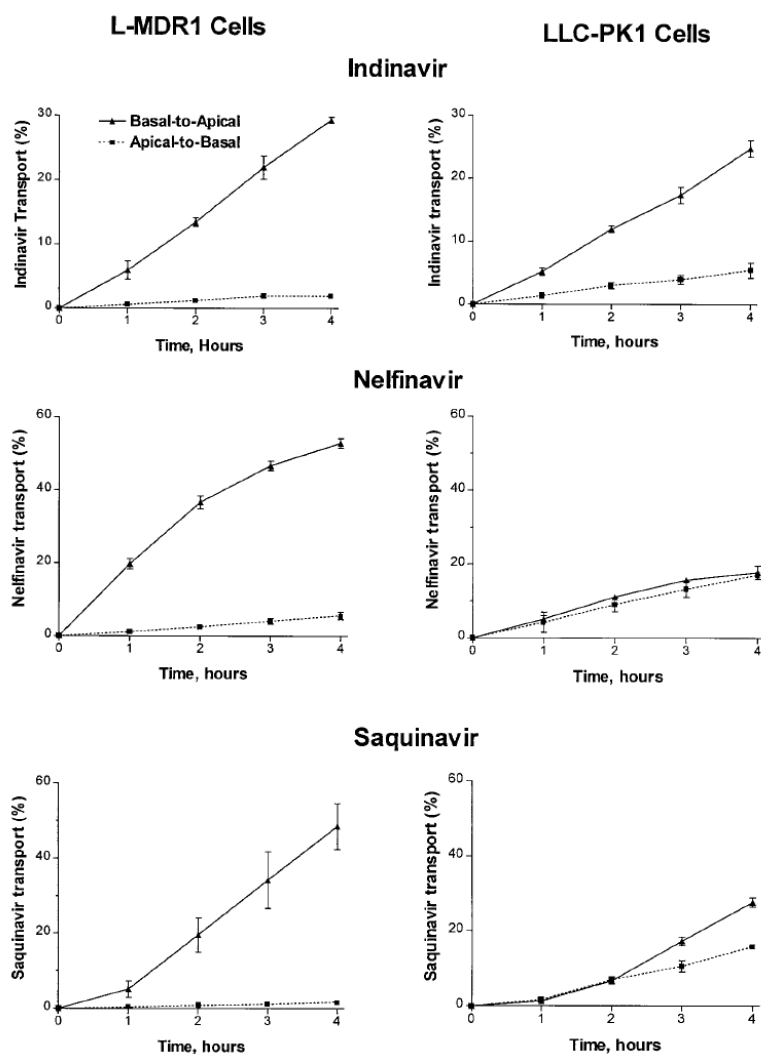


Figure 42: Transport of HIV protease inhibitors in L-MDR1 and LLC-PK1 cells<sup>58</sup>.

The drawbacks of the above mentioned cell line are the lack of commercial availability and presence of uncharacterized carriers that are active in terms of drug active transport which may lead to false results through out the project. This can be overcome by comparison of the permeability profiles with the wild type LLC-PK1 cells. But it is also possible to transfect parental LLC-PK1 cell line with human *mdr1a* and *mrp2* and *bcrp* genes for the selective expression of these proteins. It has been also reported that this cell line were superior to Caco-2 cells in adenovirus infection thus they can be used if the transduction of the Caco-2 cells is not successive<sup>196</sup>. Also it is important that wild type cells does not contain P-gp, MRP2 or BCRP

### 4.2.3. LS180

LS180 cells are derived from human colon carcinoma cells and are an established intestinal in-vitro system of intestinal mucus to measure P-gp and CYP3A4 induction. These cells are commercially available in ATCC cell line collection. Previous works conducted with this cell line are given below.

### 4.2.4. MDCK cell lines

#### 4.2.4.1. Wild type MDCK cell lines

A non-intestinal cell line, MDCK or Madin-Darby canine kidney, has also been investigated as an in vitro cell culture model for permeability screening. Although MDCK cells are a useful system for investigating renal transport processes, their application as an intestinal model requires further evaluation. The main advantage of the MDCK cell assay is its potential for increasing throughput. Unlike standard Caco-2 cells, MDCK cells may be used for permeability studies in as little as 3 days after seeding. MDCK cells grown for 2 days under standard conditions form confluent monolayers with completely developed tight junction networks and constant transepithelial electrical resistances (TEERs). One study reported that cells seeded at high densities were fully polarized by this time, whereas other studies reported that MDCK cells were partially differentiated after 3–4 days; however, they functionally expressed brush border alkaline phosphatase and polarized amino acid transporters. Apparent permeability values measured with 3-day MDCK cells correlate well with those from Caco-2 cells, which in turn correlate to in vivo intestinal absorption. Although MDCK cells seem promising as a model of passive intestinal drug transport, carrier mediated transport will likely be different from that in the human intestine because of species and organ differences. In addition to amino acid transporters, MDCK cells express the efflux transporter P-glycoprotein (P-gp), an organic cation transporter, and peptide transporters. Although transporters across species may share structural and functional characteristics, differences may arise in kinetic parameters and substrate specificity<sup>159,197,198</sup>.

Using MDCK wild type cell line in the extend of this project would not contribute to the aim of the project as determination of the specific transporter protein for related molecules since different proteins are expressed in this cell line. Thus there is no need for further evaluation of this cell line for their use in the project.

#### 4.2.4.2. Transfected MDCK cell lines

MDCK cell line was previously transfected with human *mdr1* gene and *mrp2* gene separately for the stable expression of these proteins in different clones of this cell line. MDCK cells exhibit similar growth curves as the MDCK cells but they reach the stationary phase later (10 days after seeding)<sup>199</sup>. Previous prediction of absorption using transfected MDCK cells are given below

P-glycoprotein (P-gp) expression in Caco-2 cells was compared with P-gp expression in MDCK wild- type (MDCK-WT) and MDCK-MDR1 cells using Western blotting methods. The polarized efflux activities of P-gp(s) in MDCK-MDR1 cells, MDCK-WT cells, and Caco-2 cells were compared using digoxin as a substrate. Apparent Michaelis–Menten constants ( $K_M$ ,  $V_{max}$ ) for the efflux of vinblastine in these three cell lines were determined. Apparent inhibition constants ( $K_I$ ) of

known substrates/inhibitors of P-gp were determined by measuring their effects on the efflux of digoxin in Caco-2 or MDCK-MDR1 cell monolayers. MDCK-MDR1 cells expressed higher levels of P-gp compared to Caco-2 and MDCK-WT cells, as estimated by Western blots. Two isoforms of P-gp were expressed in Caco-2 and MDCK cells migrating with molecular weights of 150 kDa and 170 kDa. In MDCK-MDR1 cells, the 150 kDa isoforms appeared to be overexpressed. The MDCK-MDR1 cells exhibited higher polarized efflux of [<sup>3</sup>H]-digoxin than did Caco-2 and MDCK-WT cells. *K<sub>M</sub>* values of vinblastine in Caco-2, MDCK-WT, and MDCK-MDR1 cells were  $89.2 \pm 26.1$ ,  $24.5 \pm 1.1$ , and  $252.8 \pm 134.7$  M, respectively, whereas *V<sub>max</sub>* values were  $1.77 \pm 0.22$ ,  $0.42 \pm 0.01$ , and  $2.43 \pm 0.86$  pmolcm<sup>-2</sup>s<sup>-1</sup>, respectively. Known P-gp substrates/inhibitors showed, in general, lower *K<sub>I</sub>* values for inhibition of digoxin efflux in Caco-2 cells than in MDCK-MDR1 cells.

Caco-2 cells and MDCK cells are derived from different species (human vs. dog) and different tissues (colonic carcinoma vs. kidney) and they serve different biologic roles. These different biologic roles may lead to differences in the lipid composition of their membrane bilayers. The phenomena of different sorting of glycosphingolipids between Caco-2 cell and MDCK cells have been reported previously. For example, Van't Hof *et al.* observed that, in MDCK and Caco-2 cells, glucosylceramide and sphingomyelin synthesized from the short-chain sphingolipid analog *N*-6-[7-nitro-2,1,3-benzoxadiazol-4-yl] aminodecanoyl-ceramide were delivered to the cell surface with different AP/BL ratios of 2–4 and 0.6–0.9, respectively. Furthermore, different strains of cells from the same tissue may have different lipid composition as well. For example, of the total glycosphingolipid content, MDCK strain I cells were reported to express 56% glucosylceramide and 6% galactosylceramide, whereas MDCK strain II cells express 28% glucosylceramide and 16% galactosylceramide (In summary, MDCK-MDR1 cells overexpressed significant amounts of P-gp, which migrated at an apparent molecular weight of 150 kDa. The MDCK-MDR1 cells exhibited increased polarized efflux of known substrates of P-gp compared to wild-type MDCK cells. Therefore, this transfected cell line may be a useful model for qualitatively screening P-gp substrate activity of drugs/drug candidates. However, the apparent kinetics constants (*K<sub>M</sub>*, *V<sub>max</sub>*) and affinity constants (*K<sub>I</sub>*) of substrates/inhibitors determined in MDCKMDR1 cells may be different from the values obtained when experiments are conducted in Caco-2 cells. These differences may result from the different levels of total P-gp expressed in Caco-2 vs. MDCK-MDR1 cells, different orientations of P-gp in the Caco-2 vs. MDCK-MDR1 cell membranes, or different partitioning of substrates/inhibitors into these two cell membrane bilayers<sup>200</sup>

To investigate whether Madin-Dabny canine kidney cells transfected with the human MRP2 gene (MDCK-MRP2) are a good model of the human intestinal mucosa MRP2 expression in Caco-2 cells was compared with the expression of this efflux transporter in MDCK-wild type (MDCK-WT) and MDCK-MRP2 cells using Western blotting methods. The polarized efflux activities of MRP2 in the MDCK-MRP2, MDCK-WT, MDCK cells transfected with the human MDR1 gene (MDCK-MDR1), and Caco-2 cells were compared using vinblastine as a substrate. Apparent Michaelis-Menten constants (*K<sub>M</sub>*, *V<sub>max</sub>*) for the efflux of vinblastine in Caco-2 and MDCK-MRP2 cells were determined in the presence of GF120918 (2 μM), which inhibits P-glycoprotein but does not affect MRP2. Apparent inhibitory constants (*K<sub>I</sub>*) of known substrates/inhibitors of MRP2 were determined by measuring their effects on the efflux of vinblastine in these cell lines. Results. MDCK-MRP2 cells expressed higher levels of MRP2 than MDCK-WT and Caco-2 cells as measured by Western blotting technique. Two isoforms of MRP2 expressed in Caco-2 and MDCK cells migrated at molecular weights of 150 kD and 190 kD. In MDCK-MRP2 cells, the 150 kD isoform appeared to be overexpressed. MDCK-MRP2 cell monolayers exhibited higher polarized efflux of vinblastine than Caco-2 and MDCK-WT cell monolayers. *K<sub>M</sub>* values for vinblastine in Caco-2 and MDCK-MRP2 cells were determined to be  $71.8 \pm 11.6$  and  $137.3 \pm 33.6$  μM, respectively, and *V<sub>max</sub>* values were determined to be  $0.54 \pm 0.03$  and  $2.45 \pm 0.31$  pmolcm<sup>-2</sup>s<sup>-1</sup> [1], respectively. Known substrates/inhibitors of MRP2 showed differences in their ability to inhibit vinblastine efflux in Caco-2 cells as compared to MDCK-MRP2 cells. These data suggest that MDCK-MRP2 cells over express only the 150 kD isoform of MRP2. The 190 kD isoform, which was also found in Caco-2 cells and MDCK-WT cells, was present in MDCK-MRP2 cells but not

over expressed. The apparent kinetics constants and affinities of some MRP2 substrates were different in Caco-2 cells and MDCK-MRP2 cells. These differences in substrate activity could result from differences in the relative expression levels of the MRP2 isoforms present in Caco-2 cells and MDCK-MRP2 cells and/or differences in the partitioning of substrates in these two cell membrane bilayers<sup>201</sup>.

The bidirectional permeation characteristics of Rhodamine 123 and Hoechst 33342, fluorescence probes of the binding sites on P-glycoprotein (P-gp), across monolayers of MDCK cells transfected with the human *MDR1* gene (MDCK-MDR1) were investigated. The ratios of the apparent permeability coefficients ( $P_{app}$ ) of Rhodamine 123 and Hoechst 33342 flux measured in the basolateral (BL) to apical (AP) direction versus the flux in the AP-to-BL direction ( $P_{app\ BL\ to\ AP}/P_{app\ AP\ to\ BL}$ ) were 115 and 177, respectively. The P-gp inhibitor GF-120918 could significantly reduce the polarized efflux of both Rhodamine 123 and Hoechst 33342. Rhodamine 123 appeared to “stimulate” the polarized efflux of Hoechst 33342 across MDCK-MDR1 cell monolayers. In contrast, Hoechst 33342 partially inhibited the polarized efflux of Rhodamine 123 across these cell monolayers whereas daunorubicin partially inhibited the polarized efflux of both Rhodamine 123 and Hoechst 33342. The uptake characteristics of Rhodamine 123 and Hoechst 33342 in MDCK-MDR1 cells were measured in the absence and presence of GF-120918 and known P-gp substrates (Hoechst 33342, Rhodamine 123, and daunorubicin). The uptake of Rhodamine 123 and Hoechst 33342 in MDCK-MDR1 cells was enhanced more than twofold by inclusion of GF-120918 (2  $\mu$ M) in the incubation medium. Daunorubicin (160  $\mu$ M) increased the relative fluorescence unit (RFU) values of cytoplasm-associated Rhodamine 123 by up to 30%. However, daunorubicin (40  $\mu$ M) and Rhodamine 123 (5  $\mu$ M) decreased the RFU values of cell membrane-associated Hoechst 33342 by 70% and 40%, respectively. To further explore what appears to be a “stimulatory” effect of daunorubicin and Rhodamine 123 on the uptake of Hoechst 33342 and a stimulatory effect of daunorubicin on Hoechst 33342 transport across cell monolayer, uptake of Hoechst 33342 into liposomes in the presence and absence of GF-120918, daunorubicin, and Rhodamine 123 was determined. GF-120918 exhibited no effect on the RFU values of liposome-associated Hoechst 33342. In contrast, Rhodamine 123 and daunorubicin decreased the fluorescence of liposome-associated Hoechst 33342 suggesting these molecules were either quenching the fluorescence of this chemical probe or displacing it from the lipid bilayer. In conclusion, these bidirectional transport data indicate that Rhodamine 123 and Hoechst 33342 are excellent substrates of P-gp in MDCK-MDR1 cells. The ability of Hoechst 33342 to partially inhibit the polarized efflux of Rhodamine 123 is consistent with these substrates binding to the same site on P-gp. In contrast, the ability of Rhodamine 123 to apparently “stimulate” the efflux of Hoechst 33342 in both the transport and uptake experiments suggests the substrates might bind to different sites on P-gp. However, experimental results using liposomes suggested that this “stimulation” phenomenon by Rhodamine 123 on Hoechst 33342 uptake and efflux might simply be an artefact. Thus, the use of Hoechst 33342 to probe the binding sites on a membrane-bound protein such as P-gp might be problematic<sup>202</sup>.

#### 4.2.5. MDCKII cell lines

MDCKII wild type cells does not express any of the transport proteins that are considered in the extend of this project (P-gp, MRP2, BCRP). But in the previous literature they were transfected with *mdr1*, *mrp2* and *bcrp* genes. As a result this gives the opportunity to detect both the affinity of the molecule to the transporter protein and to quantitatively determine the effect of the transporter proteins by comparison of the wild type cells to the transfected cells. Previous works that are gathered from the literature is given below.

MDCKII cell line was transfected with *mdr1*, cMOAT, *mrp2* and compared with Caco-2 cells in terms of protein expression with blotting experiments. The results are as follows<sup>203</sup>

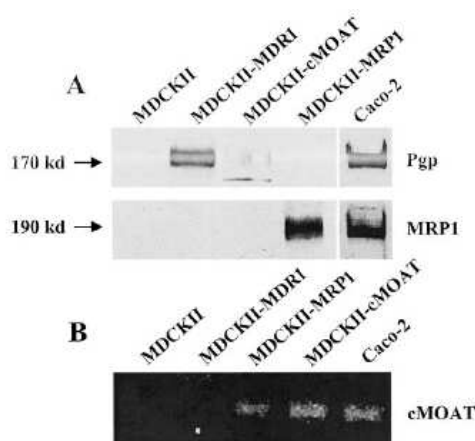


Figure 43: Over expression of P-gp MRP1 and MRP2 in MDCKII cells<sup>203</sup>.

MDCK cells are cultured using wide-ranging conditions and can produce variable results. To develop a standard protocol for studying saquinavir transport using MDCKII cells, stably transfected MDCKII cells overexpressing human P-gp (MDCKII-MDR1) and MDCKII wild-type cells (MDCKII-WT) were used to evaluate the combined effects of seeding density ( $6.9 \times 10^5$  or  $5 \times 10^4$  cells/cm<sup>2</sup>), substratum (polycarbonate  $\pm$  collagen coating) and saquinavir presence on monolayer integrity, P-gp expression, and saquinavir transport. The saquinavir efflux ratio (ratio of BL  $\rightarrow$  AP/AP  $\rightarrow$  BL permeability) for MDCKII-MDR1 cells ( $6.9 \times 10^5$  cells/cm<sup>2</sup>) was 57 with variable mannitol permeabilities. Consistent mannitol permeabilities and higher saquinavir efflux ratios were obtained with  $5 \times 10^4$  cells/cm<sup>2</sup> on polycarbonate or collagen-coated polycarbonate. The MDCKII-WT saquinavir efflux ratio was 9. Saquinavir presence increased paracellular permeability for all treatments relative to cells seeded onto collagen-coated membranes. Collagen coating caused increased P-gp expression and saquinavir efflux ratios correlated ( $r^2 = 0.96$ ) with P-gp expression levels [MDCKII-MDR1 on collagen-coated polycarbonate) > MDCKII-P-GP (on polycarbonate) > MDCKII-WT (on collagen-coated polycarbonate)]. These results directly and quantitatively link interrelated differences in cell culture conditions to changes in monolayer integrity, transporter expression, and active transport; and emphasize the critical application of controls in cell culture models<sup>204</sup>.

In this publication in vitro interaction of different benzimidazoles with the apical ATP-binding cassette drug efflux transporters, breast cancer resistance protein (BCRP/ABCG2), P-glycoprotein (ABCB1), and MRP2 (ABCC2) using MDCKII cell transduced with human MDR1, MRP2, and BCRP, and murine Bcrp1 cDNAs. The results of the transport and inhibition experiments are summarized below<sup>205</sup>.

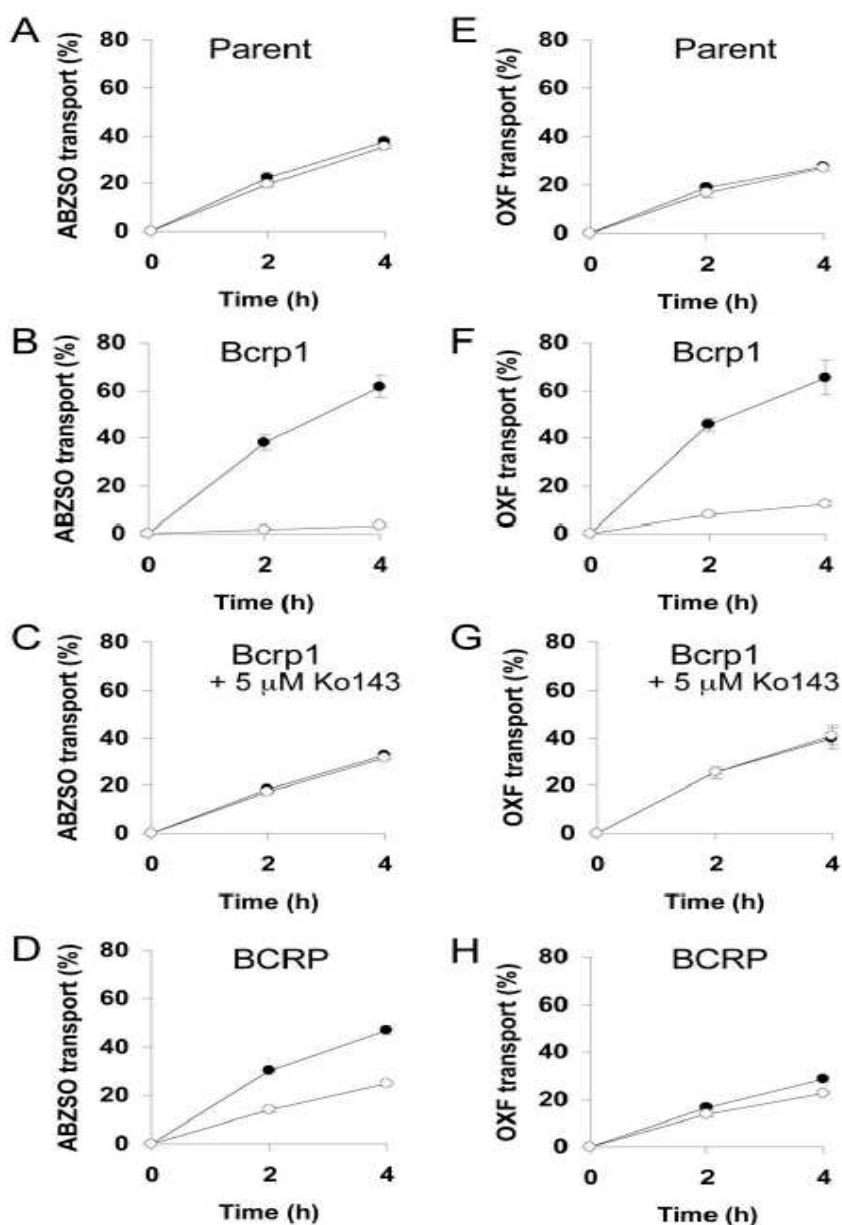


FIG. 1. Transepithelial transport of ABZSO (10  $\mu$ M, left panel) and OXF (10  $\mu$ M, right panel) in MDCKII (parent) (A and E), MDCKII-Bcrp1 (B and C, F and G), and MDCKII-BCRP (D and H) monolayers. The experiment was started with the addition of ABZSO or OXF to one compartment (basolateral or apical). After 2 and 4 h, the percentage of drug appearing in the opposite compartment was measured by HPLC and plotted. BCRP inhibitor Ko143 (C and G) was present as indicated. Results are the means; error bars indicate the standard deviations ( $n = 3$ ). Closed circles, translocation from the basolateral to the apical compartment; open circles, translocation from the apical to the basolateral compartment. The apparent permeability coefficient ( $P_{app}$ ) corresponding to 10% of transport in 1 h was  $12.3 \cdot 10^{-6}$  cm/s.

Figure 44: Graphics of the transport and inhibition experiments on BCRP protein<sup>205</sup>.

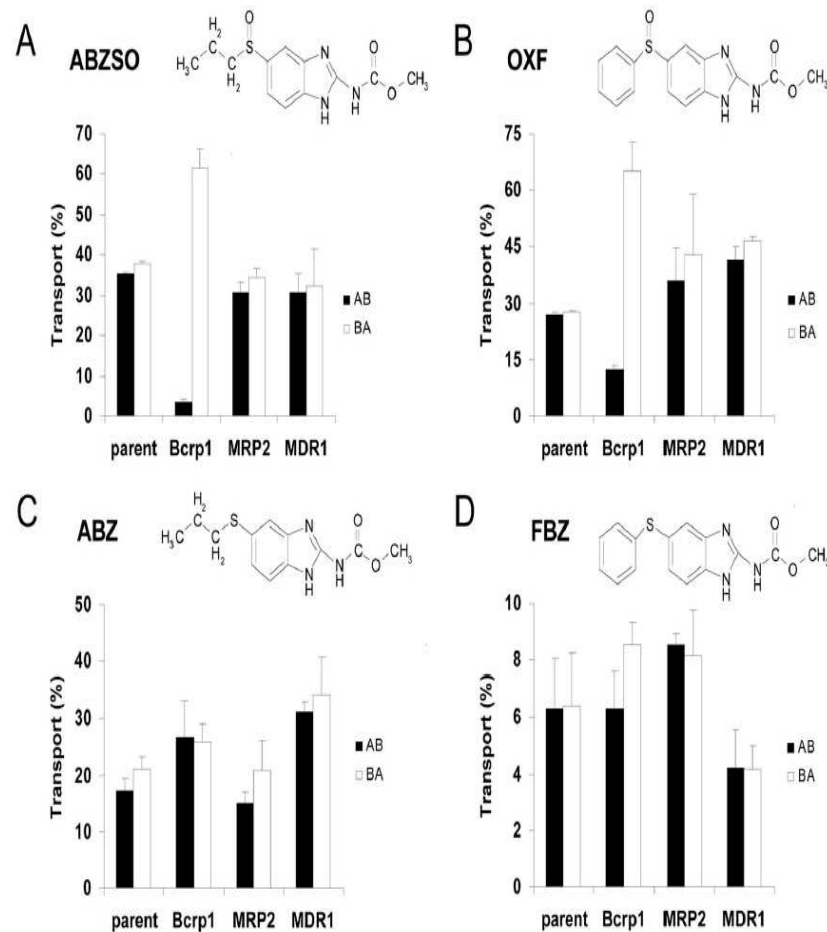


FIG. 2. Transepithelial transport of ABZSO (A), OXF (B), ABZ (C), and FBZ (D) in MDCKII (parent), MDCKII-Bcrp1, MDCKII-MRP2, MDCKII-MDR1, and monolayers. The experiment was started with the addition of the tested compound (10  $\mu$ M) to one compartment (basolateral or apical). After 4 h, the percentage of drug appearing in the opposite compartment was measured by HPLC and plotted. Results are the means; error bars indicate the standard deviations ( $n = 3$ ). BA, translocation from the basolateral to the apical compartment; AB, translocation from the apical to the basolateral compartment. The  $P_{app}$  corresponding to 10% of transport in 1 h was  $12.3 \cdot 10^{-6}$  cm/s. Chemical structures of the compounds and some data (A and B, MDCKII-Bcrp1) from Fig. 1 are included for comparison.

Figure 45: Graphics of the transport experiments with all of the proteins<sup>205</sup>.

#### 4.2.6. Caco-2 Cell Lines

Prediction of drug bioavailability is mostly proven in absorption experiments with Caco-2 cells under controlled conditions. Caco-2 cells are differentiated cells of human colorectal carcinoma which can be provided by American Type Culture Collection (ATCC). They form a monolayer and develop a well-defined brush border on the apical surface, as well as tight cellular junctions. Caco-2 cells serve as an *in vitro* model of the human intestinal epithelial cells<sup>206</sup>.

This investigation describes the expression and inter individual variability in transcript levels of multiple drug efflux systems in the human jejunum and compares the expression profiles in these cells with that of the commonly used Caco-2 cell drug absorption model. Transcript levels of ten-drug efflux proteins of the ATP-binding cassette transporter family [MDR1, MDR3, ABCB5, MRP1–6, and breast cancer resistance protein (BCRP)], lung resistance-related protein (LRP), and CYP3A4 were determined using quantitative polymerase chain reaction in jejunal biopsies from 13 healthy human subjects and in Caco-2 cells. All genes except *ABCB5* were expressed, and transcript levels varied between individuals only by a factor of 2 to 3. Surprisingly, *BCRP* and *MRP2* transcripts were more abundant in jejunum than *MDR1* transcripts. Jejunal transcript levels of the different ABC transporters spanned a range of three log units with the rank order: *BCRP* = *MRP2* > *MDR1* = *MRP3* = *MRP6* = *MRP5* = *MRP1* > *MRP4* > *MDR3*. Furthermore, transcript levels of 9 of 10 ABC transporters correlated well between jejunum and Caco-2 cells ( $r^2 = 0.90$ ). However, *BCRP* exhibited a 100-fold lower transcript level in Caco-2 cells compared with jejunum. Thus, the expression of a number of efflux protein transcripts in jejunum are equal to, or even higher than, that of *MDR1*, suggesting that the roles of these proteins (in particular *BCRP* and *MRP2*) in intestinal drug efflux have been underestimated. Also, we tentatively conclude that the Caco-2 cell line is a useful model of jejunal drug efflux, if the low expression of *BCRP* is taken into account<sup>206</sup>.

The expression levels of mRNAs for MDR1 (P-glycoprotein), multidrug resistance-associated proteins (MRP1, MRP2), and cytochrome P450 3A (CYP3A) in Caco-2 cells were quantitatively compared with those in human duodenal enterocytes, normal colorectal tissues, and colorectal adenocarcinomas. Caco-2 cells (passages 36–88) were kindly supplied by several laboratories in Japan. Human duodenal enterocytes were obtained from five healthy male volunteers. Normal colorectal tissues and colorectal adenocarcinomas were simultaneously obtained from seven patients with primary colorectal adenocarcinoma. MDR1, MRP1, MRP2, and CYP3A mRNA levels were determined by real-time quantitative polymerase chain reactions (PCR). Relative concentrations of mRNAs for target proteins (MDR1, MRP1, MRP2, and CYP3A) and glyceraldehyde-3-phosphate dehydrogenase in Caco-2 cells were  $1.00 \pm 0.15$ ,  $1.02 \pm 0.06$ ,  $0.94 \pm 0.10$ , and  $0.68 \pm 0.60$ , respectively, and those in human enterocytes were about 12, 3, 7, and 8000-fold higher than in the Caco-2 cells, respectively. In contrast, MDR1, MRP1, and CYP3A mRNA levels in Caco-2 cells were comparable to those in normal colorectal tissue and colorectal adenocarcinoma<sup>207</sup>.

Literature describing the comparison of DDI in Caco-2 cells, mouse intestine and human intestine show that the Caco-2 model not only identifies these interactions but also mimics closely their quantitative effects. This implies that all three systems have similar passive Digoxin permeability and/or similar expression of the transporters affecting digoxin permeability, primarily P-gp. The similarity is furthermore verified by the observed values for Digoxin permeability ( $P_{app}$  [ $\times 10^6$  cm/s]), in Caco-2  $2,02 \pm 0,37$ , in mouse ileum  $2,36 \pm 0,42$ , in human ileum/colon  $1,7 \pm 0,6$ . Experiments with Caco-2 cells are able to predict with some accuracy both the relative increase in absorptive  $P_{app}$  of Digoxin on co-administration of a number of drugs and the concentration range over which this effect occurs in human intestine. But changes in Digoxin permeability in Caco-2 cells appear much greater than in human. For example quinidine increases  $C_{max}$  of Digoxin by 1,43-fold in human, and by 4-fold in Caco-2. Furthermore, because interactions like inhibition are often concentration dependent it is important to perform *in vitro* interaction studies at or below the maximum concentrations likely to be obtained in the intestinal lumen *in vivo*<sup>208</sup>.

### 4.3. CONCLUSION

The aim of this project is development of a cell culture method for the prediction of absorption and drug-drug interactions of the efflux system substrates. In order to establish a good in-vitro in-vivo correlation it is for sure of crucial importance to use human colon derived cells since there are differences in the membrane properties and compositions between the kidney cells and the intestinal cells as mentioned above in the literature survey.

The objective to select the most appropriate cell line to optimally suit the overall aims of the proposal was addressed in multiple ways. In addition to the rigorous analysis of the relevant literature, results of preliminary experiments were used in the decision making process.

In particular, there has been a previous characterisation of the cell lines with respect to their MDR status. The Calcein Assay provided in vitro test data that were used for the characterization of the functional expression of MDR transporters.

Previous results obtained by the MEMTRANS partners demonstrate that the endogenous activity of MDR1/Pgp (ABCB1) is negligible in the MDCKII cell line. In contrast, Caco-2 cells exhibit considerable MDR activity that will likely contribute to significant background in the transcellular transport studies. Therefore, MDCK-2 cells seem ideal for the aims of the Proposal. In addition to the deficiency of endogenous transporters, MDCKII cells are compatible with retroviral systems and the relevant functional assays. The preliminary results obtained by convincingly demonstrate that the endogenous activity of MDR1/Pgp (ABCB1) is negligible in the MDCKII cell line. In contrast, Caco-2 cells exhibit considerable MDR activity that will likely contribute to significant background in the transcellular transport studies.

Thus, of the candidate cell lines originally proposed for WP1 (prevalidation) the scope was narrowed down to Caco-2 ATCC; MDCK-II; MDCKII-MDR1.

In conclusion, the following cell lines were selected for the evaluation of the P-gp substrates:

- The first choice for the in-vitro experiments should include Caco-2 cells.
- The second choice is the MDCKII cell line that is not expressing any of the transporter proteins in the wild type cells but can be constructed to express one of the proteins specifically. The drawbacks of this cell line are first the differences in the membrane properties and compositions compared to the colon cells since this cell line is derived from kidney tissue and second the apparent kinetic constants and substrate affinity can be different in MDCKII cell lines due to the differences in the partitioning of substrates into these two cell membrane bilayers.
- The third choice is the transfected MDCKII-MDR1 that are stably expressing one of the transporter proteins with the maximum level expression of the transporter.

Properties of the above mentioned cell lines that can affect the permeation studies are given in tables below.

#### 4.3.1. Caco-2 cells

<b>Species</b>	Human
<b>Tissue</b>	colon
<b>Days after the seeding to begin the experiments</b>	20-26
<b>Culture medium</b>	DMEM
<b>Teer values</b>	220 $\Omega$ .cm <sup>2</sup>

Table 30: Properties of Caco-2 cells

**4.3.2. MDCKII cells**

<b>Species</b>	dog
<b>Tissue</b>	kidney
<b>Days after the seeding to begin the experiments</b>	3-8
<b>Culture medium</b>	DMEM
<b>Teer values</b>	150-200 $\Omega$ .cm <sup>2</sup>

Table 31: Properties of MDCKII cells

## REFERENCES

- <sup>1</sup> Guidance for industry, Waiver of in-vivo bioavailability and bioequivalence studies for immediate release solid oral dosage forms based on a biopharmaceutics classification system, U.S. Department of Health and Human Services, Food and Drug Administration, August, 2000.
- <sup>2</sup> Varma M. V. S. *et al.* Functional role of P-Glycoprotein in limiting intestinal absorption of drugs: contribution of passive permeability to P-glycoprotein mediated efflux transport. *Mol. Pharmaceutics.*, 2(1): 12-21, 2004.
- <sup>3</sup> United States Pharmacopoeia 29, NF 24, 2006.
- <sup>4</sup> Guidance for industry, Drug Interaction Studies Study Design, Data Analysis, and Implications for Dosing and Labeling, Draft Guidance, U.S. Department of Health and Human Services, Food and Drug Administration, September, 2006.
- <sup>5</sup> Riddell J. G. *et al.* Celiprolol. A preliminary review of its pharmacodynamic and pharmacokinetic properties and its therapeutic use in hypertension and angina pectoris. *Drugs*, 34(4): 438-58, 1987.
- <sup>6</sup> Milne R. J. *et al.* Celiprolol. An updated review of its pharmacodynamic and pharmacokinetic properties and therapeutic efficacy in cardiovascular disease. *Drugs*, 41(6): 941-69, 1991.
- <sup>7</sup> Karlsson J., *et al.* Transport of celiprolol across human intestinal epithelial (Caco-2) cells: mediation of secretion by multiple transporters including P-glycoprotein. *Br. J. Pharmacol.*, 110(3): 1009-16, 1993.
- <sup>8</sup> Kuo S. M. *et al.* The contribution of intestinal secretion to the dose-dependent absorption of celiprolol. *Pharm. Res.*, 11(5): 648-53, 1994.
- <sup>9</sup> Terao T. *et al.* Active secretion of drugs from the small intestinal epithelium in rats by P-glycoprotein functioning as an absorption barrier. *J. Pharm. Pharmacol.*, 48(10): 1083-9, 1996.
- <sup>10</sup> Lilja J. J. *et al.* Rifampicin reduces plasma concentrations of celiprolol. *Eur. J. Clin. Pharmacol.*, 59(11): 819-24, 2004.
- <sup>11</sup> Lilja J. J. *et al.* Itraconazole increases but grapefruit juice greatly decreases plasma concentrations of celiprolol. *Clin Pharmacol Ther.*, 73(3): 192-8, 2003.
- <sup>12</sup> Lilja J. J. *et al.* Orange juice substantially reduces the bioavailability of the beta-adrenergic-blocking agent celiprolol. *Clin. Pharmacol. Ther.*, 75(3): 184-90, 2004.
- <sup>13</sup> Cornaire G. *et al.* *Int. J. Pharm.*, 278(1):119-31, 2004.
- <sup>14</sup> Therapeutic drugs. Dollery C ed. Second edition, Churchill Livingstone. 1999.
- <sup>15</sup> Milne R. J. *et al.* Celiprolol: an updated review of its pharmacokinetic properties and therapeutic efficacy in cardiovascular diseases. *Drugs*, 41(6): 941-969, 1991.
- <sup>16</sup> Caruso F. S. *et al.* Celiprolol: pharmacokinetic and duration of pharmacodynamic activity. *Br. J. Clin. Pract.*, 40: 12-6, 1985.
- <sup>17</sup> Lipka E. *et al.* In vivo non-linear intestinal permeability of celiprolol and propranolol in conscious dogs: evidence for intestinal secretion. *Eur. J. Pharm. Sci.*, 6(1): 75-81, 1998.
- <sup>18</sup> Shah V. P. *et al.* Bioanalytical method validation-a revisit with a decade of progress. *Pharm. Res.*, 17(12): 1551-7, 2000.
- <sup>19</sup> Caudron E. *et al.* Simultaneous determination of the acid/base antihypertensive drugs celiprolol, bisoprolol and irbesartan in human plasma by liquid chromatography. *J. Chromatogr. B. Analyt. Technol. Biomed. Life. Sci.*, 801(2): 339-45, 2004.
- <sup>20</sup> Chiu F. C. *et al.* Validated assay for the determination of celiprolol in plasma using high-performance liquid chromatography and a silanol deactivated reversed-phase support. *J. Chromatogr. B. Biomed. Appl.*, 687(2): 462-5, 1996.
- <sup>21</sup> Huizing M. T. *et al.* Pharmacokinetics of paclitaxel and metabolites in a randomized comparative study in platinum-pretreated ovarian cancer patients. *J. Clin. Oncol.*, 11(11): 2127-35, 1993.
- <sup>22</sup> Huizing, M. T. *et al.* Taxanes: a new class of antitumor agents. *Cancer Invest.*, 13(4): 381-404, 1995.
- <sup>23</sup> McGuire W. P. *et al.* Cyclophosphamide and cisplatin compared with paclitaxel in patients with stage III and stage IV ovarian cancer. *N. Engl. J. Med.*, 334(1): 1-6, 1996.
- <sup>24</sup> Jordan M. A. *et al.* Microtubules as a target for anticancer drugs. *Nat. Rev. Cancer.*, 4:253-65, 2004.
- <sup>25</sup> Gao J. *et al.* A Functional Assay for Quantitation of the Apparent Affinities of Ligands of P-Glycoprotein in Caco-2 Cells. *Pharm. Res.*, 18(2): 171-176, 2001.
- <sup>26</sup> Walle U. K. *et al.* Taxol transport by human intestinal epithelial Caco-2 cells. *Drug Metab. Dispos.*, 26(4): 343-6, 1998.
- <sup>27</sup> Woo J. S. *et al.* Enhanced Oral Bioavailability of Paclitaxel by Coadministration of the P-Glycoprotein Inhibitor KR30031. *Pharm. Res.*, 20(1): 24-30, 2003.
- <sup>28</sup> Collett A. *et al.* Predicting P-glycoprotein effects on oral absorption: correlation of transport in Caco-2 with drug pharmacokinetics in wild-type and *mdr1a*(-/-) mice in vivo. *Pharm. Res.*, 21(5): 819-26, 2004.
- <sup>29</sup> Polli J. W. *et al.* Rational use of in vitro P-glycoprotein assays in drug discovery. *J. Pharmacol. Exp. Ther.*, 299(2): 620-8, 2001.

- <sup>30</sup> Huisman M. T. *et al.* MRP2 (ABCC2) transports taxanes and confers paclitaxel resistance and both processes are stimulated by probenecid. *Int. J. Cancer*, 116(5): 824-9, 2005.
- <sup>31</sup> Doyle L. A. *et al.* Multidrug resistance mediated by the breast cancer resistance protein BCRP (ABCG2). *Oncogene*, 22(47): 7340-58, 2003.
- <sup>32</sup> Meerum Terwogt J. M. *et al.* Coadministration of oral cyclosporin A enables oral therapy with paclitaxel. *Clin. Cancer Res.*, 5(11): 3379-84, 1999.
- <sup>33</sup> Van Asperen J. *et al.* Enhanced oral bioavailability of paclitaxel in mice treated with the P-glycoprotein blocker SDZ PSC 833. *Br. J. Cancer*, 76(9): 1181-3, 1997.
- <sup>34</sup> Kruijtzter C.M. *et al.* Weekly oral paclitaxel as first-line treatment in patients with advanced gastric cancer. *Ann. Oncol.*, 14(2): 197-204, 2003.
- <sup>35</sup> Malingre M. M. *et al.* Co-administration of GF120918 significantly increases the systemic exposure to oral paclitaxel in cancer patients. *Br. J. Cancer*, 84(1): 42-7, 2001.
- <sup>36</sup> Choi J-S. *et al.* The effect of verapamil on the pharmacokinetics of paclitaxel in rats. *Eur. J. Pharm. Sci.*, 24(1): 95-100, 2005.
- <sup>37</sup> Mayer U. *et al.* Substantial excretion of digoxin via the intestinal mucosa and prevention of long-term digoxin accumulation in the brain by the mdr 1a P-glycoprotein. *Br. J. Pharmacol.*, 119(5): 1038-44, 1996.
- <sup>38</sup> Lagas J. S. *et al.* Multidrug Resistance Protein 2 is an Important Determinant of Paclitaxel Pharmacokinetics. *Clin. Cancer Res.*, 12(20 Pt 1): 6125-32, 2006.
- <sup>39</sup> Sparreboom A. *et al.* Limited oral bioavailability and active epithelial excretion of paclitaxel (Taxol) caused by P-glycoprotein in the intestine. *Proc. Natl. Acad. Sci. USA.*, 94(5): 2031-5, 1997.
- <sup>40</sup> Bardelmeijer H. A. *et al.* Increased oral bioavailability of paclitaxel by GF120918 in mice through selective modulation of p-glycoprotein. *Clin. Cancer Res.*, 6(1): 4416-21, 2000.
- <sup>41</sup> Stephens R. H. *et al.* Region dependent modulation of intestinal permeability by drug efflux transporters in vitro studies in mdr1a(-/-) mouse intestine. *J. Pharmacol. Exp. Ther.*, 303(3): 1095-01, 2002.
- <sup>42</sup> Cresteil T. *et al.* Taxol metabolism by human liver microsomes: identification of cytochrome P450 isozymes involved in its biotransformation. *Cancer Res.*, 54(2): 386-92, 1994.
- <sup>43</sup> Kumar G. N. *et al.* Cytochrome P450 3A-mediated human liver microsomal taxol 6<sub>β</sub>-hydroxylation. *J. Pharmacol. Exp. Ther.*, 268:1160-5, 1994.
- <sup>44</sup> Rahman A. *et al.* Selective biotransformation of taxol to 6-hydroxytaxol by human cytochrome P450 2C8. *Cancer Res.*, 54(21): 5543-6, 1994.
- <sup>45</sup> Sparreboom A. *et al.* Nonlinear pharmacokinetics of paclitaxel in mice results from the pharmaceutical vehicle Cremophor EL. *Cancer Res.*, 56(9): 2112-5, 1996.
- <sup>46</sup> Karlsson M. O. *et al.* Pharmacokinetic models for the saturable distribution of paclitaxel. *Drug Metab. Dispos.*, 27(10): 1220-3, 1999.
- <sup>47</sup> Wiernik P. H. *et al.* Phase I trial of taxol given as a 24-hour infusion every 21 days: responses observed in metastatic melanoma. *J. Clin. Oncol.*, 5(8): 1232-9, 1987.
- <sup>48</sup> Wiernik P. H. *et al.* Phase I clinical and pharmacokinetic study of taxol. *Cancer Res.*, 47(9): 2486-93, 1987.
- <sup>49</sup> Brown T. *et al.* Phase I trial of taxol given by a 6-hour intravenous infusion. *J. Clin. Oncol.*, 9(7): 1261-7, 1991.
- <sup>50</sup> Walle T. *et al.* Taxol metabolism and disposition in cancer patients. *Drug Metab. Dispos.*, 23(4): 506-12, 1995.
- <sup>51</sup> Alsenz J. *et al.* Active apical secretory efflux of the HIV protease inhibitors saquinavir and zidovudine in Caco-2 cell monolayers. *Pharm. Res.*, 15(3): 423-8, 1998.
- <sup>52</sup> Kasim N. A. *et al.* Molecular properties of WHO essential drugs and provisional biopharmaceutical classification. *Mol. Pharm.*, 1(1): 85-96, 2004.
- <sup>53</sup> Polli J. W. *et al.* Role of P-Glycoprotein on the CNS Disposition of Amprenavir (141W94), an HIV Protease Inhibitor. *Pharm. Res.*, 16(8): 1206-12, 1999.
- <sup>54</sup> Williams G. C. *et al.* Direct evidence that Saquinavir is transported by multidrug resistance-associated protein MRP1 and canalicular multispecific organic anion transporter MRP2. *Antimicrob. Agents Chemother.*, 46(11): 3456-62, 2002.
- <sup>55</sup> Annice E. *et al.* Saquinavir, an HIV protease inhibitor, is transported by P-glycoprotein. *J. Pharmacol. Exp. Ther.*, 286(3): 1439-45, 1998.
- <sup>56</sup> Doan K.M. *et al.* Passive Permeability and P-Glycoprotein-Mediated Efflux Differentiate Central Nervous System (CNS) and Non-CNS Marketed Drugs. *J. Pharmacol. Exp. Ther.*, 303(3): 1029-37, 2002.
- <sup>57</sup> Buss N. *et al.* Saquinavir and zidovudine pharmacokinetics following combined zidovudine and saquinavir (soft gelatin capsules) administration. *Br. J. Clin. Pharmacol.*, 52(3): 255-64, 2001.
- <sup>58</sup> Kim R. B. *et al.* The drug transporter P-glycoprotein limits oral absorption and brain entry of HIV-1 protease inhibitors. *J. Clin. Invest.*, 101(2): 289-94, 1998.
- <sup>59</sup> Bertz R. J. *et al.* Use of in vitro and in vivo data to estimate the likelihood of metabolic pharmacokinetic interactions. *Clin. Pharmacokinet.*, 32(3): 210-58, 1997.
- <sup>60</sup> Flexner C. *et al.* HIV protease inhibitors. *N. Eng. J. Med.*, 338(18): 1281-93, 1998.

- <sup>61</sup> Petri N. *et al.* Transport characteristics of fexofenadine in Caco-2 cell model. *Pharm Res.*, 21(8): 1398-404, 2004.
- <sup>62</sup> Tahara H. *et al.* P-glycoprotein plays a major role in the efflux of fexofenadine in the small intestine and blood brain barrier but only a limited role in its biliary excretion. *Drug Metab. Dispos.*, 33(7): 963-8, 2005.
- <sup>63</sup> Perloff M. D. *et al.* Fexofenadine transport in caco-2 cells: inhibition with verapamil and ritonavir. *J. Clin. Pharmacol.*, 42(11): 1269-74, 2002.
- <sup>64</sup> Cvetkovic M. *et al.* OATP and P-Glycoprotein Transporters Mediate the Cellular Uptake and Excretion of Fexofenadine. *Drug Metab. Dispos.*, 27(8): 866-71, 1999.
- <sup>65</sup> Wang Z. *et al.* Effect of St. John's wort on the pharmacokinetics of fexofenadine. *Clin. Pharmacol. Ther.*, 71(6): 414-20, 2002.
- <sup>66</sup> Tannergren C. *et al.* Multiple transport mechanisms involved in the intestinal absorption and first-pass extraction of fexofenadine. *Clin. Pharmacol. Ther.*, 74(5): 423-36, 2003.
- <sup>67</sup> Yasui-Furukori N. *et al.* Different effects of three transporting inhibitors, verapamil, cimetidine, and probenecid, on fexofenadine pharmacokinetics. *Clin. Pharmacol. Ther.*, 77(1): 17-23, 2005.
- <sup>68</sup> Hamman M. A. *et al.* The effect of rifampin administration on the disposition of fexofenadine. *Clin. Pharmacol. Ther.*, 69(3): 114-21, 2001.
- <sup>69</sup> Klein C. E. *et al.* Effect of atrasentan (ABT-627, ATN) on the pharmacokinetics (PK) of fexofenadine (FEX) *Clin. Oncol.*, 22(14S): 4723, 2004.
- <sup>70</sup> Molimard M. *et al.* Comparison of pharmacokinetics and metabolism of desloratadine, fexofenadine, levocetirizine and mizolastine in humans. *Fundam. Clin. Pharmacol.*, 18(4): 399-411, 2004.
- <sup>71</sup> Drug Information for the Health Care Professional. USP DI vol 1. 23 edition. Micromedex. 2003
- <sup>72</sup> HPLC methods for recently approved pharmaceuticals. Willey interscience. John Willey and sons.
- <sup>73</sup> Balimane P. V. *et al.* Current industrial practices of assessing permeability and P-gp interactions. *The AAPS Journal*, 8(1): E1-13, 2006.
- <sup>74</sup> Salphati L. *et al.* Effects of Ketoconazole on Digoxin absorption and disposition in Rat. *Pharmacology*, 56(6): 308-13, 1998.
- <sup>75</sup> Song S. *et al.* Effect of PSC 833, a P-glycoprotein modulator, on the disposition of vincristine and digoxin in rats. *Drug Metab. Dispos.*, 27(6): 689-94, 1999.
- <sup>76</sup> Adachi Y. *et al.* Quantitative Evaluation of the Function of Small Intestinal P-Glycoprotein: Comparative Studies Between in Situ and in Vitro. *Pharm. Res.*, 20(8): 1163-9, 2003.
- <sup>77</sup> Schinkel A. H. *et al.* Absence of the mdr1a P-Glycoprotein in mice affects tissue distribution and pharmacokinetics of dexamethasone, digoxin and cyclosporin A. *J. Clin. Invest.*, 96(4): 1698-705, 1995.
- <sup>78</sup> Schwab D. *et al.* Comparison of in vitro P-glycoprotein screening assays: recommendations for their use in drug discovery. *J. Med. Chem.*, 46(9): 1716-25, 2003.
- <sup>79</sup> Xianhua C. *et al.* Permeability dominates in vivo intestinal absorption of P-gp substrate with high solubility and high permeability. *Mol. Pharm.*, 2:329-340, 2004.
- <sup>80</sup> Matsson P. *et al.* Exploring the Role of Different Drug Transport Routes in Permeability Screening. *J. Med. Chem.*, 48(2): 604-13, 2005.
- <sup>81</sup> Cavet M. E. *et al.* Transport and epithelial secretion of the cardiac glycoside, digoxin, by human intestinal epithelial (Caco-2) cells. *Br. J. Pharmacol.*, 118(6): 1389-96, 1996.
- <sup>82</sup> Fromm M. F. *et al.* Inhibition of P-glycoprotein-mediated drug transport: A unifying mechanism to explain the interaction between digoxin and quinidine. *Circulation*. 99(4): 552-7, 1999.
- <sup>83</sup> Balayssac D. *et al.* Does inhibition of P-glycoprotein lead to drug-drug interactions?. *Toxicol. Lett.*, 156(3): 319-329, 2005.
- <sup>84</sup> Tanaka H. *et al.* Effect of clarithromycin on steady-state digoxin concentrations. *Ann. Pharmacother.*, 37(2): 178-81, 2003.
- <sup>85</sup> Rengelshausen J. *et al.* Contribution of increased oral bioavailability and reduced nonglomerular renal clearance of digoxin to the digoxin-clarithromycin interaction. *Br. J. Clin. Pharmacol.*, 56(1): 32-8, 2003.
- <sup>86</sup> Johne A. *et al.* Pharmacokinetic interaction of digoxin with an herbal extract from St John's wort. *Clin. Pharmacol. Ther.* 66(4): 338-45, 1999.
- <sup>87</sup> Boyd R. A. *et al.* Atorvastatin coadministration may increase digoxin concentrations by inhibition of intestinal p-glycoprotein-mediated secretion. *J. Clin. Pharmacol.*, 40(1): 91-8, 2000.
- <sup>88</sup> Reinhard D. *et al.* Substantial pharmacokinetics interaction between digoxin and ritonavir in healthy volunteers. *Clin. Pharmacol. Ther.*, 76(1): 73-84, 2004.
- <sup>89</sup> Westphal K. *et al.* Oral bioavailability of digoxin is enhanced by talinolol: Evidence for involvement of Intestinal P-glycoprotein. *Clin. Pharmacol. Ther.*, 68(1): 6-12, 2000.
- <sup>90</sup> Zhao Y. H. *et al.* Atorvastatin coadministration may increase digoxin concentrations by inhibition of intestinal P-glycoprotein-mediated secretion. *J. Pharm. Sci.*, 90(6): 749-84, 2001.

- <sup>91</sup> Smith T. W. Pharmacokinetics, bioavailability and serum levels of cardiac glycosides. *J. Am. Coll. Cardiol.*, 5(Suppl A): 43A-50A, 1985.
- <sup>92</sup> Sietsema W. K. The absolute oral bioavailability of selected drugs. *Int. J. Clin. Pharmacol. Ther. Toxicol.*, 27(4): 179-211, 1989.
- <sup>93</sup> Spahn-Langguth H. *et al.* P-glycoprotein transporters and the gastrointestinal tract: evaluation of the potential in vivo relevance of in vitro data employing talinolol as model compound. *Int. J. Clin. Pharmacol. Ther.*, 36(1): 16-24, 1998.
- <sup>94</sup> Gramatte T. *et al.* Intestinal secretion of intravenous talinolol is inhibited by luminal R-verapamil. *Clin. Pharmacol. Ther.*, 66(3): 239-45, 1999.
- <sup>95</sup> Westphal K. *et al.* Induction of P-glycoprotein by rifampin increases intestinal secretion of talinolol in human beings: A new type of drug/drug interaction, *Clin. Pharmacol. Ther.*, 68:345-355, 2000.
- <sup>96</sup> Bogman K. *et al.* P-glycoprotein and surfactants: Effects on intestinal talinolol absorption. *Clin. Pharmacol. Ther.*, 77: 24-32, 2005.
- <sup>97</sup> Trausch B. *et al.* Disposition and bioavailability of the beta 1-adrenoceptor antagonist talinolol in man. *Biopharm. Drug. Dispos.*, 16(5): 403-14, 1995.
- <sup>98</sup> Doran A. *et al.* The impact of P-glycoprotein on the disposition of drugs targeted for indications of the central nervous system: evaluation using the MDR1A/1B knockout mouse model. *Drug Metab. Dispos.*, 33(1): 165-74, 2005.
- <sup>99</sup> Von Moltke L. L. *et al.* Drug transporters in psychopharmacology-are they important? *J. Clin. Psychopharmacol.*, 20(3): 291-4, 2000.
- <sup>100</sup> Schinkel A. H. *et al.* P-glycoprotein in the blood-brain barrier of mice influences the brain penetration and pharmacological activity of many drugs. *J. Clin. Invest.*, 97(11): 2517-24, 1996.
- <sup>101</sup> Dagenais C. *et al.* Effect of mdr1a P-glycoprotein gene disruption, gender, and substrate concentration on brain uptake of selected compounds. *Pharm. Res.*, 18(7): 957-63, 2001.
- <sup>102</sup> Hou T. J. *et al.* ADME evaluation in drug discovery. 5. Correlation of Caco-2 permeation with simple molecular properties. *J. Chem. Inf. Comput. Sci.*, 44(5): 1585-600, 2004.
- <sup>103</sup> Yamazaki M. *et al.* In vitro substrate identification studies for p-glycoprotein-mediated transport: species difference and predictability of in vivo results. *J. Pharmacol. Exp. Ther.*, 296(3): 723-35, 2001.
- <sup>104</sup> Lee J. S. *et al.* Rhodamine efflux patterns predict P-glycoprotein substrates in the National Cancer Institute drug screen. *Mol Pharmacol.*, 46(4): 627-38, 1994.
- <sup>105</sup> Cisternino S. *et al.* Screening of multidrug-resistance sensitive drugs by in situ brain perfusion in P-glycoprotein-deficient mice. *Pharm. Res.*, 18(2): 183-90, 2001.
- <sup>106</sup> Goh L. B. *et al.* Endogenous drug transporters in in vitro and in vivo models for the prediction of drug disposition in man. *Biochem Pharmacol.*, 64(11): 1569-78, 2002.
- <sup>107</sup> Saitoh H. *et al.* Limited interaction between tacrolimus and P-glycoprotein in the rat small intestine. *Eur. J. Pharm. Sci.*, 28(1-2): 34-42, 2006.
- <sup>108</sup> Flanagan S. D. *et al.* Comparison of furosemide and vinblastine secretion from cell lines over expressing multidrug resistance protein and multi drug resistance associated proteins (MRP1 and MRP2). *Pharmacology*, 64(3): 126-34, 2002.
- <sup>109</sup> Stephens R. H. *et al.* Kinetic profiling of P-glycoprotein mediated drug efflux in rat and human intestinal epithelia. *J. Pharmacol. Exp. Ther.*, 296(2): 584-91, 2001.
- <sup>110</sup> Kruijtzter C. M. *et al.* Increased oral bioavailability of topotecan in combination with the breast cancer resistance protein and P-glycoprotein inhibitor GF120918. *J. Clin. Oncol.*, 20(13): 2943-50, 2002.
- <sup>111</sup> Hendricks C.B. *et al.* Effect of P-glycoprotein expression on the accumulation and cytotoxicity of topotecan (SF&K 104864), a new camptothecin analogue. *Cancer Res.*, 52(8): 2268-78, 1992.
- <sup>112</sup> Johan W. J. *et al.* Role of breast cancer resistance protein in the bioavailability and fetal penetration of topotecan. *J. Nat. Cancer Ins.*, 92(20): 1651-56, 2000.
- <sup>113</sup> Zhang S. *et al.* Flavonoids chrysin and benzoflavone, potent breast cancer resistance protein inhibitors have no significant effect on topotecan pharmacokinetics in rats or MDR1A/1B (-/-) mice. *Drug. Metab. Dispos.*, 33(3): 341-8, 2005.
- <sup>114</sup> Schellens J. H. *et al.* Bioavailability and pharmacokinetics of oral topotecan: a new topoisomerase I inhibitor. *Br J Cancer.*, 73(10): 1268-71, 1996.
- <sup>115</sup> Bachmakov I. *et al.* Characterization of  $\beta$ -adrenoreceptor antagonists as substrates and inhibitors of the drug transporter P-glycoprotein, *Fundam. Clin. Pharmacol.*, 20(3): 273-282, 2006.
- <sup>116</sup> Cho H. Y. *et al.* Improvement and validation of a HPLC method for examining the effects of the MDR1 gene polymorphism on sparfloxacin pharmacokinetics. *J. Chromatogr. B. Analyt. Technol. Biomed. Life Sci.*, 834(1-2): 84-92, 2006.
- <sup>117</sup> Hooijberg J. H. *et al.* Antifolate resistance mediated by the multidrug resistance proteins MRP1 and MRP2. *Cancer Res.*, 59(11): 2532-5, 1999.
- <sup>118</sup> Chen C. *et al.* Impact of MRP2 on the biliary excretion and intestinal absorption of furosemide, probenecid and methotrexate using eisai hyperbilirubinemic rats. *Pharm. Res.*, 20(1): 31-7, 2003.

- <sup>119</sup> Chen Z. *et al.* Analysis of Methotrexate and folate transport by multidrug resistance protein 4: MRP4 is a major component of the methotrexate efflux system. *Cancer Res.*, 62(11): 3144-50, 2002.
- <sup>120</sup> <http://redpoll.pharmacy.ualberta.ca/drugbank/index.html>
- <sup>121</sup> <http://www.tsrlinc.com/search3.cfm>
- <sup>122</sup> <http://www.rxlist.com/>
- <sup>123</sup> Dagenais C. *et al.* Variable modulation of opioid brain uptake by P-glycoprotein in mice. *Biochem. Pharmacol.*, 67(2): 269-76, 2004.
- <sup>124</sup> Saeki T. *et al.* Human P-glycoprotein transports cyclosporin A and FK506. *J. Biol. Chem.*, 268(9): 6077-80, 1993.
- <sup>125</sup> Kuzuya T. *et al.* Amlodipine, but not MDR1 polymorphisms, alters the pharmacokinetics of cyclosporine A in Japanese kidney transplant recipients. *Transplantation*. 76(5): 865-8, 2003.
- <sup>126</sup> Zhao Y. H. *et al.* Quantitative relationship between rat intestinal absorption and Abraham descriptors. *Eur. J. Med. Chem.*, 38(11-12): 939-47, 2003.
- <sup>127</sup> Dresser G. K. *et al.* Pharmacokinetic-pharmacodynamic consequences and clinical relevance of cytochrome P450 3A4 inhibition. *Clin. Pharmacokinet.*, 38(1): 41-57, 2000.
- <sup>128</sup> van Kalken C. K. *et al.* Cortisol is transported by the multidrug resistance gene product P-glycoprotein. *Br. J. Cancer*. 67(2): 284-9, 1993.
- <sup>129</sup> Schuetz E. G. *et al.* P-glycoprotein: a major determinant of rifampicin-inducible expression of cytochrome P4503A in mice and humans. *Proc. Natl. Acad. Sci. U S A.* 93(9): 4001-5, 1996.
- <sup>130</sup> Burman W. J. *et al.* Comparative pharmacokinetics and pharmacodynamics of the rifamycin antibacterials. *Clin. Pharmacokinet.* 40(5): 327-41, 2001.
- <sup>131</sup> Alvarez M. *et al.* Generation of a drug resistance profile by quantitation of mdr-1/P-glycoprotein in the cell lines of the National Cancer Institute Anticancer Drug Screen. *J. Clin. Invest.*, 95(5): 2205-14, 1995.
- <sup>132</sup> Takeshita H. *et al.* Experimental models for the study of drug resistance in osteosarcoma: P-glycoprotein-positive, murine osteosarcoma cell lines. *J. Bone Joint. Surg. Am.*, 78(3): 366-75, 1996.
- <sup>133</sup> Mechetner E. B. *et al.* Efficient inhibition of P-glycoprotein-mediated multidrug resistance with a monoclonal antibody. *Proc. Natl. Acad. Sci. U S A.* 89(13): 5824-8, 1992.
- <sup>134</sup> Troutman M. D. *et al.* Efflux ratio cannot assess P-glycoprotein-mediated attenuation of absorptive transport: asymmetric effect of P-glycoprotein on absorptive and secretory transport across Caco-2 cell monolayers. *Pharm. Res.*, 20(8): 1200-9, 2003.
- <sup>135</sup> R. H. *et al.* Resolution of P-glycoprotein and non-P-glycoprotein effects on drug permeability using intestinal tissues from mdr1a (-/-) mice. *Br. J. Pharmacol.*, 135(8): 2038-46, 2002.
- <sup>136</sup> Goodman & Gilman's. *The Pharmacological Basis of Therapeutics*. Ninth Edition, The McGraw-Hill Companies, 1995.
- <sup>137</sup> Kim R. B. *et al.* Interrelationship between substrates and inhibitors of human CYP3A and P-glycoprotein. *Pharm. Res.*, 16(3): 408-14, 1999.
- <sup>138</sup> Bergstrom C. A. *et al.* Absorption classification of oral drugs based on molecular surface properties. *J. Med. Chem.*, 46(4): 558-70, 2003.
- <sup>139</sup> Banerjee S. K. *et al.* Bioavailability of tobramycin after oral delivery in FVB mice using CRL-1605 copolymer, an inhibitor of P-glycoprotein. *Life Sci.*, 67(16): 2011-6, 2000.
- <sup>140</sup> Schinkel A. H. *et al.* Disruption of the mouse mdr1a P-glycoprotein gene leads to a deficiency in the blood-brain barrier and to increased sensitivity to drugs. *Cell*, 77(4): 491-502, 1994.
- <sup>141</sup> Saito T. *et al.* Homozygous disruption of the mdr1a P-glycoprotein gene affects blood-nerve barrier function in mice administered with neurotoxic drugs. *Acta Otolaryngol.*, 121(6): 735-42, 2001.
- <sup>142</sup> Krukemyer J. J. *et al.* Comparison of single-dose and steady-state nadolol plasma concentrations. *Pharm. Res.*, 7(9): 953-6, 1990.
- <sup>143</sup> Wang Q. *et al.* Evaluation of the MDR-MDCK cell line as a permeability screen for the blood-brain barrier. *Int. J. Pharm.* 288(2): 349-59, 2005.
- <sup>144</sup> Shirakawa K. *et al.* Interaction of docetaxel ("Taxotere") with human P-glycoprotein. *Jpn. J. Cancer. Res.*, 90(12): 1380-6, 1999.
- <sup>145</sup> Wils P. *et al.* Polarized transport of docetaxel and vinblastine mediated by P-glycoprotein in human intestinal epithelial cell monolayers. *Biochem. Pharmacol.*, 48(7): 1528-30, 1994.
- <sup>146</sup> Malingre M. M. *et al.* Coadministration of cyclosporine strongly enhances the oral bioavailability of docetaxel. *J. Clin. Oncol.*, 19(4): 1160-6, 2001.
- <sup>147</sup> Kuppens I. E. *et al.* Oral bioavailability of docetaxel in combination with OC144-093 (ONT-093). *Cancer Chemother Pharmacol.*, 55(1): 72-8, 2005.
- <sup>148</sup> Van der Sandt I.C. *et al.* Assessment of active transport of HIV protease inhibitors in various cell lines and the in vitro blood-brain barrier. *AIDS*. 15(4): 483-91, 2001.

- <sup>149</sup> Stenberg P. *et al.* Experimental and computational screening models for the prediction of intestinal drug absorption. *J. Med. Chem.*, 44(12): 1927-37, 2001
- <sup>150</sup> Watanabe K. *et al.* Studies on intestinal absorption of sulpiride (2): transepithelial transport of sulpiride across the human intestinal cell line Caco-2. *Biol. Pharm. Bull.*, 25(10): 1345-50, 2002.
- <sup>151</sup> Baluom M. *et al.* Improved intestinal absorption of sulpiride in rats with synchronized oral delivery systems. *J. Control Release.* 70(1-2): 139-47, 2001.
- <sup>152</sup> Willmann S. *et al.* A physiological model for the estimation of the fraction dose absorbed in humans. *J. Med. Chem.*, 47(16): 4022-31, 2004.
- <sup>153</sup> Wiesel F.A. *et al.* The pharmacokinetics of intravenous and oral sulpiride in healthy human subjects. *Eur. J. Clin. Pharmacol.*, 17(5): 385-91, 1980.
- <sup>154</sup> Pachot J. I. *et al.* Experimental estimation of the role of P-Glycoprotein in the pharmacokinetic behaviour of telithromycin, a novel ketolide, in comparison with roxithromycin and other macrolides using the Caco-2 cell model. *J. Pharm. Pharm. Sci.*, 6(1): 1-12, 2003.
- <sup>155</sup> Amsden G. W. *et al.* A study of the pharmacokinetics of azithromycin and nelfinavir when coadministered in healthy volunteers. *J. Clin. Pharmacol.*, 40(12 Pt 2): 1522-7, 2000.
- <sup>156</sup> Page R. L. *et al.* Possible interaction between intravenous azithromycin and oral cyclosporine. *Pharmacotherapy.* 21(11):1436-43, 2001.
- <sup>157</sup> Zhanel G. G. *et al.* Review of macrolides and ketolides: focus on respiratory tract infections. *Drugs.* 61(4): 443-98, 2001.
- <sup>158</sup> Valenzuela B. *et al.* Modelling intestinal absorption of salbutamol sulphate in rats. *Int. J. Pharm.*, 314(1): 21-30, 2006.
- <sup>159</sup> Guo A. *et al.* Delineating the contribution of secretory transporters in the efflux of etoposide using Madin-Darby canine kidney (MDCK) cells overexpressing P-glycoprotein (P-gp), multidrug resistance-associated protein (MRP1), and canalicular multispecific organic anion transporter (cMOAT). *Drug Metab. Dispos.*, 30(4): 457-63, 2002.
- <sup>160</sup> Makhlof K. *et al.* Potential of beta2-adrenoceptor agonists as add-on therapy for multiple sclerosis: focus on salbutamol (albuterol). *CNS Drugs.* 16(1): 1-8, 2002.
- <sup>161</sup> Boulton D. W. *et al.* The pharmacokinetics of levosalbutamol: what are the clinical implications? *Clinical Pharmacokinet.*, 40(1):23-41, 2001.
- <sup>162</sup> Liang E. *et al.* Mechanisms of transport and structure permeability relationship of sulfasalazine and its analogs in Caco-2 cell monolayers. *Pharm. Res.*, 17(10): 1168-74, 2000.
- <sup>163</sup> Zaher H. *et al.* Breast cancer resistance protein is a major determinant of sulfasalazine absorption and elimination in the mouse. *Mol. Pharm.*, 3(1): 55-61, 2006.
- <sup>164</sup> Tirona R. G. Ethnic differences in statin disposition. *Clin. Pharmacol. Ther.*, 78(4): 311-6, 2005.
- <sup>165</sup> Huang L. *et al.* ATP dependent transport of rosuvastatin in membrane vesicles expressing breast cancer resistance protein. *Drug Metab. Dispos.*, 34(5): 738-42, 2006.
- <sup>166</sup> Cooper K. J. *et al.* Lack of effect of ketoconazole on the pharmacokinetics of rosuvastatin in healthy subjects. *J. Clin. Pharmacol.*, 55(1): 94-9, 2003.
- <sup>167</sup> Hirano M. *et al.* Involvement of BCRP in the biliary excretion of pitavastatin. *Mol. Pharm.*, 68(3):800-7, 2005.
- <sup>168</sup> Varma M. V. S. *et al.* Prediction of *in vivo* intestinal absorption enhancement on P-glycoprotein inhibition, from rat *in situ* permeability. *J. Pharm. Sci.*, 94(8): 1694-704, 2005.
- <sup>169</sup> Lindenberg M. *et al.* Classification of orally administered drugs on the World Health Organization Model list of Essential Medicines according to the biopharmaceutics classification system. *Eur. J. Pharm. Biopharm.*, 58(2): 265-78, 2004.
- <sup>170</sup> Thiel-Demby V. E. *et al.* In vitro absorption and secretory quotients: practical criteria derived from a study of 331 compounds to assess for the impact of P-glycoprotein mediated efflux on drug candidates, *J. Pharm. Sci.*, 93(10): 2567-72, 2004.
- <sup>171</sup> Schrickx J. *et al.* Ochrotaxin A secretion by ATP dependent membrane transporters in Caco-2 cells. *Arch. Toxicol.*, 80(5): 243-9, 2006.
- <sup>172</sup> Allen J. D. *et al.* Potent and specific inhibition of the BCRP multi-drug Transporter in vitro and in mouse intestine by a novel analogue of Fumitremorgin C1. *Mol. Cancer Ther.*, 1(6): 417-25, 2002.
- <sup>173</sup> Xia C. Q. *et al.* Expression, localization, and functional characteristics of BCRP in Caco-2 cells. *Drug Metab. Dispos.*, 33(5): 637-643, 2005.
- <sup>174</sup> Dantzig A. H. *et al.* Selectivity of the multidrug resistance modulator LY335979 for the P-glycoprotein and effect on cytochrome P-450 activities. *J. Pharmacol. Exp. Ther.*, 290(2): 854-62, 1999.
- <sup>175</sup> Chen Z. S. *et al.* Effect of multidrug resistance reversing agents on transporting activity of human cMOAT. *Mol. Pharm.*, 56(6): 1219-1228, 1999.
- <sup>176</sup> Robey R. W. *et al.* Overexpression of the ATP-binding cassette half transporter ABCG2 in flavopiridol-resistant human breast cancer cells. *Clin. Cancer Res.*, 7(1): 145-52, 2001.
- <sup>177</sup> Volk E. L. *et al.* Wild type Breast cancer resistance protein is a Methotrexate polyglutamate transporter. *Cancer Res.*, 63(17): 5538-43, 2003.

- <sup>178</sup> Rabindran S. K. *et al.* Fumitremorgin C reverses multidrug resistance cells transfected with the breast cancer resistance protein. *Cancer Res.*, 60(1): 47-50, 2000.
- <sup>179</sup> Hidalgo I. J. *et al.* Characterization of the human colon carcinoma cell line (Caco-2) as a model system for intestinal epithelial permeability. *Gastroenterology*. 96(3): 736-49, 1989.
- <sup>180</sup> Lu S. *et al.* Transport properties are not altered across Caco-2 cells with heightened TEER despite underlying physiological and ultrastructural changes. *J. Pharm. Sci.*, 85(3): 270-273, 1996.
- <sup>181</sup> Irvine J. D. *et al.* MDCK (Madin-Darby canine kidney) cells: A tool for membrane permeability screening. *J. Pharm. Sci.*, 88(1): 28-33, 1999.
- <sup>182</sup> Madgula V. L. *et al.* Transport of decursin and decursinol angelate across Caco-2 and MDR-MDCK cell monolayers: in vitro models for intestinal and blood-brain barrier permeability. *Planta Med.*, 73(4): 330-5, 2007.
- <sup>183</sup> Sandri G. *et al.* Nanoparticles based on N-trimethylchitosan: evaluation of absorption properties using in vitro (Caco-2 cells) and ex vivo (excised rat jejunum) models. *Eur. J. Pharm. Biopharm.*, 65(1): 68-77, 2007.
- <sup>184</sup> Zhou Y. *et al.* The chemical species of aluminum influences its paracellular flux across and uptake into Caco-2 cells, a model of gastrointestinal absorption. *Toxicol. Sci.*, 87(1): 15-26, 2005.
- <sup>185</sup> Saitoh R. *et al.* Correction of Permeability with Pore Radius of Tight Junctions in Caco-2 Monolayers Improves the Prediction of the Dose Fraction of Hydrophilic Drugs Absorbed by Humans. *Pharm. Res.*, 21(5): 749-755, 2004.
- <sup>186</sup> Vogt M. *et al.* Biowaiver monographs for immediate release solid oral dosage forms: prednisolone. *J. Pharm. Sci.*, 96(6): 1480-9, 2007.
- <sup>187</sup> Polli J. E. *et al.* Summary workshop report: Biopharmaceutics Classification System-implementation challenges and extension opportunities, *J. Pharm. Sci.*, 93(6): 1375-81, 2004.
- <sup>188</sup> Neuhoﬀ S. *et al.* Impact of extracellular protein binding on passive and active drug transport across Caco-2 cells. *Pharm. Res.*, 23(2): 350-9, 2006.
- <sup>189</sup> Cho C. *et al.* Carrier mediated uptake of Rhodamine 123: Implications on its use for MDR research. *Biochem. Biophys. Res. Commun.*, 279(1): 124-30, 2000.
- <sup>190</sup> Neyfakh A. A. Use of fluorescent dyes as molecular probes for the study of multidrug resistance. *Exp. Cell Res.*, 174(1): 168-176, 1988.
- <sup>191</sup> Cormet-Boyaka E. *et al.* Secretion of Sparfloxacin from the human intestinal Caco-2 cell line is altered by P-glycoprotein inhibitors. *Antimicrob. Agents Chemother.*, 42(10): 2607-11, 1998.
- <sup>192</sup> Services, U.S.D.o.H.a.H., FDA, and CDER, Guidance for industry Drug interaction studies - study design, data analysis, and implications for dosing and labeling. p. 52, 2006.
- <sup>193</sup> Da Violante G. *et al.* Short term Caco-2/TC7 cell culture: comparison between conventional 21-d and a commercially available 3-d system. *Biol. Pharm. Bull.*, 27(12): 1986-92, 2004.
- <sup>194</sup> Marie-Catherine G. *et al.* Correlation Between Oral Drug Absorption in Humans, and Apparent Drug Permeability in TC-7 Cells, A Human Epithelial Intestinal Cell Line: Comparison with the Parental Caco-2 Cell Line. *Pharm. Res.*, 15(5): 726-733, 2004.
- <sup>195</sup> van der Sandt I. C. *et al.* Specificity of doxorubicin versus rhodamine-123 in assessing P-glycoprotein functionality in the LLC-PK1, LLC-PK1:MDR1 and Caco-2 cell lines. *Eur. J. Pharm. Sci.*, 11(3): 207-14, 2000.
- <sup>196</sup> Brimer C. *et al.* Creation of polarized cells coexpressing CYP3A4, NADPH cytochrome P450 reductase and MDR1/P-glycoprotein. *Pharm. Res.*, 17(7): 803-10, 2000.
- <sup>197</sup> Putnam W. S. *et al.* Functional characterization of monocarboxylic acid, large neutral amino acid, bile acid and peptide transporters, and P-glycoprotein in MDCK and Caco-2 cells. *J. Pharm. Sci.*, 91(12): 2622-35, 2002.
- <sup>198</sup> Ito S. *et al.* Modeling of P-glycoprotein-involved epithelial drug transport in MDCK cells. *Am. J. Physiol.*, 277(1 Pt 2): F84-96, 1999.
- <sup>199</sup> Braun A. *et al.* Cell cultures as tools in biopharmacy. *Eur. J. Pharm. Sci.*, 11(2): S51-60, 2000.
- <sup>200</sup> Tang F. Are MDCK cells transfected with the human MDR1 gene a good model of the human intestinal mucosa? *Pharm. Res.*, 19(6): 765-72, 2002.
- <sup>201</sup> Tang F. *et al.* Are MDCK cells transfected with the human MRP2 gene a good model of the human intestinal mucosa? *Pharm. Res.*, 19(6): 773-9, 2002.
- <sup>202</sup> Tang F. *et al.* Bidirectional transport of rhodamine 123 and Hoechst 33342, fluorescence probes of the binding sites on P-glycoprotein, across MDCK-MDR1 cell monolayers. *J. Pharm. Sci.*, 93(5): 1185-94, 2004.
- <sup>203</sup> Luo F. R., *et al.* Intestinal transport of irinotecan in Caco-2 cells and MDCK II cells overexpressing efflux transporters P-gp, cMOAT, and MRP1. *Drug Metab. Dispos.*, 30(7): 763-70, 2002.
- <sup>204</sup> Williams G. C. *et al.* The effect of cell culture conditions on saquinavir transport through, and interactions with, MDCKII cells overexpressing hMDR1. *J. Pharm. Sci.*, 92(10): 1957-67, 2003.
- <sup>205</sup> Merino G. *et al.* Transport of anthelmintic benzimidazole drugs by breast cancer resistance protein (BCRP/ABCG2). *Drug. Metab. Dispos.*, 33(5): 614-8, 2005.
- <sup>206</sup> Taipalensuu J., *et al.*, Correlation of gene expression of ten drug efflux proteins of the ATP-binding cassette transporter family in normal human jejunum and in human intestinal epithelial Caco-2 cell monolayers. *J. Pharmacol. Exp. Ther.*, 299(1): 64-70, 2001.

---

<sup>207</sup> Nakamura T. *et al.* Real-time quantitative polymerase chain reaction for MDR1, MRP1, MRP2, and CYP3A-mRNA levels in Caco-2 cell lines, human duodenal entero-cytes, normal colorectal tissues, and colorectal adenocarcinomas. *Drug Metab. Dispos.*, 30(1): 4-6, 2002.

<sup>208</sup> Collett A. *et al.* Comparison of P-glycoprotein-mediated drug-digoxin interactions in Caco-2 with human and rodent intestine: relevance to in vivo prediction. *Eur. J. Pharm. Sci.*, 26(5): 386-93, 2005.